

Computing f -Divergences and Distances of High-Dimensional Probability Density Functions — Low-Rank Tensor Approximations —

Alexander Litvinenko^{* a}, Youssef Marzouk^b, Hermann G. Matthies^c,
Marco Scavino^d, and Alessio Spantini^b

^aRheinisch-Westfälische Technische Hochschule (RWTH) Aachen, Germany

^bMIT, Cambridge (MA), USA

^cTechnische Universität Braunschweig, Brunswick, Germany

^dUniversidad de la República, Instituto de Estadística (IESTA), Montevideo, Uruguay

16th November 2021

Abstract

Very often, in the course of uncertainty quantification tasks or data analysis, one has to deal with high-dimensional random variables (RVs) (with values in \mathbb{R}^d). Just like any other random variable, a high-dimensional RV can be described by its probability density (**pdf**) and/or by the corresponding probability characteristic functions (**pcf**), or by a polynomial chaos (PCE) or similar expansion, or some more general representation as a function of other, known, random variables (functional representation). Here the interest is mainly to compute characterisations like the entropy, or relations between two distributions, like their Kullback-Leibler divergence, or more general measures such as f -divergences, among others. These are all computed from the **pdf**, which is often not available directly, and it is a computational challenge to even represent it in a numerically feasible fashion in case the dimension d is even moderately large. It is an even stronger numerical challenge to then actually compute said characterisations in the high-dimensional case. In this regard, in order to achieve a computationally feasible task, we propose to represent the density by a high order tensor product, and approximate this in a low-rank format. We investigate the connection between the low-rank approximability of the d -dimensional random variable, its **pcf**, and its **pdf**. We show how to go from the **pcf** or functional representation to the **pdf**. This allows us to reduce the computational complexity and storage cost from $\mathcal{O}(n^d)$ to $\mathcal{O}(dnr^\alpha)$, where n is the number of discretisation points in one direction or dimension, $r \ll n$ is the maximal tensor rank, and α a small integer.

The characterisations such as entropy or the f -divergences need the possibility to compute point-wise functions of the **pdf**. This normally rather trivial task becomes more difficult when the **pdf** is approximated in a low-rank tensor format, as the point values are not directly accessible any more. The data is considered as an

^{*}Corresponding author: RWTH Aachen, 52072 Aachen, Germany,
e-mail: Litvinenko@uq.rwth-aachen.de

element of a high order tensor space. The considered algorithms are independent of the representation of the data as a tensor. All that we require is that the data can be considered as an element of an associative, commutative algebra with an inner product. Such an algebra is isomorphic to a commutative sub-algebra of the usual matrix algebra, allowing the use of matrix algorithms to accomplish the mentioned tasks. The algorithms to be described are iterative methods or truncated series expansions for particular functions of the tensor, which will then exhibit the desired result. We allow the actual computational representation to be a lossy compression, and we allow the algebra operations to be performed in an approximate fashion, so as to maintain a high compression level. One such example which we address explicitly is the representation of data as a tensor with compression in the form of a low-rank representation. The suggested technique, in order to be employed efficiently, assumes that all involved tensors have a low rank, and the rank is not increasing strongly after linear algebra operations. In the last Section 6, we show some exemplary numerical examples of applications of this framework to approximate high-dimensional density functions of α -stable type—given only through their characteristic function—and compute divergences and distances between such probability distributions.

Keywords: high-dimensional probability density, Kullback-Leibler divergence, f-divergence, distance, tensor representation, computational algorithms, low-rank approximation

MSC Classification: 41A05 · 41A45 · 41A63 · 60-08 · 60E07 · 60E10 · 62-08 · 62E17 · 62H10 · 65C20 · 65F55 · 65F60 · 94A17

Contents

Contents	i
1 Introduction	1
1.1 Motivation	1
1.2 Main idea	2
1.2.1 Discrete low-rank representation of the density	3
1.2.2 Discrete low-rank representation of the characteristic function	4
1.2.3 Low-rank representation of high-dimensional random variables	5
1.2.4 Computing quantities of interest	6
1.3 Working diagram	7
1.4 Literature review	8
1.5 Outline of the paper	9
2 Theoretical background	10
2.1 Notation and summary of basic descriptors	10
2.1.1 Basic descriptors	11
2.1.2 Distribution measure and probability density	11
2.1.3 Probability characteristic function	13
2.2 Relations through the Fourier transform	14
2.2.1 Geometric and algebraic structures	14
2.2.2 Characterising functions and transforms	15
2.3 Grid functions and finite dimensional algebras on tensors	16

2.3.1	Grid discretisation of high-dimensional functions	16
2.3.2	The convolution and Hadamard algebras	18
2.3.3	Using the discrete Fourier transform	20
2.3.4	Functions on the Hadamard algebra	21
3	Computation of moments and divergences	23
3.1	Statistics and moments	23
3.2	Computing divergences	25
4	Tensor formats	26
4.1	The canonical polyadic (CP) tensor format	27
4.2	The Tensor Train format	28
5	Algorithms	30
5.1	Discrete low-rank representation and Fourier transforms	31
5.2	Consistency of data	32
5.3	Overview of methods to compute tensor functions	33
5.4	Iterative methods	34
5.4.1	Perturbed iteration	34
5.4.2	Iteration functions	35
5.5	Series expansions	38
5.6	Direct approximation of $\mathbf{v} := f(\mathbf{w})$	39
6	Numerical examples	39
7	Conclusion	43
	References	45

1 Introduction

In statistics and probability, and in particular in the vigorous field of uncertainty quantification (UQ) [44, 89, 88], one often has to deal with high-dimensional random variables (RVs) with values in \mathbb{R}^d . These RVs have to be computationally represented in some way. For even moderately large dimension d , just the mere storage of the results is a challenge. Thus the results of such computations have to be represented in some “sparse” form.

1.1 Motivation

Often one is interested in characteristic quantities of interest (QoI), i.e. functionals of the RV or its probability density function (**pdf**), so that one has to computationally efficiently operate on the *sparse* stored form. One apparently quite efficient way to deal with such high-dimensional RVs is to view them as elements of some tensor product space of tensors of high order — typically the order corresponds to the dimension [55]. Such tensors can be approximated by low-rank tensors, and thus it becomes feasible to deal with them numerically. Here we concentrate solely on real valued continuous RVs which possess a probability density function (**pdf**), so another possibility is the representation of the **pdf** in some computationally advantageous form.

Possible quantities of interest (QoI) are often defined or only accessible in some specific representation of the RV. We are thinking of QoIs such as the entropy, the Kullback-Leibler divergence, or more generally f -divergences, as well as Hellinger distances, and (central) and generalised moments, to name a few such QoIs [83, 91, 113]. Some are defined and can efficiently be computed with a functional representation of the RV, and some are defined and efficiently computed if one has access to the point values of the **pdf**, the case to be considered here.

For the computation we propose a discrete low-rank tensor representation of the **pdf**. We shall sketch three possibilities on how to arrive at such a low-rank representation of the density. One is via tensor function representations [13, 8, 55, 48, 15] of the probability density function (**pdf**) [29, 104], another via an analogous representation of the (probability) characteristic function (**pcf**) [111, 107, 121], and a third one is via a low-rank representation of a random variable (RV) — e.g. [30, 23].

Connecting and connected with these different representations — next to the already mentioned probability characteristic function (**pcf**) — are other well known characterising objects like the moment generating function or the second characteristic or cumulant generating function, and we show how these may be efficiently computed as well in a low-rank tensor format.

Thus the motivating factors for a low-rank tensor compression include the following [78, 55]:

- the storage cost is reduced to linear or even sub-linear in the dimension;
- the approximation accuracy is controlled by the tensor rank;
- algebraic operations can be performed in cost linear or even sub-linear in the dimension;
- it can be combined with the fast Fourier transform (FT), yielding a *superfast* Fourier transform [93, 26]. The appropriately scaled FT is a unitary transformation, i.e. it does not change the norm. Therefore, applying a FT to a **pcf** (or to its low-rank approximation) does not amplify numerical errors.

On the other hand, general limitations of such a tensor compression technique are that

- it could be time consuming to compute a compression, or in particular a low-rank tensor decomposition;
- with sampling or point evaluation, it requires an axes-parallel mesh;
- after algebraic manipulations, a re-compression may be necessary;
- although many functions have a low-rank representation, in practice only some theoretical estimates for the rank exist.

But the fact still remains that there are situations where storage of all items is not feasible, or operating on all items is out of the question, so that some kind of compression has to be employed, and low-rank tensor techniques offer a very promising avenue [78, 55].

1.2 Main idea

Let us give an example which motivates much of the following formulation and development. Assume that one is dealing with a random vector $\boldsymbol{\xi}$ in a high-dimensional vector space \mathbb{R}^d , i.e.

$$\boldsymbol{\xi} = [\xi_1, \dots, \xi_d]^\top : \Omega \rightarrow \mathbb{R}^d,$$

defined on a suitable probability space Ω . Further assume that this random vector has a density $p_{\boldsymbol{\xi}} : \mathbb{R}^d \rightarrow \mathbb{R}$ (probability density function — **pdf**), and that we want to compute — as a simple example of the possible tasks envisioned — the *differential entropy* (see also Eq. (65)), the *expectation* of the negative logarithm of the **pdf**. This requires the point-wise logarithm of $p_{\boldsymbol{\xi}}$:

$$h(p_{\boldsymbol{\xi}}) := \mathbb{E}(-\ln(p_{\boldsymbol{\xi}}(\mathbf{y}))) := \int_{\mathbb{R}^d} -\ln(p_{\boldsymbol{\xi}}(\mathbf{y}))p_{\boldsymbol{\xi}}(\mathbf{y}) \, d\mathbf{y}. \quad (1)$$

Even if in many cases one may have an analytical expression resp. approximation for the **pdf** $p_{\boldsymbol{\xi}}$, it still may not be possible to compute the above integral analytically, and so we propose to do this numerically. This immediately provokes the *curse of dimensionality*, as the numerical evaluation of such high dimensional integrals can be very expensive, with work proportional n^d , where $n \in \mathbb{N}$ is a discretisation parameter (see the following section 1.2.1). In the following, we shall propose one possible approach to alleviate the computational burden.

The goal is a discrete low-rank tensor point evaluation of the **pdf**. The first starting point in section 1.2.1 is the assumption that one has or may obtain a low-rank tensor function representation [13, 8, 55, 48, 15] of the probability density function (**pdf**) [29, 104]. The second possible starting point in section 1.2.2 is that one has such a low-rank tensor function of the **pcf** [87, 111, 107, 121, 10]. Then via the Fourier transform one may come back to the **pdf**. And the third possibility sketched in section 1.2.3 is that one has a sparse or low-rank representation of a high-dimensional random variable (RV). From this one may evaluate the **pcf** on a tensor grid, and from there then via the Fourier transform again arrive at a low-rank approximation of the **pdf**.

1.2.1 Discrete low-rank representation of the density

Let us further assume that the pdf of the high-dimensional RV has its support in a compact hyper-rectangle

$$\text{supp } p_{\xi} := \text{cl}\{\mathbf{y} \in \mathbb{R}^d \mid p_{\xi}(\mathbf{y}) \neq 0\} \subseteq \bigtimes_{\nu=1}^d [\xi_{\nu}^{(\min)}, \xi_{\nu}^{(\max)}] \subset \mathbb{R}^d.$$

A fully discrete representation of the pdf can be achieved (further details will be provided in Section 2) by picking in each dimension $1 \leq \nu \leq d$ of \mathbb{R}^d an equidistant grid vector $\hat{\mathbf{x}}_{\nu} := (\hat{x}_{1,\nu}, \dots, \hat{x}_{M_{\nu},\nu})$ of size M_{ν} , such that $\hat{x}_{1,\nu} \leq \xi_{\nu}^{(\min)}$ and $\hat{x}_{M_{\nu},\nu} \geq \xi_{\nu}^{(\max)}$. The size M_{ν} could be different for each dimension ν , but for the sake of simplicity here we assume them all equal to n , i.e. each $\hat{\mathbf{x}}_{\nu} \in \mathbb{R}^n$. The whole grid will be denoted by $\hat{\mathbf{X}} = \bigtimes_{\nu=1}^d \hat{\mathbf{x}}_{\nu} = (\hat{X})_{(\nu,i_1,\dots,i_d)}$ with $1 \leq i_{\nu} \leq M_{\nu}$.

The notation $\mathbf{P} := p_{\xi}(\hat{\mathbf{X}})$ will denote the tensor $\mathbf{P} \in \bigotimes_{\nu=1}^d \mathbb{R}^{M_{\nu}} =: \mathcal{T} = (\mathbb{R}^n)^d = \mathbb{R}^N$, with $\dim \mathcal{T} = \prod_{\nu=1}^d M_{\nu} =: N = n^d$, the components of which are the evaluation of the pdf p_{ξ} on the grid $\hat{\mathbf{X}}$

$$\mathbf{P} := p_{\xi}(\hat{\mathbf{X}}) := (P_{i_1,\dots,i_d}) := (p_{\xi}(\hat{x}_{i_1,1}, \dots, \hat{x}_{i_d,d})), \quad 1 \leq i_{\nu} \leq M_{\nu}, \quad 1 \leq \nu \leq d.$$

If n and especially the dimension d are even moderately large, the total dimension $N = n^d$ is very quickly a huge number, maybe even so that it is not possible to reasonably store that amount of information.

Sometimes the density p_{ξ} is — at least approximately — given as an analytical expression, and it may be possible to approximate it [59] through a low-rank function tensor representation. In the simplest case this would look like

$$p_{\xi}(\mathbf{y}) \approx \tilde{p}_{\xi}(\mathbf{y}) = \sum_{\ell=1}^R \bigotimes_{\nu=1}^d p_{\ell,\nu}(y_{\nu}), \quad (2)$$

where each $p_{\ell,\nu}$ is only a function of the real variable y_{ν} in dimension ν . This is a so-called *canonical polyadic* (CP) tensor representation [59] (cf. Section 4), and it becomes computationally viable when the *rank* R can be chosen fairly small $R \ll N$. The multi-dimensional Gaussian distribution with diagonal covariance matrix is an obvious simple case in point with $R = 1$. Now it becomes possible for each $1 \leq \nu \leq d$ to evaluate the $p_{\ell,\nu}$ on the grid vector $\hat{\mathbf{x}}_{\nu}$ for all $1 \leq \ell \leq R$, giving

$$\mathbf{p}_{\ell,\nu} := (p_{\ell,\nu}(\hat{x}_{1,\nu}), \dots, p_{\ell,\nu}(\hat{x}_{M_{\nu},\nu})) \in \mathbb{R}^{M_{\nu}}.$$

This is a building block for a possible low-rank CP representation of the tensor \mathbf{P} , as now

$$\mathbf{P} \approx \sum_{\ell=1}^R \bigotimes_{\nu=1}^d \mathbf{p}_{\ell,\nu}. \quad (3)$$

More details and descriptions about this and other low-rank tensor approximations will be given in Section 4.

To evaluate now numerically an expression like the differential entropy Eq. (1), the integral is replaced by a numerical quadrature

$$h(p_{\xi}) \approx \sum_{i_1=1}^{M_1} \cdots \sum_{i_d=1}^{M_d} -\ln(P_{i_1,\dots,i_d}) P_{i_1,\dots,i_d} w_{i_1,\dots,i_d}, \quad (4)$$

where w_{i_1, \dots, i_d} are integration weights, which will all be chosen equal $w_{i_1, \dots, i_d} \propto N^{-1}$, cf. Section 2 and Section 3.

The challenge in Eq. (4) is the huge number of terms in the sum. Here the low-rank representation Eq. (3) can be used to advantage, cf. Section 2, but then the challenge is to compute the logarithm in Eq. (4) when \mathbf{P} is in the representation Eq. (3), cf. section 2.3.4. For this certain algebraic properties of the space \mathcal{T} will be used, as will be explained in Section 2 and Section 5.

There are of course other ways to arrive at a discrete low-rank representation of a high-dimensional function. One group of such possible methods are the various “cross”-procedures [36, 100, 8, 7, 25, 31]. In any case, this is not supposed to be an exhaustive survey of such methods, and only intended to give some hints and point to some possibilities.

1.2.2 Discrete low-rank representation of the characteristic function

Again, at other times the (probability) characteristic function (pcf) φ_ξ of the density (cf. section 2.1.3) —

$$\varphi_\xi(\mathbf{t}) := \mathbb{E}(\exp(i \langle \xi | \mathbf{t} \rangle)) := \int_{\mathbb{R}^d} p_\xi(\mathbf{y}) \exp(i \langle \mathbf{y} | \mathbf{t} \rangle) d\mathbf{y} =: \mathcal{F}_d(p_\xi)(\mathbf{t}), \quad (5)$$

where $\mathbf{t} = (t_1, t_2, \dots, t_d) \in \mathbb{R}^d$ is the dual variable to $\mathbf{y} \in \mathbb{R}^d$, $\langle \mathbf{y} | \mathbf{t} \rangle = \sum_{j=1}^d y_j t_j$ is the canonical inner product on \mathbb{R}^d , and \mathcal{F}_d is the probabilist’s d -dimensional Fourier transform Eq. (22) — may be given [10], at least approximately, as an analytical expression (similar to Eq. (2))

$$\varphi_\xi(\mathbf{t}) \approx \tilde{\varphi}_\xi(\mathbf{t}) = \sum_{\ell=1}^R \bigotimes_{\nu=1}^d \varphi_{\ell, \nu}(t_\nu), \quad (6)$$

where the $\varphi_{\ell, \nu}(t_\nu)$ are one-dimensional functions. Examples of such a situation are *elliptically contoured α -stable distributions*, or also *symmetric infinitely divisible distributions* [10]. From this it may be deduced that an approximate low-rank expression of the pdf is given by (cf. Eq. (2))

$$p_\xi(\mathbf{y}) \approx \tilde{p}_\xi(\mathbf{y}) = \mathcal{F}_d^{-1}(\varphi_\xi)\mathbf{y} = \sum_{\ell=1}^R \bigotimes_{\nu=1}^d \mathcal{F}_1^{-1}(\varphi_{\ell, \nu})(y_\nu), \quad (7)$$

see Eq. (24), where \mathcal{F}_1^{-1} is the *one-dimensional* probabilist’s inverse Fourier transform.

For the discrete grid $\hat{\mathbf{X}}$, there is a corresponding *dual grid* $\hat{\mathbf{T}} = (\hat{T})_{(\nu, i_1, \dots, i_d)}$ with $1 \leq i_\nu \leq M_\nu$ for the discrete Fourier transform [16] (cf. section 2.3.1) of same size and dimensions. Similarly to the pdf evaluated on the grid $\hat{\mathbf{X}}$ and represented by the tensor \mathbf{P} , the pcf will be used in a discrete setting evaluated on this dual grid $\hat{\mathbf{T}}$

$$\Phi := \varphi_\xi(\hat{\mathbf{T}}) := (\Phi_{i_1, \dots, i_d}) := (\varphi_\xi(\hat{t}_{i_1, 1}, \dots, \hat{t}_{i_d, d})), \quad 1 \leq i_\nu \leq M_\nu, \quad 1 \leq \nu \leq d.$$

From Eq. (6) it is now easy to see that, as in Eq. (3)

$$\Phi \approx \sum_{\ell=1}^R \bigotimes_{\nu=1}^d \varphi_{\ell, \nu},$$

where the vectors $\varphi_{\ell, \nu}$ are the evaluations of the one-dimensional functions $\varphi_{\ell, \nu}$ from Eq. (6), given by

$$\varphi_{\ell, \nu} := (\varphi_{\ell, \nu}(\hat{t}_{1, \nu}), \dots, \varphi_{\ell, \nu}(\hat{t}_{M_\nu, \nu})) \in \mathbb{R}^{M_\nu}.$$

From these vectors $\boldsymbol{\varphi}_{\ell,\nu}$ one may now compute with the discrete one-dimensional inverse Fourier transform — for the sake of simplicity again denoted by \mathcal{F}_1^{-1} , cf. section 2.3.3 — the vectors $\mathbf{p}_{\ell,\nu} = \mathcal{F}_1^{-1}(\boldsymbol{\varphi}_{\ell,\nu})$, such that from Eq. (7) one arrives at an expression corresponding to Eq. (3):

$$\mathbf{P} = \mathcal{F}_d^{-1}(\boldsymbol{\Phi}) \approx \sum_{\ell=1}^R \bigotimes_{\nu=1}^d \mathcal{F}_1^{-1}(\boldsymbol{\varphi}_{\ell,\nu}) = \sum_{\ell=1}^R \bigotimes_{\nu=1}^d \mathbf{p}_{\ell,\nu}.$$

Thus one again obtains a numerical low-rank representation for the density as in the previous section 1.2.1. Obviously, the cross-methods [36, 100, 8, 7, 25, 31] alluded to in that section 1.2.1 can be used here too, to directly obtain a low-rank representation of the **pcf**. Then again, with the help of the discrete inverse Fourier transforms, one arrives at a low-rank representation of the **pdf**.

1.2.3 Low-rank representation of high-dimensional random variables

Random vectors of high dimension $\boldsymbol{\xi}$ occur also when random fields resp. stochastic processes are discretised, often given through their so-called Karhunen-Loève expansion (KLE) [85, 67, 68] of $\boldsymbol{\xi}$:

$$\boldsymbol{\xi}(\omega) = \sum_{k=0}^d \lambda_k^{1/2} \zeta_k(\omega) \mathbf{v}_k. \quad (8)$$

This places the random vector $\boldsymbol{\xi}(\omega) = [\dots, \xi_k(\omega), \dots]$, a function of the two variables (ω, k) , in the tensor product $L_2(\Omega) \otimes \mathbb{R}^d$, and the Karhunen-Loève expansion Eq. (8) is a *separated* representation of this tensor of second order. Often the singular values $\lambda_k^{1/2}$ decay quickly as k grows, so that one may obtain a good approximation with only r terms. When $r \ll d$, this is exactly the prototype of a *low-rank* approximation we are after, and it is fairly obvious that it can lead to large computational savings.

To see in a nutshell where this leads to, assume further that the uncorrelated RVs $\zeta_k(\omega)$ may be expanded in Wiener's polynomial chaos expansion (PCE), see e.g. [66], with multi-variate polynomials $\Psi_{\boldsymbol{\alpha}}(\boldsymbol{\theta}(\omega)) := \prod_{j=1}^d \psi_{\alpha_j}(\theta_j(\omega))$ in *iid* standard normalised Gaussians $\boldsymbol{\theta}(\omega) = (\theta_1(\omega), \dots, \theta_d(\omega))$, where $\boldsymbol{\alpha} = (\alpha_1, \dots, \alpha_d)$ is a multi-index and the $\psi_{\alpha_j}(\theta_j(\omega))$ are uni-variate polynomials:

$$\zeta_k(\omega) = \sum_{\boldsymbol{\alpha}} \zeta_k^{(\boldsymbol{\alpha})} \Psi_{\boldsymbol{\alpha}}(\boldsymbol{\theta}(\omega)).$$

Inserting this into the KLE, one obtains a combined truncated KLE / PCE

$$\boldsymbol{\xi}(\omega) \approx \sum_{k=0}^r \lambda_k^{1/2} \left(\sum_{\boldsymbol{\alpha}} \zeta_k^{(\boldsymbol{\alpha})} \Psi_{\boldsymbol{\alpha}}(\boldsymbol{\theta}(\omega)) \right) \mathbf{v}_k = \sum_{\boldsymbol{\alpha}} \boldsymbol{\xi}^{(\boldsymbol{\alpha})} \Psi_{\boldsymbol{\alpha}}(\boldsymbol{\theta}(\omega)), \quad (9)$$

where $\boldsymbol{\xi}^{(\boldsymbol{\alpha})} = \sum_{k=0}^d \lambda_k^{1/2} \zeta_k^{(\boldsymbol{\alpha})} \mathbf{v}_k \in \mathbb{R}^d$. Arguably, now the tensor — a multi-dimensional array — $\mathbf{Z} = (\lambda_k^{1/2} \zeta_k^{(\alpha_1, \dots, \alpha_d)})$ resp. $\Xi = (\zeta_k^{(\alpha_1, \dots, \alpha_d)})$ represents the RV $\boldsymbol{\xi}$.

Such a tensor can — as before — be represented in the *canonical polyadic* (CP) format [59], say with low *CP-rank* R :

$$\mathbf{Z} \approx \sum_{r=1}^R \bigotimes_{k=0}^d \mathbf{z}_r^{(k)} = \sum_{r=1}^R \mathbf{z}_r. \quad (10)$$

Here — assuming $\mathbf{z}_r^{(0)} \in \mathbb{R}^d$ and $\mathbf{z}_r^{(k)} \in \mathbb{R}^{M_k}$ for $1 \leq k \leq d$ — each elementary tensor $\mathbf{z}_r = \bigotimes_{k=0}^d \mathbf{z}_r^{(k)} \in \mathbb{R}^d \otimes \bigotimes_{k=1}^d \mathbb{R}^{M_k}$ requires only $d + \sum_{k=1}^d M_k$ pieces of information, in

total $R \times (d + \sum_{k=1}^d M_k)$, compared to $d \times \prod_{k=1}^d M_k$ for the full tensor. A similar low-rank representation may be possible for the PCE coefficient tensor Ξ .

If we view the collection of functions $\Psi_\alpha(\boldsymbol{\theta}(\omega))$ as one tensor-valued function $\boldsymbol{\Psi}(\boldsymbol{\theta}) = (\Psi_\alpha(\boldsymbol{\theta}))$ with values in $\otimes_{k=1}^d \mathbb{R}^{M_k}$, then the evaluation of $\boldsymbol{\xi}(\boldsymbol{\theta})$ in Eq. (9) can be written as a contraction over all of the α -indices — the inner product in $\otimes_{k=1}^d \mathbb{R}^{M_k}$ — of the two tensors Ξ and $\boldsymbol{\Psi}(\boldsymbol{\theta})$:

$$\boldsymbol{\xi}(\boldsymbol{\theta}) = \langle \Xi | \boldsymbol{\Psi}(\boldsymbol{\theta}) \rangle_\alpha. \quad (11)$$

Having Ξ in a low-rank representation then leads to a low-rank representation of the random vector $\boldsymbol{\xi}(\boldsymbol{\theta})$, to obtain a formula for a quick evaluation of the pcf of $\boldsymbol{\xi}(\boldsymbol{\theta})$:

$$\varphi_\xi(\mathbf{t}) = \mathbb{E}(\exp(i \langle \mathbf{t} | \boldsymbol{\xi}(\boldsymbol{\theta}) \rangle_{\mathbb{R}^d})) \approx \mathbb{E}(\exp(i \langle \mathbf{t} | \langle \Xi | \boldsymbol{\Psi}(\boldsymbol{\theta}) \rangle_\alpha \rangle_{\mathbb{R}^d})), \quad (12)$$

giving us the pcf of $\boldsymbol{\xi}(\boldsymbol{\theta})$ in a low-rank tensor function format. Now we are back to the situation in the preceding 1.2.2, and may proceed from there to achieve — via a discrete low-rank representation $\boldsymbol{\Phi}$ of the low-rank function representation in Eq. (12) — a low-rank tensor function representation for the density p_ξ of $\boldsymbol{\xi}(\boldsymbol{\theta})$, and thus for the discrete representation tensor of the density \mathbf{P} , as alluded to in the previous sections above.

1.2.4 Computing quantities of interest

To compute QoIs such as the differential entropy, the Kullback-Leibler (KL) divergence, more general f -divergences, or the Bregman- and Jensen-Shannon-divergences, as well as Hellinger distances — see Section 3 for the distances and divergences considered — functions such as powers, the square root, the logarithm, and the inverse have to be computed point-wise on the pdf. But in a compressed format such as low-rank tensor formats — e.g. in the CP-format in Eq. (2) — the point values are not directly accessible. An important contribution of this paper is to show that such computations are still possible efficiently by operating directly on the compressed format. This will be enabled by identifying both the pcf and the pdf as elements of algebras. A similar idea was already used in [33, 39] for post-processing low-rank representations of random variables, and here it is to be extended to densities and characteristic functions. It is well-known that algebras can be represented as linear operators resp. matrices in the finite-dimensional case (e.g. [110]), and one can employ the spectral calculus of linear operators in order to obtain these point-wise evaluations in a low-rank format. In the concrete case here this boils down to using algorithms which were developed to compute functions of matrices [64].

Therefore, special sparse/low-rank data structures are needed. We suggest to use the low-rank tensor train (TT) data format [100, 101]. Other known tensor formats, such as: canonical polyadic (CP), Tucker, and hierarchical Tucker (HT) could be also applied [55, 70, 75, 12]. For the sake of simplicity of exposition, the CP tensor format is considered in the main part of the paper, when direct reference to a low-rank format is necessary. The computations are also possible in other compressed formats, and we shall give pointers as to what the requirements are, and what other formats can be used just as well. In [39] the computations of the operations of the algebra were already given for various tensor formats, and they may also be found e.g. in [55, 70, 75, 12], so that we may be brief here. For numerical experiments we use the Tensor Train (TT) software library TT-tool [101].

1.3 Working diagram

Diagram 1.3 demonstrates two ways to compute a low-rank approximation of a given **pdf**. Either one applies tensor algorithms directly to the **pdf**, or one goes through the **pcf**. Namely, first, one computes a low-rank approximation of the **pcf** and then, by applying the inverse FFT (IFFT), one obtains a low-rank approximation of **pdf**. Having computed a low-rank approximation, one may compute the f -divergence, moments, and make sampling cheaper.

Consider two scenarios: the **pdf** is either available, or not available (unknown). In contrast to the **pdf**, the **pcf** function always exist (but is not always known analytically). If it is possible to compute a low-rank approximation of the **pdf** directly, then we do it. If not, we try to compute a low-rank approximation of the **pcf**, which may look simpler than the **pdf**. A low-rank approximation may exist or may not exist. If it exists, we can try to find it with low-rank techniques.

The low-rank representation of the high-dimensional **pdf** will simplify integration and sampling. Instead of integrating in d -dimensional space, we will integrate in d one-dimensional spaces. As a consequence, the computational cost and the memory storage will be drastically reduced, $\mathcal{O}(dnr^\alpha)$ instead of $\mathcal{O}(n^d)$, where $\alpha = 2$ or 3 . The obtained low-rank approximation of the **pdf** can be later used in multivariate statistics, in Bayesian inference, in data assimilation, and in uncertainty quantification applications.

In the cases when the multidimensional **pdf** function is not available (either does not exist, is unknown in analytical form, or hard to compute), one may start computations with the **pcf**. For instance, a low-rank approximation of **pcf** can be easier to compute than of **pdf**. After that, by applying IFFT the **pdf** in a low-rank format can be obtained. We illustrated this idea on the diagram below. Additionally, there is a large class of multivariate **pdfs** for which the approximation properties of the corresponding **pcfs** are well studied. [79]. If φ_ξ is integrable, the inversion theorem [87] states that, the **pdf** of ξ on \mathbb{R}^d can be computed from the **pcf** $\varphi_\xi(\mathbf{t})$ by the inverse FT (for details see Section 2.1.3).

The Diagram 1 illustrates the suggested numerical approach. Usually, the **pdf** is used to compute the Bayesian update, data assimilation, or optimal design procedures. These tasks may require computing the f -divergence, Kullback-Leibler divergence (KLD), differential entropy, or the information gain. But what to do if the **pdf** is not available? The **pdf** can be estimated (if it exists) from a sample set, but this works only for small dimensions, due to enormous computing cost in higher dimensions. Therefore, we suggest to use “sparse formats” like low-rank approximations. In case one has a RV ξ as functional representation in a “sparse formats” like e.g. a low-rank approximation, we indicate how to obtain its **pcf** as a “sparse formats” like the low-rank approximation. In again other cases, the **pcf** may be given or estimated in a “sparse formats” like a low-rank approximation. Then, by applying the inverse FFT, one can compute the low-rank approximation of the **pdf**. The concluding step is to compute desired QoIs like the f -divergence, the KLD, and others directly from the low-rank **pdf**.

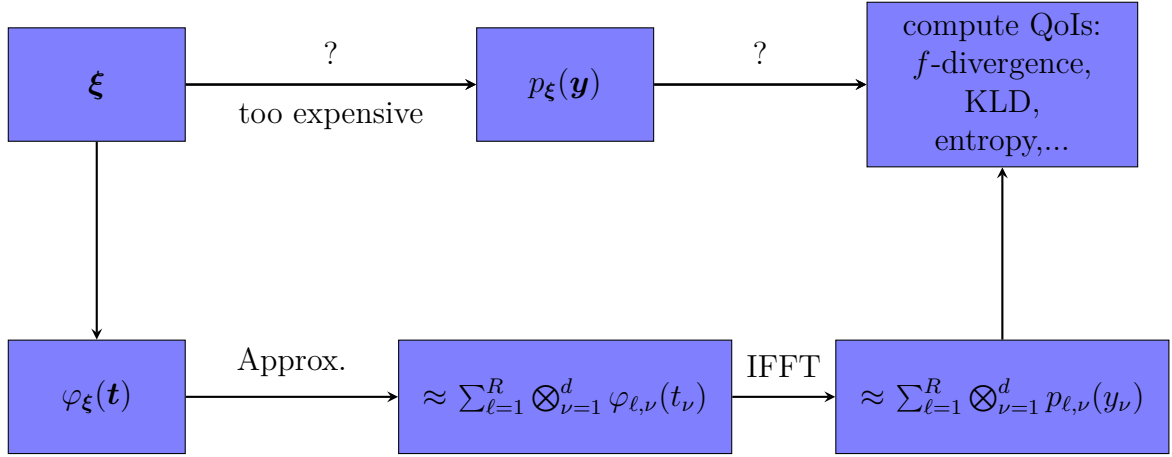


Diagram 1: Our goal is to compute such QoIs as the f -divergence, the KLD, the differential entropy and others for high-dimensional RVs. One can do it either from the RV ξ or its pcf or pdf . If the pdf is not available, one may start with its pcf , and compute a low-rank approximation of the pcf , then apply the IFFT to obtain a low-rank approximation of the pdf , and then compute the desired QoI. As a by-product obtains a low-rank approximation of the pdf .

1.4 Literature review

The well known connections between the above mentioned concepts, to be briefly reviewed in Section 2, can be translated into a discrete setting, where the RV resp. the other characterising functions like density, characteristic function, etc., appear in a discretised version, where they may be seen as an element of a tensor space. This opens the possibility to manipulate and use them with the tools of low-rank tensor approximations, and to use these to compute the desired QoI.

In this work we would like to explore the usefulness and applicability of these techniques in probability. In probability theory, given a d -dimensional random variable, it is well known that its characterisation is provided by the probability characteristic function [87] (Feller and Lévi theorems). Therefore, our contribution will focus on approximation techniques for representing characteristic functions in low-rank tensor format. Previous approaches to approximate characteristic functions were not able to handle high-dimensional random variables, e.g. [87, 111, 121]. Our approach can overcome these difficulties.

The transformations of characterising objects and the computation of QoIs will be achieved by computing a function of the representing tensor. The proposed algorithms are iterative in nature, and the convergence tolerance can be adapted to the reconstruction error. The basic idea for the algorithms, which operate only on the algebraic structure, is an iterative scheme which converges to a result which solves the desired problem in some way. Such iterations typically destroy the compressed representation, so they have to be combined with re-compression or truncation. Other numerical methods which rely on the use of the pcf may also benefit from the proposed approach; e.g. the idea to use Markov Chain Monte Carlo methods in the Fourier domain to sample from a density proportional to the absolute value of the underlying characteristic function is presented in [10].

In a very recent paper [104], the authors estimate tensor train (TT) ranks for approximated multivariate Gaussian pdfs . In [29], the authors use the TT-format to approximate multivariate probability distributions. There they analyse properties of the obtained

low-rank approximation and use it as a prior distribution in the Markov Chain Monte Carlo approach. In [121, 122], the author develops numerical inversion of characteristic functions.

Low-rank tensor techniques proved to be very successful in such areas as numerical mathematics [39, 33, 81, 75, 55, 12], computational chemistry [70], statistics [84] and others [54]. Many known types of Green’s functions were approximated in the low-rank tensor format [75, 72, 73], which resulted in drastically reducing the computational cost and storage. In these papers, the authors research the separability of multi-dimensional kernels and covariance functions, develop numerical algorithms for computing low-rank representations, and estimate the approximation accuracy as well as the computational costs.

General tensor formats and their low-rank approximations, in quantum physics also known as *tensor networks*, are described in [119, 106, 41, 94, 18, 14]. For the mathematical and numerical point of view we refer to the review [78], the monographs [59, 70, 75], and to the literature survey on low-rank approximations [54].

1.5 Outline of the paper

After introduction and motivation, we review some theory in Section 2. We operate with two types of objects: **pdfs** and **pcfs**, which are defined in appropriate spaces. To compute various functions of these objects we need to define algebras on **pdfs** and on **pcfs**: the convolution algebra and the point-wise multiplication algebra, respectively. After discretisation of the **pdf** and the **pcf** we obtain tensors, and the point-wise multiplication algebra becomes the Hadamard algebra, whereas the continuous convolution algebra becomes the discrete convolution algebra.

The discrete versions of the **pdf** and the **pcf** are represented by “sparse” approximations, in our case we propose to use low-rank tensor approximations. As the different QoIs require one to compute point-wise functions of the **pdf** (e.g. like the logarithm in Eq. (4)), but as these point-wise values are not directly accessible due to the “sparse” approximation, another way has to be found to compute a point-wise function like the logarithm without going away from “sparse” approximations. To this end the discretised **pdf** and **pcf** are viewed as tensors equipped with a discrete version of the point-wise product, the so-called Hadamard product. With this product they become (commutative) C^* -algebras, so it is possible to define algebraically the desired functions on these tensors, and on their “sparse” approximation.

We use matrix algebra algorithms [64] to define the functions $\exp(\cdot)$, $\log(\cdot)$, $\sqrt{(\cdot)}$ and $\text{sign}(\cdot)$. These algorithms are classically formulated for an algebra of linear mappings (matrices), which includes definitions of the inverse, adjoint, sum and product. But as many algorithms are formulated purely abstractly in algebraic terms, they can be used for any other algebra, and hence also in this case. Since some algorithms are developed only for self-adjoint or positive definite matrices, we need to define these notions also in the algebra we are using. In this way we also define the convolution algebra on discretised **pdfs**, which is needed, for example, when adding two RVs.

Assuming that the **pdf** has been represented in such an algebraic setting, in Section 3 we explain how to compute statistical moments and divergences in this discretised framework, using only the abstract discrete operations, independent of any particular representation. In Section 4 we show as an example how the algebraic operations may be actually implemented on a low-rank tensor format, namely first on the simpler canonical polyadic (CP) tensor decomposition, where we recall all required definitions and properties. This

tensor format is the easiest one to explain our ideas. In our example computations later in Section 6 we actually use the tensor-train (TT) format, but here the explanation is more complicated. The actual algorithms—developed for matrices—which can be used to compute various functions of **pdfs** are either iterations or truncated series expansions, and are listed in Section 5. Again, we use only the abstract discrete operations, and the algorithms are independent of any particular representation. In Section 6 we give some numerical examples, and Section 7 concludes.

2 Theoretical background

The two entities we will be working with are the probability density function (**pdf**) and the corresponding probability characteristic function (**pcf**). These are connected by the Fourier transform. The ultimate goal is to use discretised versions of these two descriptors of a random variable to compute for example the **pdf** of a mixture model or the **pdf** of the sum of two independent RVs, or quantities of interest (QoIs) like moments or other statistics like the relative entropy of a RV, or — for two **pdf**(s) — their Kullback-Leibler- or more general f -divergences. Additionally to introducing the notation, this section serves to collect the basic properties which the different descriptors of a RV have to satisfy, as it will be important to preserve these properties in the discretisation to be discussed in Subsection 2.3.

We briefly recall in Subsection 2.1 the connections between a high-dimensional random variable, its distribution (**cdf**) and probability density function (**pdf**), the (probability) characteristic function (**pcf**), and the second characteristic or cumulant generating function [107, 87, 121], as well as their fundamental properties and operations with them. The discretised versions of these properties and operations will later be used in the numerical computations.

In the following Subsection 2.2, the geometric and algebraic properties of probability density functions (**pdf**) and probability characteristic functions (**pcf**) will be recalled, as they will be the basis for the discretised treatment of the compressed low-rank tensor format. In order to be able to evaluate the point-wise functions of the **pdf** which are necessary to compute the various divergences and other characteristics mentioned above, it is necessary to view the **pdf** as well as the **pcf** as elements of function algebras, which has to be conserved by the discretisation and low-rank representation. This section therefore serves as a reminder of which functions one has to compute on the discrete representations of the RV, the **cdf**, **pdf**, and the **pcf**. Subsequently, we outline in Subsection 2.3 the theoretical background for low-rank representations and possibilities for a discretisation which can take advantage of this.

2.1 Notation and summary of basic descriptors

The purpose of this summary is on one hand to recall the basic characterisations of RVs, and on the other to prepare for the numerical treatment of these entities in a compressed format by collecting the necessary functions one needs for converting between them. For the numerical representations it is important to observe that the constraining conditions are also preserved in the discretised case, therefore they are especially emphasised.

Assume that one is dealing with a random vector $\boldsymbol{\xi}$ which lives in a high-dimensional vector space \mathcal{V} . As we are mainly interested in numerical computations, we shall directly identify the vector space \mathcal{V} through choice of a basis with an appropriate $\mathbb{R}^d = \mathcal{V}$, where

the dimension $d = \dim \mathcal{V}$ is assumed to be a large number. Let us remark that we employ the canonical Euclidean inner product $\langle \mathbf{x} | \mathbf{y} \rangle_{\mathcal{V}} := \sum_{k=1}^d x_k y_k$ on $\mathcal{V} = \mathbb{R}^d$, which is used to identify the space $\mathcal{V} = \mathbb{R}^d$ with its dual. We also assume the usual order structure on $\mathbb{R}^d = \mathcal{V}$, so that $\mathbf{x} \leq \mathbf{y}$ iff $x_k \leq y_k$ for $k = 1, \dots, d$, resp. $\mathbf{y} - \mathbf{x} \in \mathbb{R}_+^d = \mathcal{V}_+$, with positive cone $\mathbb{R}_+^d = \mathcal{V}_+ = \{\mathbf{x} \in \mathbb{R}^d \mid x_1 \geq 0, \dots, x_d \geq 0\}$.

A finite dimensional random vector — a vector of scalar random variables (RVs) — is formally $\boldsymbol{\xi} = [\xi_1, \dots, \xi_d]^\top : \Omega \rightarrow \mathcal{V} = \mathbb{R}^d$ a measurable mapping w.r.t. the Borel- σ -algebra $\mathfrak{B}(\mathbb{R}^d)$ on \mathbb{R}^d , defined on a probability space $(\Omega, \mathfrak{A}, \mathbb{P})$, where Ω is the set of elementary events, \mathfrak{A} the σ -algebra, and \mathbb{P} the probability measure. The associated expectation operator is denoted by $\mathbb{E}(\cdot)$, the mean as $\bar{\boldsymbol{\xi}} := \mathbb{E}(\boldsymbol{\xi}) \in \mathbb{R}^d$, and the mean zero random part as $\tilde{\boldsymbol{\xi}} := \boldsymbol{\xi} - \bar{\boldsymbol{\xi}}$.

2.1.1 Basic descriptors

Basic descriptors of a RV are its moments. The *moments* \mathbf{X}_k and *central moments* Ξ_k of $\boldsymbol{\xi}$ of order $k \in \mathbb{N}_0$ — assuming they exist — are denoted as

$$\mathbf{X}_k = \mathbb{E}(\boldsymbol{\xi}^{\otimes k}) \in (\mathbb{R}^d)^{\otimes k}, \quad \Xi_k = \mathbb{E}(\tilde{\boldsymbol{\xi}}^{\otimes k}) \in (\mathbb{R}^d)^{\otimes k}. \quad (13)$$

where for $\mathbf{x} \in \mathbb{R}^d$ one sets $\mathbf{x}^{\otimes k} = \bigotimes_{j=1}^k \mathbf{x}$. The second central moment — the *covariance* matrix — is also denoted as $\boldsymbol{\Sigma}_{\boldsymbol{\xi}} = \text{cov} \boldsymbol{\xi} = \Xi_2 = \mathbf{X}_2 - \bar{\boldsymbol{\xi}} \otimes \bar{\boldsymbol{\xi}} \in \mathcal{V} \otimes \mathcal{V} = (\mathbb{R}^d)^{\otimes 2} \cong \mathcal{L}(\mathcal{V})$.

If $\boldsymbol{\eta}$ is another random vector with values in $\mathcal{U} = \mathbb{R}^n$, the *mixed* and *mixed central* moments are denoted by

$$\mathbf{Y}_{k,\ell} = \mathbb{E}(\boldsymbol{\xi}^{\otimes k} \otimes \boldsymbol{\eta}^{\otimes \ell}) \quad \text{and} \quad \boldsymbol{\tau}_{k,\ell} = \mathbb{E}(\tilde{\boldsymbol{\xi}}^{\otimes k} \otimes \tilde{\boldsymbol{\eta}}^{\otimes \ell}) \in (\mathbb{R}^d)^{\otimes k} \otimes (\mathbb{R}^n)^{\otimes \ell}. \quad (14)$$

The *covariance* is also denoted as $\text{cov}(\boldsymbol{\xi}, \boldsymbol{\eta}) = \boldsymbol{\tau}_{1,1} = \mathbf{Y}_{1,1} - \bar{\boldsymbol{\xi}} \otimes \bar{\boldsymbol{\eta}} \in \mathcal{V} \otimes \mathcal{U} = \mathbb{R}^d \otimes \mathbb{R}^n \cong \mathcal{L}(\mathcal{U}, \mathcal{V}) = \mathcal{L}(\mathbb{R}^n, \mathbb{R}^d)$.

2.1.2 Distribution measure and probability density

The *distribution measure* $P_{\boldsymbol{\xi}}$ of $\boldsymbol{\xi}$ for a subset $\mathcal{E} \subseteq \mathbb{R}^d$ in the Borel algebra is as usual the *push-forward* $\boldsymbol{\xi}_* \mathbb{P}$ of the original measure \mathbb{P} :

$$P_{\boldsymbol{\xi}}(\mathcal{E}) := \boldsymbol{\xi}_* \mathbb{P}(\mathcal{E}) := \mathbb{P}(\boldsymbol{\xi}^{-1}(\mathcal{E})) = \mathbb{E}(\mathbb{1}_{\mathcal{E}}(\boldsymbol{\xi})), \quad (15)$$

where the *characteristic indicator function* $\mathbb{1}_{\mathcal{E}}(\mathbf{y})$ at $\mathbf{y} \in \mathbb{R}^d$ of such a Borel set $\mathcal{E} \in \mathfrak{B}(\mathbb{R}^d)$ is unity if $\mathbf{y} \in \mathcal{E}$ and vanishes otherwise.

In light of Lebesgue's decomposition theorem [87] for the distribution measure $P_{\boldsymbol{\xi}}(\mathcal{E})$ w.r.t. Lebesgue measure Λ on $\mathfrak{B}(\mathbb{R}^d)$, we will consider here only RVs with absolutely continuous distribution measure, i.e. we assume $P_{\boldsymbol{\xi}}(\mathcal{E}) \leq C\Lambda(\mathcal{E})$ for all $\mathcal{E} \in \mathfrak{B}(\mathbb{R}^d)$ with some constant $C > 0$.

This constraint results in an absolutely continuous *cumulative distribution function* (cdf) of $\boldsymbol{\xi}$ — defined for $\mathbf{y} \in \mathbb{R}^d = \mathcal{V}$ via semi-infinite intervals $\mathcal{E}_{\mathbf{y}} = \times_{k=1}^d]-\infty, y_k] \in \mathfrak{B}(\mathbb{R}^d)$ as

$$F_{\boldsymbol{\xi}}(\mathbf{y}) := P_{\boldsymbol{\xi}}(\mathcal{E}_{\mathbf{y}}) = \mathbb{P}(\boldsymbol{\xi} \leq \mathbf{y}) = \mathbb{E}(\mathbb{1}_{\mathcal{E}_{\mathbf{y}}}(\boldsymbol{\xi})). \quad (16)$$

The well known properties of $F_{\boldsymbol{\xi}}$ such as positivity $F_{\boldsymbol{\xi}}(\mathbf{y}) \geq 0$, and the monotonicity $F_{\boldsymbol{\xi}}(\mathbf{y}_1) \leq F_{\boldsymbol{\xi}}(\mathbf{y}_2)$ for $\mathbf{y}_1 \leq \mathbf{y}_2$, as well as $F_{\boldsymbol{\xi}}(\mathbf{y}) \rightarrow 0$ as $\mathbf{y} \rightarrow -\infty$ and $F_{\boldsymbol{\xi}}(\mathbf{y}) \rightarrow 1$ as $\mathbf{y} \rightarrow +\infty$, should be replicated in any discretised setting. As $P_{\boldsymbol{\xi}}(\mathcal{E})$ is absolutely continuous, it

has a Radon-Nikodým derivative $p_{\boldsymbol{\xi}}(\mathbf{y}) = dP_{\boldsymbol{\xi}}/d\mathbf{y} \in L_1(\mathbb{R}^d, \mathbb{R})$ w.r.t. Lebesgue measure, the *probability density function* (pdf) of $\boldsymbol{\xi}$, which is also the weak derivative of $F_{\boldsymbol{\xi}}(\mathbf{y})$:

$$p_{\boldsymbol{\xi}}(\mathbf{y}) = \frac{d}{d\mathbf{y}} P_{\boldsymbol{\xi}}(\mathbf{y}) = \frac{\partial^d}{\partial y_1 \dots \partial y_d} F_{\boldsymbol{\xi}}(\mathbf{y}); \text{ with } p_{\boldsymbol{\xi}} \geq 0, \text{ and } \int_{\mathbb{R}^d} p_{\boldsymbol{\xi}}(\mathbf{x}) d\mathbf{x} = 1. \quad (17)$$

These are quasi defining relations for a pdf, they are directly implied by the properties of the cdf $F_{\boldsymbol{\xi}}$, and are important to be preserved under discretisation and compressed low-rank approximation. The positivity requirement in Eq. (17) means that geometrically speaking densities are in the positive convex cone of $L_1(\mathbb{R}^d, \mathbb{R})$, and the integral relation means that they lie on a particular hyperplane. The intersection of these two closed convex sets is where the probability densities live, denoted by

$$\mathfrak{D} := \{p \mid p \geq 0\} \cap \{p \mid \int_{\mathbb{R}^d} p(\mathbf{x}) d\mathbf{x} = 1\} \subset L_1(\mathbb{R}^d, \mathbb{R}), \quad (18)$$

is again closed and convex. In addition one notes that due to the positivity the constraint of unit integral also implies that $\|p_{\boldsymbol{\xi}}\|_1 = \int_{\mathbb{R}^d} |p_{\boldsymbol{\xi}}(\mathbf{x})| d\mathbf{x} = 1$, i.e. $p_{\boldsymbol{\xi}}$ is on the unit sphere. That \mathfrak{D} in Eq. (18) is convex means also that convex combinations of densities $p_{\boldsymbol{\xi}_1}, \dots, p_{\boldsymbol{\xi}_m} \in \mathfrak{D}$, namely $p_{\boldsymbol{\xi}_M}(\mathbf{x}) = \sum_{\ell=1}^m \beta_{\ell} p_{\boldsymbol{\xi}_{\ell}}(\mathbf{x})$ — with $\beta_{\ell} \geq 0, \sum_{\ell} \beta_{\ell} = 1$ — are again densities; these correspond to *mixture models* for a RV $\boldsymbol{\xi}_M$.

Direct *quantities of interest* (QoIs) are usually expected values of functions of $\boldsymbol{\xi}$, i.e. quantities like $g = \mathbb{E}(g(\boldsymbol{\xi})) \in \mathbb{R}^m = \mathcal{Y}$ with a measurable $g : \mathbb{R}^d = \mathcal{V} \rightarrow \mathbb{R}^m = \mathcal{Y}$. Obviously the moments and central moments Eq. (13) are special cases of this, as is the characteristic function Eq. (22). These quantities may alternatively be computed by integrating over the pdf $p_{\boldsymbol{\xi}}$ and \mathbb{R}^d :

$$\begin{aligned} g = \mathbb{E}(g(\boldsymbol{\xi})) &= \int_{\mathbb{R}^d} g(\mathbf{x}) P_{\boldsymbol{\xi}}(d\mathbf{x}) = \int_{\mathbb{R}^d} g(\mathbf{x}) dF_{\boldsymbol{\xi}}(\mathbf{x}) \\ &= \int_{\mathbb{R}^d} g(\mathbf{x}) p_{\boldsymbol{\xi}}(\mathbf{x}) d\mathbf{x} =: \mathbb{E}_{p_{\boldsymbol{\xi}}}(g) \in \mathcal{Y}, \end{aligned} \quad (19)$$

where the second integral is to be understood as a Lebesgue-Stieltjes integral. Taking as QoI $g_k : \mathbf{x} \mapsto \mathbf{x}^{\otimes k}$ (cf. Eq. (13)), one has $\bar{\boldsymbol{\xi}} = \mathbf{X}_1 = \int \mathbf{x} p_{\boldsymbol{\xi}}(\mathbf{x}) d\mathbf{x}$ for the mean, and for the higher moments

$$\mathbf{X}_k = \int_{\mathbb{R}^d} g_k(\mathbf{x}) p_{\boldsymbol{\xi}}(\mathbf{x}) d\mathbf{x} = \mathbb{E}_{p_{\boldsymbol{\xi}}}(\mathbf{x}^{\otimes k}), \quad \Xi_k = \mathbb{E}_{p_{\boldsymbol{\xi}}}((\mathbf{x} - \bar{\boldsymbol{\xi}})^{\otimes k}), \quad (20)$$

and especially $\boldsymbol{\Sigma}_{\boldsymbol{\xi}} = \Xi_2 = \mathbb{E}_{p_{\boldsymbol{\xi}}}((\mathbf{x} - \bar{\boldsymbol{\xi}})^{\otimes 2})$ for the covariance.

As is well known [110], the Banach space $L_1(\mathbb{R}^d, \mathbb{R})$ is a commutative Banach algebra when the space is equipped with the convolution product, i.e. for $p, q \in L_1(\mathbb{R}^d, \mathbb{R})$

$$(p * q)(\mathbf{y}) := \int_{\mathbb{R}^d} p(\mathbf{y} - \mathbf{x}) q(\mathbf{x}) d\mathbf{x}. \quad (21)$$

Observe that if p and q are density functions, so is $p * q$. This reflects the well known fact that if $p_{\boldsymbol{\xi}}$ is the density of the RV $\boldsymbol{\xi}$, and $p_{\boldsymbol{\eta}}$ is the density of the independent RV $\boldsymbol{\eta}$, then $p_{\boldsymbol{\xi}} * p_{\boldsymbol{\eta}}$ is the density of the RV $\boldsymbol{\xi} + \boldsymbol{\eta}$. It also means that the closed convex set \mathfrak{D} is stable under convolution of its members.

The last topic to touch on to collect the requirements for the discretised low-rank representation of the pdf is to look at what is required for the computation of e.g. the *differential entropy* of a RV. Recall that the differential entropy of a pdf $p_{\boldsymbol{\xi}}$ is defined

as $h(p_\xi) := \mathbb{E}_{p_\xi}(-\log(p_\xi)) = -\int_{\mathbb{R}^d} \log(p_\xi(\mathbf{x}))p_\xi(\mathbf{x}) \, d\mathbf{x}$. Hence, in order to compute the differential entropy $h(p_\xi)$, one has to be able to compute *point-wise* functions of the **pdf**; in this case the logarithm. This and other point-wise function needed for the various divergences, like the square root, pose quite a challenge for a compressed low-rank representation, and will be addressed later in Section 5.

To summarise, for the discrete compressed low-rank representation of a **pdf**, the vector space structure is needed to compute convex combinations and the convolution algebra structure is needed to compute convolutions, as well as the ability to compute point-wise functions like the log, the square root, etc. Additionally, positivity has to be checked, as well as the condition that the **pdf** integrates to unity. The last requirement, the ability to compute the Fourier transform, will be explained in the following.

2.1.3 Probability characteristic function

The *characteristic function* or probability characteristic function (**pcf**) of the RV ξ is defined via Eq. (19) as a QoI with $g_t(\mathbf{x}) = \exp(i \langle \mathbf{t} | \mathbf{x} \rangle)$, i.e. the probabilist's Fourier transform — in other fields this is considered as the non-unitary version of the *inverse* Fourier transform [16] — of the **pdf**:

$$\begin{aligned} \varphi_\xi(\mathbf{t}) &:= \mathbb{E}(g_t(\xi)) = \mathbb{E}(\exp(i \langle \mathbf{t} | \xi \rangle)) = \int_{\mathbb{R}^d} \exp(i \langle \mathbf{t} | \mathbf{x} \rangle) P_\xi(d\mathbf{x}) \\ &= \int_{\mathbb{R}^d} \exp(i \langle \mathbf{t} | \mathbf{x} \rangle) p_\xi(\mathbf{x}) \, d\mathbf{x} = \mathbb{E}_{p_\xi}(\exp(i \langle \mathbf{t} | \cdot \rangle)) =: \mathcal{F}_d(p_\xi)(\mathbf{t}). \end{aligned} \quad (22)$$

Well known [87, 121] facts about characteristic functions $\varphi_\xi : \mathbb{R}^d \rightarrow \mathbb{C}$ are that they are bounded and uniformly continuous — $\varphi_\xi \in C_{bu}(\mathbb{R}^d, \mathbb{C})$ — and satisfy $|\varphi_\xi(\mathbf{t})| \leq \varphi_\xi(0) = 1$ for all $\mathbf{t} \in \mathbb{R}^d$, i.e. $\|\varphi_\xi\|_\infty = 1$. These conditions tell us that all probability characteristic functions lie on a hyperplane in the vector space $C_{bu}(\mathbb{R}^d, \mathbb{C})$, obviously reflecting the hyperplane condition — unit integral — for the **pdf**.

The **pcf** is a complex-valued function, but as it is the Fourier transform of the real and positive **pdf**, it has to satisfy some further constraints. To be able to properly formulate this, one defines an anti-linear involution or \star -operation “ \star ” as $\varphi_\xi^*(\mathbf{t}) := \bar{\varphi}_\xi(-\mathbf{t})$, where the overbar denotes the complex conjugate. Now, as the **pdf** p_ξ in Eq. (22) is a real function, this implies [16, 87] that φ_ξ is Hermitean, i.e. invariant w.r.t. the conjugation induced by the \star -involution; so it satisfies $\varphi_\xi^*(\mathbf{t}) = \bar{\varphi}_\xi(-\mathbf{t}) = \varphi_\xi(\mathbf{t})$. This real subspace of Hermitean functions will be denoted by $\mathcal{H} \subset C_{bu}(\mathbb{R}^d, \mathbb{C})$.

As is well known [110], the Banach space $C_b(\mathbb{R}^d, \mathbb{C})$ together with point-wise multiplication and the \star -operation is a commutative C^* -algebra. As is easily seen, the real subspace \mathcal{H} of Hermitean functions is a *real* sub-algebra. As p_ξ is non-negative [87], the characteristic function φ_ξ has to be a positive definite function: for any $n \in \mathbb{N}$ and distinct points $\{\mathbf{t}_k \in \mathbb{R}^d\}_{k=1}^n$, the matrix $\Phi_\xi = (\varphi_\xi(\mathbf{t}_i - \mathbf{t}_j))_{i,j} \in \mathbb{C}^{n \times n}$ is Hermitean positive semi-definite in \mathbb{C}^n . The positive definite functions form a convex cone in \mathcal{H} .

This last condition reflects the positivity of the **pdf**. These conditions will not be so easy to directly ascertain on a discretised and compressed low-rank representation of φ_ξ , and are simpler checked on the **pdf** p_ξ . As the positive semi-definite functions form a real convex cone in \mathcal{H} , this means that the **pcf** is in the intersection of this cone and the hyperplane with unit value at the origin in \mathcal{H} , again a closed and convex set, denoted by

$$\mathcal{C} = \mathcal{H} \cap \{\varphi \mid \varphi(0) = 1\} \cap \{\varphi \mid \varphi \text{ is positive semi-definite} \} \subset C_{bu}(\mathbb{R}^d, \mathbb{C}). \quad (23)$$

Thus real convex combinations of probability characteristic functions are again probability characteristic functions, namely of mixture models, reflecting the analogous result for probability density functions in \mathfrak{D} in Eq. (18).

It is also easily seen that the point-wise product of two probability characteristic functions is again a **pcf**, and hence the set \mathfrak{C} in Eq. (23) is stable under point-wise products. This reflects the fact that the point-wise product $\varphi_{\xi} \cdot \varphi_{\eta}$ of two independent RVs ξ and η is just the **pcf** of their sum. This is the analogue to the previous statement about the convolution of two probability density functions. It is now obvious that $\mathcal{F}_d(\mathfrak{D}) \subseteq \mathfrak{C}$, and — as will be stated explicitly later — the Fourier transform is a real algebra homomorphism between the real convolution algebra $L_1(\mathbb{R}^d, \mathbb{R})$ and the real multiplication sub-algebra $\mathcal{H} \subset C_{bu}(\mathbb{R}^d, \mathbb{C})$ of Hermitean functions.

Naturally, the **pdf** p_{ξ} is given by the inverse relation of Eq. (22) [87, 16], which is the probabilist's inverse Fourier transform

$$p_{\xi}(\mathbf{y}) = \frac{1}{(2\pi)^d} \int_{\mathbb{R}^d} \exp(-i \langle \mathbf{t} | \mathbf{y} \rangle) \varphi_{\xi}(\mathbf{t}) d\mathbf{t} = \mathcal{F}_d^{-1}(\varphi_{\xi})(\mathbf{y}). \quad (24)$$

To summarise, for the discrete compressed low-rank representation of a **pcf**, the real vector space structure is needed to compute convex combinations, and the multiplication algebra structure is needed to compute products. Additionally, positive definiteness of approximations has to be checked, as well as the condition that the **pcf** is unity at the origin. This will be addressed later. The last requirement to be mentioned is the ability to compute the inverse Fourier transform.

2.2 Relations through the Fourier transform

This section collects a few algebraic and geometric properties, both from characteristic functions and densities, and connects these with the Fourier transform. In the following, the probabilist's Fourier transform \mathcal{F}_d in Eq. (22) will simply be referred to as *the Fourier transform (FT)*.

2.2.1 Geometric and algebraic structures

The Fourier transform is known [16, 87] to connect the algebraic convolution structure on probability densities described previously with the corresponding multiplication structure on characteristic functions. Let $p, q \in L_1(\mathbb{R}^d, \mathbb{R})$ be integrable real-valued functions in the convolution Banach-algebra, and denote their Fourier transforms (FT in Eq. (22)) by $\phi = \mathcal{F}_d(p), \psi = \mathcal{F}_d(q) \in \mathcal{H}$ (as p, q are real, their FT is Hermitean), then the Fourier transform and its inverse Eq. (24) has the following well known [16, 87] property:

$$\mathcal{F}_d(p * q) = \mathcal{F}_d(p) \cdot \mathcal{F}_d(q) = \phi \cdot \psi \quad \Leftrightarrow \quad p * q = \mathcal{F}_d^{-1}(\phi \cdot \psi). \quad (25)$$

Here it is important to see that the Fourier transform (FT) is a real algebra homomorphism between the real convolution Banach-algebra $L_1(\mathbb{R}^d, \mathbb{R})$ and the real multiplication algebra \mathcal{H} of Hermitean functions. In light of later developments, let us mention in passing [110] that any algebra can be represented by linear operators, and especially that any commutative or Abelian Banach-C*-algebra can be represented by a sub-algebra of simultaneously diagonalisable operators, and that it is isomorphic to the multiplication algebra of continuous functions on a locally compact set — the so-called Gel'fand representation. This so-called uniform multiplication algebra — a sub-algebra of the full

maximal Abelian W^* -multiplication algebra of L_∞ functions — can be seen as the simultaneous spectral resolution or diagonalisation of the linear representation operators. In this view the (unitary version of the) FT diagonalises the convolution algebra, and confirms that the Fourier functions may be viewed as the generalised eigenfunctions of any convolution operator.

In our context, further well known [16, 110] properties of the FT, which will be needed later, are

$$\mathcal{F}_d(L_1(\mathbb{R}^d, \mathbb{R})) \subseteq \mathcal{H} \quad (26)$$

$$\mathcal{F}_d(\{p \in L_1(\mathbb{R}^d, \mathbb{R}) \mid p(\mathbf{x}) \geq 0 \text{ a.e. in } \mathbb{R}^d\}) \subseteq \{\phi \in \mathcal{H} \mid \phi \text{ is positive definite}\} \quad (27)$$

$$\mathcal{F}_d(\{p \in L_1(\mathbb{R}^d, \mathbb{R}) \mid \int_{\mathbb{R}^d} p(\mathbf{x}) \, d\mathbf{x} = 1\}) \subseteq \{\phi \in \mathcal{H} \mid \phi(0) = 1\}. \quad (28)$$

While all these relations were already mentioned, here they can be summarised as follows: Eq. (26) is the correspondence between real-valued functions and Hermitean Fourier transforms \mathcal{H} , and Eq. (27) says that the positive convex cone in $L_1(\mathbb{R}^d, \mathbb{R})$ corresponds to the convex cone of positive-definite functions in \mathcal{H} , whereas the last relation Eq. (28) is the correspondence between the hyperplane with unit integral in $L_1(\mathbb{R}^d, \mathbb{R})$ with the hyperplane with unit value at the origin in \mathcal{H} . These relations will be used in the discretised low-rank setting in the following Subsection 2.3 to ascertain the correctness of the approximations. This means that as the pdf satisfies $p_\xi \in \mathfrak{D}$ in Eq. (18), so the discretised version will have to satisfy a similar discrete constraint, and dually, as the pcf satisfies $\varphi_\xi \in \mathfrak{C}$ in Eq. (23), the discretised version of this quantity will have to satisfy a similar discrete constraint.

2.2.2 Characterising functions and transforms

Another well known property [16, 110] of the Fourier transform that will be needed in the future is how it connects derivatives and multiplication by the co-ordinates. We assume that all derivatives appearing in the sequel exist and are well defined. In fact, from Eq. (22) one gleans that

$$(-i \partial_{t_k}) \varphi_\xi(\mathbf{t}) = \int_{\mathbb{R}^d} x_k \exp(i \langle \mathbf{t} \mid \mathbf{x} \rangle) p_\xi(\mathbf{x}) \, d\mathbf{x} = \mathcal{F}_d(x_k p_\xi(\mathbf{x}))(\mathbf{t}). \quad (29)$$

This relation shows the well known general way of evaluating derivatives via the Fourier transform: for any well-behaved function $f : \mathbb{R}^d \rightarrow \mathbb{C}$, one has

$$(-i \partial_{t_k}) f(\mathbf{t}) = \mathcal{F}_d(x_k \mathcal{F}_d^{-1}(f)(\mathbf{x}))(\mathbf{t}). \quad (30)$$

Coming back to Eq. (29) one has in particular $(-i) \nabla \varphi_\xi(\mathbf{0}) = (-i) D \varphi_\xi(\mathbf{0}) = \bar{\xi}$ for the gradient or first derivative. If one denotes the order k tensor of k -th derivatives of φ_ξ by

$$D^k \varphi_\xi(\mathbf{t}) = \left(\frac{\partial^k}{\partial_{t_{i_1}} \dots \partial_{t_{i_k}}} \varphi_\xi(\mathbf{t}) \right), \quad 1 \leq i_1, \dots, i_k \leq d,$$

one obtains the well-known relation

$$(-i)^k D^k \varphi_\xi(\mathbf{0}) = \int_{\mathbb{R}^d} \mathbf{x}^{\otimes k} p_\xi(\mathbf{x}) \, d\mathbf{x} = \mathcal{F}_d(\mathbf{x}^{\otimes k} p_\xi(\mathbf{x}))(\mathbf{0}) = \mathbf{X}_k, \quad k \in \mathbb{N}_0. \quad (31)$$

Similar relations as Eq. (31) can be obtained by other characterising functions. The *second characteristic* function [87] — confusingly sometimes also labeled as cumulant

generating function (cf. Eq. (35)) — whose derivative tensors of order k are essentially the *cumulants* \mathbf{K}_k of $\boldsymbol{\xi}$, is defined as the point-wise logarithm of the *pcf* :

$$\chi_{\boldsymbol{\xi}}(\mathbf{t}) := \log(\varphi_{\boldsymbol{\xi}}(\mathbf{t})) = \log(\mathbb{E}(\exp(i \langle \mathbf{t} | \boldsymbol{\xi} \rangle))) , \quad \text{with } (-i)^k D^k \chi_{\boldsymbol{\xi}}(\mathbf{0}) =: \mathbf{K}_k, \quad k \in \mathbb{N}_0. \quad (32)$$

The relations Eq. (31) and Eq. (32) involve the slightly annoying imaginary unit. To stay with completely real functions one may switch from the Fourier transform in Eq. (22) or Eq. (32) to the Laplace transform, at the price of working with functions which may not be defined for all $\mathbf{t} \in \mathbb{R}^d$, but maybe only in a small neighbourhood around $\mathbf{0} \in \mathbb{R}^d$. The *moment generating* function is defined as [87] essentially the reflected *Laplace transform* of the density, or as evaluation of the characteristic function Eq. (22) for purely imaginary arguments:

$$M_{\boldsymbol{\xi}}(\mathbf{t}) := \mathbb{E}(\exp(\langle \mathbf{t} | \boldsymbol{\xi} \rangle)) = \int_{\mathbb{R}^d} \exp(\langle \mathbf{t} | \mathbf{x} \rangle) p_{\boldsymbol{\xi}}(\mathbf{x}) \, d\mathbf{x} = \mathcal{L}_d(p_{\boldsymbol{\xi}})(-\mathbf{t}) = \varphi_{\boldsymbol{\xi}}(-i \mathbf{t}), \quad (33)$$

where $\mathcal{L}_d(p_{\boldsymbol{\xi}})(\mathbf{t}) = \int \exp(\langle -\mathbf{t} | \mathbf{x} \rangle) p_{\boldsymbol{\xi}}(\mathbf{x}) \, d\mathbf{x}$ is the two-sided d -dimensional *Laplace* transform of $p_{\boldsymbol{\xi}}$. As in Eq. (31), one obtains

$$D^k M_{\boldsymbol{\xi}}(\mathbf{0}) = \int_{\mathbb{R}^d} \mathbf{x}^{\otimes k} p_{\boldsymbol{\xi}}(\mathbf{x}) \, d\mathbf{x} = \mathbf{X}_k, \quad k \in \mathbb{N}_0. \quad (34)$$

Closely related is the *cumulant generating* function [87], the point-wise logarithm of the moment generating function $M_{\boldsymbol{\xi}}$ in Eq. (33):

$$K_{\boldsymbol{\xi}}(\mathbf{t}) := \log(M_{\boldsymbol{\xi}}(\mathbf{t})) = \log(\mathbb{E}(\exp(\langle \mathbf{t} | \boldsymbol{\xi} \rangle))) , \quad \text{with } D^k K_{\boldsymbol{\xi}}(\mathbf{0}) = \mathbf{K}_k, \quad k \in \mathbb{N}_0. \quad (35)$$

2.3 Grid functions and finite dimensional algebras on tensors

It was already pointed out in Section 1 that we want to discretise both the *pdf* and the *pcf* , by representing them on a discrete and finite grid. We start with the *pdf* . The first thing usually to do is to centre everything around the mean $\bar{\boldsymbol{\xi}}$ of the RV $\boldsymbol{\xi}$, i.e. to shift co-ordinates on \mathbb{R}^d by $\mathbf{x} \mapsto \mathbf{x} - \bar{\boldsymbol{\xi}}$. Another way of saying this is to state that we work with the centred RV $\tilde{\boldsymbol{\xi}}$. We assume from now implicitly that this has been done. The values of the RV $\boldsymbol{\xi}$ will thus be around the origin $\mathbf{0} \in \mathbb{R}^d$.

2.3.1 Grid discretisation of high-dimensional functions

To achieve a fully discrete representation of the *pdf* and the *pcf* , in each dimension $1 \leq \nu \leq d$ of \mathbb{R}^d we pick a grid vector $\hat{\mathbf{x}}_{\nu} := (\hat{x}_{1,\nu}, \dots, \hat{x}_{M_{\nu},\nu})$ of size M_{ν} (cf. section 1.2.1). As already mentioned, we want to use the discrete fast Fourier transform (FFT) algorithm, hence we use an equidistant sampling grid with the origin in the middle. This way $\hat{x}_{i_{\nu},\nu} = \hat{x}_{1,\nu} + (i_{\nu} - 1)\Delta_{x_{\nu}}$, with the increment vector denoted by $\Delta_{\mathbf{x}} = (\Delta_{x_1}, \dots, \Delta_{x_d})$. The whole grid can be represented as $\hat{\mathbf{X}} = \times_{\nu=1}^d \hat{\mathbf{x}}_{\nu}$, and we assume that it covers the support of $p_{\boldsymbol{\xi}}(\mathbf{x})$. Observe, as with the FFT functions are implicitly assumed to be periodic [16], the total d -dimensional volume covered is

$$V = \prod_{\nu=1}^d M_{\nu} \Delta_{x_{\nu}}, \quad (36)$$

and the integration rule is implicitly the iterated trapezoidal rule on a periodic grid, hence each point carries the same integration weight V/N .

As already alluded to in Section 1, the notation $\mathbf{P} := p_\xi(\hat{\mathbf{X}})$ denotes the tensor $\mathbf{P} \in \bigotimes_{\nu=1}^d \mathbb{R}^{M_\nu} =: \mathcal{T}$, a finite dimensional space with $\dim \mathcal{T} = \prod_{\nu=1}^d M_\nu =: N$, the components of which are the evaluation of the pdf p_ξ on the grid $\hat{\mathbf{X}}$

$$\mathbf{P} := p_\xi(\hat{\mathbf{X}}) := (P_{i_1, \dots, i_d}) := (p_\xi(\hat{x}_{i_1,1}, \dots, \hat{x}_{i_d,d})), \quad 1 \leq i_\nu \leq M_\nu, \quad 1 \leq \nu \leq d, \quad (37)$$

similarly for any other scalar function $f(\mathbf{x})$ on \mathbb{R}^d . The grid itself $\hat{\mathbf{X}}$ can be seen as d scalar functions evaluated on the grid, i.e. $\hat{\mathbf{X}} \in \mathcal{T}^d$, one for each co-ordinate of $\mathbf{x} = (x_1, \dots, x_d)$, where each co-ordinate function evaluated is

$$x_\ell(\hat{\mathbf{X}}) = (x_\ell(\hat{x}_{i_1,1}, \dots, \hat{x}_{i_d,d})) = ((x_\ell)_{i_1, \dots, i_d}) := (\hat{x}_{i_\ell, \ell}), \quad 1 \leq i_\nu \leq M_\nu, \quad 1 \leq \nu \leq d, \quad 1 \leq \ell \leq d.$$

As $\hat{\mathbf{X}}$ is characterised by the $(d+1)$ indices (ℓ, i_1, \dots, i_d) , it can be seen as a tensor of order $(d+1)$, an element of $\mathbb{R}^d \otimes \mathcal{T} = \mathcal{V} \otimes \mathcal{T}$, such that $\hat{X}_{\ell, i_1, \dots, i_d} = \hat{x}_{i_\ell, \ell}$. The vector of all co-ordinate function tensors — the evaluation of the vector-valued function $\mathbf{x} \mapsto \mathbf{x}$ (i.e. the identity) — will be denoted by

$$\mathbf{x} := (x_1(\hat{\mathbf{X}}), \dots, x_d(\hat{\mathbf{X}})), \quad \text{with } x_{i_1, \dots, i_d} = \hat{\mathbf{X}}_{:, i_1, \dots, i_d} = (\hat{x}_{i_1,1}, \dots, \hat{x}_{i_d,d}), \quad (38)$$

using the *MATLAB*-like notation with the colon (:), i.e. at index position i_1, \dots, i_d sits the vector $(\hat{x}_{i_1,1}, \dots, \hat{x}_{i_d,d}) \in \mathcal{V} = \mathbb{R}^d$. This notation is extended to tensor products via

$$\mathbf{x}^{\otimes k} := (x_1(\hat{\mathbf{X}}), \dots, x_d(\hat{\mathbf{X}}))^{\otimes k}, \quad \text{i.e. } x_{i_1, \dots, i_d}^{\otimes k} = (\hat{\mathbf{X}}_{:, i_1, \dots, i_d})^{\otimes k} = (\hat{x}_{i_1,1}, \dots, \hat{x}_{i_d,d})^{\otimes k}. \quad (39)$$

Similarly, any other vector valued function $\mathbf{g} : \mathcal{V} \rightarrow \mathbb{R}^m = \mathcal{Y}$, when evaluated on the grid $\hat{\mathbf{X}}$, may be viewed as a tensor $\mathbf{g}(\hat{\mathbf{X}}) \in \mathcal{Y} \otimes \mathcal{T}$, which at index position i_1, \dots, i_d carries the vector $\mathbf{g}(x_{i_1, \dots, i_d}) = \mathbf{g}(\hat{x}_{i_1,1}, \dots, \hat{x}_{i_d,d}) \in \mathcal{Y}$.

To achieve a similar discrete representation of the **pcf** (see section 2.1.3), one may make use of a discrete version of the relation Eq. (22), especially $\varphi_\xi(\mathbf{t}) = \mathcal{F}_d(p_\xi)(\mathbf{t})$. We shall denote the discrete d -dimensional Fourier transform on the grid $\hat{\mathbf{X}}$ again by \mathcal{F}_d for the sake of simplicity, and the dual grid [16] for the transform will be denoted by $\hat{\mathbf{T}} = \times_{\nu=1}^d \hat{\mathbf{t}}_\nu$, where in each dimension the dual grid vector is $\hat{\mathbf{t}}_\nu := (\hat{t}_{1,\nu}, \dots, \hat{t}_{M_\nu,\nu})$. As is well known [16], if in dimension ν one has $L_\nu = M_\nu \Delta_{x_\nu}$ as *period length* for the equidistantly spaced grid with grid spacing Δ_{x_ν} , then $\hat{t}_{M_\nu,\nu} = \pi/\Delta_{x_\nu}$ is the highest (Nyquist) *frequency*, and the equidistant spacing of the dual grid in dimension ν is $2\pi/L_\nu$. It is assumed that the origin $\mathbf{0} \in \mathbb{R}^d$ is in the dual grid, $\mathbf{0} \in \hat{\mathbf{T}}$, and we denote the index of the origin in the grid with $\mathbf{j}^0 = (j_1^0, \dots, j_d^0)$, i.e. $(\hat{t}_{j_1^0,1}, \dots, \hat{t}_{j_d^0,d}) = \mathbf{0} = (0, \dots, 0)$. This point will be important in some of the statistics resp. Qois to be described later in Section 3. As before, the whole grid can be seen as an order $(d+1)$ tensor $\hat{\mathbf{T}} \in \mathbb{R}^d \otimes \mathcal{T} = \mathcal{V} \otimes \mathcal{T}$.

Similarly, the **pcf** will be used through a representing tensor on the dual grid (cf. section 1.2.1), i.e. the tensor $\Phi := \phi_\xi(\hat{\mathbf{T}}) \in \mathcal{T}$ with components

$$\Phi := (\phi_{i_1, \dots, i_d}) := \varphi_\xi(\hat{\mathbf{T}}) := (\varphi_\xi(\hat{t}_{i_1,1}, \dots, \hat{t}_{i_d,d})), \quad 1 \leq i_\nu \leq M_\nu, \quad 1 \leq \nu \leq d. \quad (40)$$

It is on these grid representations $\mathbf{P} := p_\xi(\hat{\mathbf{X}})$ of the **pdf** and $\Phi := \phi_\xi(\hat{\mathbf{T}})$ of the **pcf** that we propose to operate on to compute the desired quantities of interest, e.g. the differential entropy. A more comprehensive list of such quantities of interest is given in Section 3.

It was already noted that even for modest values of dimension d and number of discretisation points n the total amount of data $N = n^d$ may become huge or even non-manageable, and one has to resort to some kind of compressed representation resp. approximation. Here we advocate for low-rank tensor representations to allow for efficient

computation, which will be treated in Section 4. In such a representation it becomes difficult to compute point-wise functions (like the log) of values of particular tensors required for particular statistics (cf. Section 3), as they are not accessible directly. To still be able to do these computations, we will rely on certain algebraic properties, cf. Section 5. These algebraic relations have been pointed out for the non-discrete entities in the preceding sections, as well as the rôle of the Fourier transform in connecting them. It is now important to ascertain that such algebraic relations also hold for the grid-discrete quantities, this will be done in the following section 2.3.2. The continuous Fourier transform has to be replaced by the discrete Fourier transform or sum, as described in section 2.3.3. How these algebraic operations can be performed in some low-rank representations will be described in Section 4. The use of these algebraic structures in the computation of point-wise functions will be shown in section 2.3.4. The actual algorithms using these algebraic structures are collected in Section 5.

2.3.2 The convolution and Hadamard algebras

The set of tensors in which the representations of **pdf** and **pcf** live, $\mathcal{T} = \bigotimes_{\nu=1}^d \mathbb{R}^{M_\nu} \cong \mathbb{R}^N$ is clearly a vector space. The Section 4 will explain how the vector operations can be numerically performed in the low-rank representation. This assures that convex linear combinations of different probability densities or characteristic functions can be computed. Furthermore one makes \mathcal{T} into a Euclidean space by extending the canonical inner products on the \mathbb{R}^{M_ν} onto \mathcal{T} . With elementary tensors $\mathbf{r} = \bigotimes_{\nu=1}^d \mathbf{r}_\nu, \mathbf{s} = \bigotimes_{\nu=1}^d \mathbf{s}_\nu, \in \mathcal{T}$, it is simply

$$\langle \mathbf{r} | \mathbf{s} \rangle_{\mathcal{T}} := \prod_{\nu=1}^d \langle \mathbf{r}_\nu | \mathbf{s}_\nu \rangle_{\mathbb{R}^{M_\nu}}, \quad (41)$$

and then extended to all of \mathcal{T} by linearity.

It is convenient to extend this inner product to larger tensor products [55], and only perform a partial inner product. For example, if $\mathbf{S} = \mathbf{y} \otimes \mathbf{r}$ is an elementary tensor in $\mathcal{Y} \otimes \mathcal{T}$, and $\mathbf{u} \in \mathcal{T}$, then the partial product, denoted as before, is

$$\langle \mathbf{S} | \mathbf{u} \rangle_{\mathcal{T}} := \langle \mathbf{y} \otimes \mathbf{r} | \mathbf{u} \rangle_{\mathcal{T}} = \langle \mathbf{r} | \mathbf{u} \rangle_{\mathcal{T}} \mathbf{y} \in \mathcal{Y}, \quad (42)$$

and then extended to all of $\mathcal{Y} \otimes \mathcal{T}$ by linearity. It is practically a contraction over all indices related to \mathcal{T} .

The next task is to introduce the algebraic structures. For $\mathbf{r} = (r_1, \dots, r_n), \mathbf{s} = (s_1, \dots, s_n) \in \mathbb{R}^n$, where n stands for any of the $M_\nu, 1 \leq \nu \leq d$, we want to define the *circular convolution* [16, 55] $\mathbf{z} := (z_1, \dots, z_n) = \mathbf{r} * \mathbf{s} \in \mathbb{R}^n$ component-wise as

$$z_k := \sum_{\ell=1}^n r_\ell s_m, \quad m = ((k - \ell) \bmod n) + 1; \quad 1 \leq k \leq n. \quad (43)$$

This is an associative and commutative product; the convolution algebra on \mathbb{R}^n . It is the discrete version of the convolution algebra $L_1(\mathbb{R}^d, \mathbb{R})$ considered in section 2.1.2 and following. One should point out [16] that two steps are involved in going from \mathbb{R}^d resp. \mathbb{R} to the finite grids $\hat{\mathbf{X}}$ resp. $\hat{\mathbf{x}}_\nu$: One is the truncation of the infinite domain, say \mathbb{R} in dimension ν , to a finite one — the interval $[\xi_\nu^{(\min)}, \xi_\nu^{(\max)}]$. This picks only certain discrete frequencies or wavenumbers [16] from the continuum in the Fourier transform, and they are all multiples of a basic frequency resp. wavenumber. The second step is the use of a finite grid, this picks a finite number of the discrete frequencies. The effect of this is to

make everything implicitly periodic, through periodic continuation. This is reflected in the use of the *circular* convolution.

Having defined the circular convolution on each \mathbb{R}^{M_ν} , it is not difficult to extend it to $\mathcal{T} = \bigotimes_{\nu=1}^d \mathbb{R}^{M_\nu}$. With elementary tensors $\mathbf{r} = \bigotimes_{\nu=1}^d \mathbf{r}_\nu, \mathbf{s} = \bigotimes_{\nu=1}^d \mathbf{s}_\nu \in \mathcal{T}$ it is simply

$$\mathbf{z} = \mathbf{r} * \mathbf{s} := \bigotimes_{\nu=1}^d \mathbf{r}_\nu * \mathbf{s}_\nu, \quad (44)$$

and extended to all of \mathcal{T} by linearity. This again is an associative and commutative product; the convolution algebra on \mathcal{T} . In passing one may remark that the statement that the discrete version Φ of the pcf is Hermitean positive definite is equivalent with the statement that the linear (in \mathbf{r}) operator $\mathbf{K}_\Phi : \mathbf{r} \mapsto \Phi * \mathbf{r}$ is Hermitean or self-adjoint and positive definite; \mathbf{K}_Φ is the operator of convolution with Φ .

The other product we need is the discrete version of the point-wise product. This is the Hadamard product, and again it is first formulated component-wise on \mathbb{R}^n : For $\mathbf{r} = (r_1, \dots, r_n), \mathbf{s} = (s_1, \dots, s_n) \in \mathbb{R}^n$ it is denoted by [55] $\mathbf{z} := (z_1, \dots, z_n) = \mathbf{r} \odot \mathbf{s} \in \mathbb{R}^n$ and defined component-wise as

$$z_k := r_k \cdot s_k, \quad 1 \leq k \leq n. \quad (45)$$

This also is an associative and commutative product; the Hadamard algebra on \mathbb{R}^n . Having defined the Hadamard product on \mathbb{R}^n , it is again extended to $\mathcal{T} = \bigotimes_{\nu=1}^d \mathbb{R}^{M_\nu}$. With elementary tensors $\mathbf{r} = \bigotimes_{\nu=1}^d \mathbf{r}_\nu$ and $\mathbf{s} = \bigotimes_{\nu=1}^d \mathbf{s}_\nu \in \mathcal{T}$ it is defined as

$$\mathbf{z} = \mathbf{r} \odot \mathbf{s} := \bigotimes_{\nu=1}^d \mathbf{r}_\nu \odot \mathbf{s}_\nu, \quad (46)$$

and extended to all of \mathcal{T} by linearity. And again this is an associative and commutative product; the Hadamard algebra on \mathcal{T} .

The interaction with the inner product is quite simple, it is an elementary calculation to verify that for $\mathbf{w}, \mathbf{r}, \mathbf{s} \in \mathcal{T}$

$$\langle \mathbf{w} \odot \mathbf{r} \mid \mathbf{s} \rangle_{\mathcal{T}} = \langle \mathbf{r} \mid \mathbf{w} \odot \mathbf{s} \rangle_{\mathcal{T}}, \quad (47)$$

which means that the linear (in \mathbf{r}) operation of Hadamard multiplication by \mathbf{w} , i.e. $\mathbf{L}_\mathbf{w} : \mathbf{r} \mapsto \mathbf{w} \odot \mathbf{r}$, is self-adjoint.

It is easily seen that the Hadamard algebra has a multiplicative unit, which we denote by $\mathbf{1} = (1_{i_1, \dots, i_d})$ — the tensor with all ones — satisfying $\mathbf{r} \odot \mathbf{1} = \mathbf{r}$ for any $\mathbf{r} \in \mathcal{T}$. Defining $\mathbf{1}_\nu := (1, \dots, 1) \in \mathbb{R}^{M_\nu}$, a vector of all ones in dimension ν (which is the Hadamard unit for the Hadamard algebra on \mathbb{R}^{M_ν}), it is not difficult to see that the Hadamard unit on the tensor product has rank one: $\mathbf{1} = \bigotimes_{\nu=1}^d \mathbf{1}_\nu$; it is the simple tensor product of the Hadamard units on each \mathbb{R}^{M_ν} .

The unit further allows to introduce a discrete expectation or integral operator. Recall that we have a tensor quadrature grid, equi-spaced in each dimension, in order to use the FFT. As mentioned before, each point has the integration weight V/N , with V given in Eq. (36). Hence for a tensor \mathbf{P} , representing a function $p(\mathbf{x})$ evaluated on the grid, the approximate integral is

$$\int p(\mathbf{x}) \, d\mathbf{x} \approx \mathcal{S}(\mathbf{P}) := \frac{V}{N} \langle \mathbf{P} \mid \mathbf{1} \rangle_{\mathcal{T}}. \quad (48)$$

Obviously Eq. (48) is only a convenient way of writing the approximate integral, and there is no need to actually compute the inner product with $\mathbf{1}$, i.e. multiply each entry

in the low-rank representation of \mathbf{P} with unity. This Eq. (48) can be simply extended to discrete integrands of the form $\mathbf{S} \in \mathcal{Y} \otimes \mathcal{T}$ through the use of the partial inner product Eq. (42) with the result $\mathcal{S}(\mathbf{S}) \in \mathcal{Y}$. If \mathbf{F} is a tensor which represents the samples of a function $f(\mathbf{x})$, i.e. $\mathbf{F} = f(\hat{\mathbf{X}})$, and \mathbf{P} represents the pdf p_{ξ} , then one may define a discrete version of the expectation by

$$\mathbb{E}(f(\xi)) = \mathbb{E}_{p_{\xi}}(f) = \int_{\mathbb{R}^d} f(\mathbf{x}) p_{\xi}(\mathbf{x}) \, d\mathbf{x} \approx \mathcal{S}(\mathbf{F} \odot \mathbf{P}) = \frac{V}{N} \langle \mathbf{F} \mid \mathbf{P} \rangle_{\mathcal{T}} =: \mathbb{E}_{\mathbf{P}}(\mathbf{F}). \quad (49)$$

Again this can be extended to tensors $\mathbf{S} \in \mathcal{Y} \otimes \mathcal{T}$.

The convolution algebra $(\mathcal{T}, *)$ will be used when dealing with discrete tensor product versions of probability densities, whereas the *point-wise* product Hadamard algebra (\mathcal{T}, \odot) will be used when dealing with discrete tensor product versions of probability characteristic functions. In addition, the Hadamard algebra will also be employed when one has to compute point-wise functions of either the pcf or the pdf.

2.3.3 Using the discrete Fourier transform

Now we want to translate the statements in Subsection 2.2 into the present discrete setting. Let $\mathbf{p}, \mathbf{q} \in \mathcal{T}$ be two tensors, and $\boldsymbol{\phi} = \mathcal{F}_d(\mathbf{p}), \boldsymbol{\psi} = \mathcal{F}_d(\mathbf{q}) \in \mathcal{T}$ their discrete Fourier transforms. Then one has just as in Eq. (25)

$$\mathcal{F}_d(\mathbf{p} * \mathbf{q}) = \mathcal{F}_d(\mathbf{p}) \odot \mathcal{F}_d(\mathbf{q}) = \boldsymbol{\phi} \odot \boldsymbol{\psi} \quad \Leftrightarrow \quad \mathbf{p} * \mathbf{q} = \mathcal{F}_d^{-1}(\boldsymbol{\phi} \odot \boldsymbol{\psi}), \quad (50)$$

showing that the discrete Fourier transform (FT) is an algebra isomorphism between the convolution algebra $(\mathcal{T}, *)$ and the Hadamard algebra (\mathcal{T}, \odot) . This makes it relatively easy to compute the discrete convolution of the tensor representations of two densities, say p represented by \mathbf{P} , and q represented by \mathbf{Q} : Then the density $p * q$ corresponds to $\mathbf{P} * \mathbf{Q}$, computed with their Fourier transforms $\boldsymbol{\phi} = \mathcal{F}_d(\mathbf{P})$ and $\boldsymbol{\psi} = \mathcal{F}_d(\mathbf{Q})$ as

$$\mathbf{P} * \mathbf{Q} = \mathcal{F}_d^{-1}(\boldsymbol{\phi} \odot \boldsymbol{\psi}) = \mathcal{F}_d^{-1}(\mathcal{F}_d(\mathbf{P}) \odot \mathcal{F}_d(\mathbf{Q})). \quad (51)$$

Now it is possible to give a finite dimensional interpretation of the diagonalisation resp. eigen-decomposition of the operators representing the continuous convolution algebra mentioned in section 2.2.1. For a real tensor \mathbf{w} , the Hadamard multiplication operator $\mathbf{L}_{\mathbf{w}}$ of Hadamard multiplication with \mathbf{w} was defined above. As the Hadamard algebra is commutative, the Hadamard multiplication operators commute with each other. Thus it is theoretically clear [110] that they can be simultaneously diagonalised. But it is elementary to see this explicitly. If the arbitrary tensor $\mathbf{r} \in \mathcal{T}$ were written as a vector, the action $\mathbf{L}_{\mathbf{w}}(\mathbf{r}) = \mathbf{w} \odot \mathbf{r}$ would be the action of a diagonal matrix, and diagonal matrices obviously commute. This means that $\mathbf{L}_{\mathbf{w}}$ is fully diagonalised, and the components w_{j_1, \dots, j_d} of the tensor \mathbf{w} are in fact the diagonal elements, i.e. the eigenvalues of $\mathbf{L}_{\mathbf{w}}$. Obviously, to an eigenvalue w_{j_1, \dots, j_d} belongs the canonical unit vector with the same index as eigenvector, in tensor notation the eigenvector is $\mathbf{v}^{(j_1, \dots, j_d)} = (\delta_{(j_1, \dots, j_d), (i_1, \dots, i_d)})_{i_1, \dots, i_d}$, i.e. $\mathbf{L}_{\mathbf{w}}(\mathbf{v}^{(j_1, \dots, j_d)}) = w_{j_1, \dots, j_d} \mathbf{v}^{(j_1, \dots, j_d)}$.

Let $\boldsymbol{\phi} = \mathcal{F}_d^{-1}(\mathbf{w})$, and let $\mathbf{r} \in \mathcal{T}$ be any tensor. The convolution operator $\mathbf{K}_{\boldsymbol{\phi}}$ of convolution with a Hermitean $\boldsymbol{\phi}$ was defined above. One then has

$$\mathbf{K}_{\boldsymbol{\phi}}(\mathbf{r}) = \boldsymbol{\phi} * \mathbf{r} = \mathcal{F}_d^{-1}(\mathcal{F}_d(\boldsymbol{\phi}) \odot \mathcal{F}_d(\mathbf{r})) = \mathcal{F}_d^{-1}(\mathbf{w} \odot \mathcal{F}_d(\mathbf{r})) = \mathcal{F}_d^{-1}(\mathbf{L}_{\mathbf{w}}(\mathcal{F}_d(\mathbf{r}))), \quad \text{or} \quad (52)$$

$$\mathbf{L}_{\mathbf{w}}(\mathbf{r}) = \mathbf{w} \odot \mathbf{r} = \mathcal{F}_d(\boldsymbol{\phi}) \odot \mathbf{r} = \mathcal{F}_d(\boldsymbol{\phi} * \mathcal{F}_d^{-1}(\mathbf{r})) = \mathcal{F}_d(\mathbf{K}_{\boldsymbol{\phi}}(\mathcal{F}_d^{-1}(\mathbf{r}))). \quad (53)$$

This shows that \mathbf{K}_ϕ and \mathbf{L}_w are unitarily equivalent and have the same eigenvalues; and since those of \mathbf{L}_w are the components w_{j_1, \dots, j_d} of the tensor w , those of \mathbf{K}_ϕ are the same, i.e. the components of $w = \mathcal{F}_d(\phi)$, the Fourier transform of the Hermitean convolution tensor ϕ .

When manipulating tensors which represent discrete versions of the pdf resp. the pcf, one wants to make sure that these manipulations do not destroy the fundamental properties of these objects. Let us consider discrete densities first, and assume that $\mathbf{P} \in \mathcal{T}$ is the discrete representation of a density. Then we should expect $\mathbf{P} \geq 0$, i.e. for each $1 \leq i_\nu \leq M_\nu$, $1 \leq \nu \leq d$: $P_{i_1, \dots, i_d} \geq 0$. We have tacitly assumed that \mathbf{P} is also real-valued; this is not necessarily so if it is computed with the involvement of the FT. But this condition is easy to check, as usually the real and imaginary parts of a complex tensor are approximated separately; one only has to make sure the imaginary part is identical to zero — or even better, not computed or stored at all by using a half-length compressed real version of the FFT. This incidentally insures that its FT $\phi = \mathcal{F}_d(\mathbf{P})$ is Hermitean. This condition is preserved by the discrete FT. Coming back to the positivity of \mathbf{P} , this can be checked by computing its *minimum* component P_{\min} ; this minimum should be non-negative. If it happens to be negative, those components can be removed and set to zero. It will be explained later on how to do this. Observing this will also automatically make its FT ϕ positive definite.

A further condition is that the density integrates to unity. Hence in the discrete setting we should expect $\mathcal{S}(\mathbf{P}) = 1$. Incidentally, if $\phi = \mathcal{F}_d(\mathbf{P})$ is its FT, then from Eq. (79) one gleans that this is equivalent with $\phi_{j^0} = \phi_{j_1^0, \dots, j_d^0} = 1$. If \mathbf{P} does not meet this condition, then it can be rescaled appropriately.

2.3.4 Functions on the Hadamard algebra

The last task which will be described here in connection with low-rank tensor approximations is how to compute point-wise functions $f(w)$ of a real tensor $w \in \mathcal{T}$, which means the same function applied to each component. This is important for example if one has to compute $\log(w)$ in order to evaluate the differential entropy mentioned earlier.

Normally, in a full representation, this computation is no problem. But in a low-rank representation, the component values are not directly accessible and have to be computed, and even if they were computed, the question remains on how to bring the result again into a low-rank format. Here it is explored how the Hadamard algebra can be used to accomplish this function evaluation, continuing [33, 39]. This builds on generally well known results [110] on how to compute functions of self-adjoint linear operators, and abstractly on how to compute functions of self-adjoint elements in a C*-algebra. More specifically, as will be seen later, one may use well known algorithms for (real and self-adjoint) matrices [64] to actually do the calculations. One should bear in mind that in the following short description, the arguments presented would hold in any unital C*-algebra, but if concrete examples are used, these are given for the Hadamard algebra.

The simplest functions like linear combinations follow from the vector space structure of \mathcal{T} . The next in complexity are powers. We define for $m \in \mathbb{N}_0$ as usual recursively the power by $\mathbf{r}^{\odot m} := \mathbf{r}^{\odot(m-1)} \odot \mathbf{r}$, and naturally $\mathbf{r}^{\odot 0} = \mathbf{1}$. This way one may evaluate *polynomials*; i.e. if $f_p(t) = \sum_{m=0}^M \beta_m t^m$ is a polynomial in the real variable t with real coefficients $\beta_m \in \mathbb{R}$, then it is now clear how to compute $f_p(\mathbf{r}) \in \mathcal{T}$ for $\mathbf{r} \in \mathcal{T}$, namely by replacing t^m with $\mathbf{r}^{\odot m}$ in the formula for f_p .

The next function to look at is the inverse, $f_i(t) = 1/t = t^{-1}$. The existence of a unit allows the definition of an inverse element: $\mathbf{r} \in \mathcal{T}$ is called invertible, if there exists a —

unique — element $\mathbf{w} \in \mathcal{T}$ such that $\mathbf{r} \odot \mathbf{w} = \mathbf{1}$; it is denoted by $\mathbf{w} = \mathbf{r}^{\odot -1}$. It is obvious that for $\mathbf{r} \in \mathcal{T}$ to have a Hadamard inverse, no component can vanish, $r_{i_1, \dots, i_d} \neq 0$ for all $1 \leq i_\nu \leq M_\nu$, $1 \leq \nu \leq d$; and in that case $\mathbf{r}^{\odot -1} = (1/r_{i_1, \dots, i_d})$. This is up to now only a definition of $f_i(\mathbf{r}) = \mathbf{r}^{\odot -1}$, and not yet an algebraic way of computing it.

The next in complexity are power series $f_{ps}(t) = \sum_{m=0}^{\infty} \beta_m t^m$, or more generally $f_{ps}(t) = \sum_{m=0}^{\infty} \beta_m (t - t_0)^m$, with real coefficients. They are usually approximated by truncation, which is a polynomial. It may be observed that the power series $f_{ps}(\mathbf{r})$ will converge iff all the values of \mathbf{r} are inside the radius of convergence around $t_0 \in \mathbb{R}$. In case f_h is a holomorphic function in a complex domain containing the values of \mathbf{r} , it can also be evaluated in the algebra via Cauchy's formula:

$$f_h(\mathbf{r}) = \oint_{\Gamma} f_h(z) (z \cdot \mathbf{1} - \mathbf{r})^{\odot -1} dz \in \mathcal{T}, \quad (54)$$

where Γ is a contour in \mathbb{C} inside the domain of holomorphy, with all values of \mathbf{r} inside the contour.

We now turn our attention on how to compute a general function $f(\mathbf{r})$ — where f is a real valued function defined on a subset of \mathbb{R} which includes all the values of \mathbf{r} — with purely algebraic methods, i.e. with operations from the algebra, in a similar way as it was already displayed in the trivial case of polynomials and also for power series. Generally, for this one needs to consider algebra representations, i.e. algebra homomorphism with some sub-algebra of linear operators. It was already pointed out in Subsection 2.2 that any algebra can be represented as a sub-algebra of the algebra of linear operators on a vector space, and in the previous section 2.3.2 this representation $\mathbf{w} \mapsto \mathbf{L}_{\mathbf{w}}$ was already explicitly addressed, and it was noted that the $\mathbf{L}_{\mathbf{w}}$ are all self-adjoint on the finite dimensional Hilbert space \mathcal{T} . This is called the (left) *regular representation* [110].

The representation $\mathbf{w} \mapsto \mathbf{L}_{\mathbf{w}}$ from the algebra (\mathcal{T}, \odot) into the algebra $(\mathcal{L}(\mathcal{T}), \circ)$ — the algebra of linear operators with concatenation “ \circ ” as multiplication — is an injective algebra homomorphism onto an Abelian sub-algebra of $\mathcal{L}(\mathcal{T})$ of self-adjoint operators, as (\mathcal{T}, \odot) is Abelian and all members are real, i.e. self-adjoint. It was already explicitly shown in the previous section 2.3.2 that all the operators $\mathbf{L}_{\mathbf{w}}$ are in fact already in diagonal form, so the image Abelian sub-algebra is isomorphic to the algebra of diagonal matrices. Now the general way to compute a function $f(\mathbf{w})$ is to use the spectral calculus [110] of self-adjoint operators to compute $f(\mathbf{L}_{\mathbf{w}})$, and then to use the inverse of the representation $\mathbf{w} \mapsto \mathbf{L}_{\mathbf{w}}$ on the relevant Abelian sub-algebra.

While this general theory will work in any unital algebra and was mentioned for general orientation, the situation here is much simpler, as we already have seen explicitly in section 2.3.2 that the operators $\mathbf{L}_{\mathbf{w}}$ can be represented by diagonal matrices.

This matrix representation means that *matrix algorithms*, which only use the matrix algebra operations, can be used to compute $f(\mathbf{L}_{\mathbf{w}})$ to represent $f(\mathbf{w})$, see e.g. [64]. The algorithms will explicitly be addressed later in Section 5. This is quite the opposite of what one wants to do normally, where access to the spectral decomposition resp. eigen-representation would be used directly to compute such a function $f(\mathbf{w})$, and the matrix algorithms mentioned are used when the eigen-decomposition is regarded as too costly. Here we will show that one has a low-rank form of the eigen-representation, and the point-wise application of a function $f(\mathbf{w})$ is regarded as too costly, whereas the matrix algorithms can be efficiently carried out in low-rank format.

This concrete representation of (\mathcal{T}, \odot) on the Abelian unital algebra of diagonal $N \times N$ matrices is easily seen to be in fact an algebra isomorphism. Due to this representation isomorphism, one may use the matrix algorithms directly on the Hadamard algebra, and

there is no need to actually use matrices. It was already shown in section 2.3.2 that the eigenvalues of $\mathbf{L}_{\mathbf{w}}$ are the component values of \mathbf{w} . With that in mind, it may be mentioned in passing that as the spectrum resp. set of eigenvalues of $\mathbf{L}_{\mathbf{w}}$ is a finite set, any function $f(\mathbf{w})$ could be interpolated by a polynomial. But this is not practical, as the polynomial would in general have degree $N = \dim \mathcal{T}$, which we assume to be a huge number, so that typically the matrix algorithms are more economical. Also, this means that the maximum value of \mathbf{w} is the largest eigenvalue of $\mathbf{L}_{\mathbf{w}}$, and the minimum value of \mathbf{w} is the smallest eigenvalue, hinting at concrete algorithms to find the maximum and minimum value of \mathbf{w} .

The Section 4 will explain how the Hadamard algebra operations like multiplication with a scalar, addition of two low-rank tensors, or the Hadamard product can be carried out for the CP- and tensor-train-formats.

3 Computation of moments and divergences

While Section 2 recalled the statistic and characterisations of RVs resp. probability distributions or rather **pdfs**, and additionally explained how a low-rank tensor representation on a discrete grid could be achieved, the purpose is here to make this specific within the framework of tensor representations explained in Subsection 2.3. There is was also shown how to use the FT in the low-rank format. Moreover, here the computation of various distances and divergences between probability density functions will be treated in this discrete setting. It is thereby assumed that point-wise functions of the low-rank tensor representation can be computed as alluded to in section 2.3.4. The Section 4 will show how to perform the basic algebra operations in a low-rank tensor format, and the following Section 5 will explain in more detail and give actual algorithms how those required point-wise functions can also be computed in a low-rank format. Here it assumed that these operations—basic algebra and point-wise functions—can be carried out at least approximately, and with that the first topic will be the computation of the elementary statistics and other QoIs. Thereafter, some exemplary distances and divergences will be discussed, noting the point-wise functions which are required to compute them.

It should be recalled that the basic assumption here is that the starting point is either access to the probability characteristic function (**pcf**) section 2.1.3, or the probability density function (**pdf**) section 2.1.2, or directly to the underlying random variable (RV) Subsection 2.1. It will be also recalled how to go between **pdf** and **pcf** and vice versa, and how to compute the other characterising functions mentioned in section 2.2.2.

3.1 Statistics and moments

If it is desired to compute some QoI — the expected value of a function $\mathbf{g}(\boldsymbol{\xi})$ (with $\mathbf{g} : \mathbb{R}^d \rightarrow \mathcal{Y}$) of the RV $\boldsymbol{\xi}$ like in Eq. (19), then it is first necessary to represent this function in low-rank format on the grid $\hat{\mathbf{X}}$, i.e. to find $\mathbf{G} = \mathbf{g}(\hat{\mathbf{X}}) \in \mathcal{Y} \otimes \mathcal{T}$. If \mathbf{P} represents the **pdf** $p_{\boldsymbol{\xi}}$, the discrete version of the expectation was already given in Eq. (49):

$$\mathbf{g} = \mathbb{E}_{p_{\boldsymbol{\xi}}}(\mathbf{g}) = \int_{\mathbb{R}^d} \mathbf{g}(\mathbf{x}) p_{\boldsymbol{\xi}}(\mathbf{x}) \, d\mathbf{x} \approx \mathbb{E}_{\mathbf{P}}(\mathbf{G}) = \frac{V}{N} \langle \mathbf{G} \mid \mathbf{P} \rangle_{\mathcal{T}}. \quad (55)$$

Moments are a special case of Eq. (55): for the mean one takes the tensor \mathbf{x} from Eq. (38) or for higher moments the tensor $\mathbf{x}^{\otimes k}$ from Eq. (39) to give

$$\bar{\boldsymbol{\xi}} = \mathbf{X}_1 \approx \mathbb{E}_{\mathbf{P}}(\mathbf{x}), \quad \text{and } \mathbf{X}_k \approx \mathbb{E}_{\mathbf{P}}(\mathbf{x}^{\otimes k}), \, k \in \mathbb{N}_0. \quad (56)$$

For mixed moments these relations can be used in an analogous fashion.

The moments can also be computed through characterising functions, and some of these and their relations with moments were already discussed in section 2.2.2. Here the discrete versions of these relations on the low-rank representation will be discussed. Again, the items which are assumed to be in a low-rank representation are either the probability density p_ξ with low-rank representation \mathbf{P} , or the characteristic function φ_ξ with low rank representation Φ . Their relation was already discussed in Eq. (80):

$$\Phi = \mathcal{F}_d(\mathbf{P}), \text{ and } \mathbf{P} = \mathcal{F}_d^{-1}(\Phi).$$

Hence, having one of them, it is easy to obtain the other one. From Eq. (31) one obtains a second route — typically involving more numerical work — to the approximate computation of the moments Eq. (56):

$$\bar{\xi} = \mathbf{X}_1 \approx \mathbb{E}_{\mathbf{P}}(\mathbf{x}) = (\mathcal{F}_d(\mathbf{x} \odot \mathbf{P}))_{j^0} = (\mathcal{F}_d(\mathbf{x} \odot \mathcal{F}_d^{-1}(\Phi)))_{j^0}, \quad \text{and} \quad (57)$$

$$\mathbf{X}_k \approx \mathbb{E}_{\mathbf{P}}(\mathbf{x}^{\otimes k}) = (\mathcal{F}_d(\mathbf{x}^{\otimes k} \odot \mathbf{P}))_{j^0} = (\mathcal{F}_d(\mathbf{x}^{\otimes k} \odot \mathcal{F}_d^{-1}(\Phi)))_{j^0}, \quad k \in \mathbb{N}_0. \quad (58)$$

Other characterising functions were sketched at the end of section 2.2.2. The simplest one is the second characteristic function $\chi_\xi(\mathbf{t}) = \log(\varphi_\xi(\mathbf{t}))$ from Eq. (32). Given the tensor Φ representing φ_ξ , this is just the point-wise logarithm

$$\mathbf{r} = \log(\Phi), \quad \text{such that } \mathbf{r} = \chi_\xi(\hat{\mathbf{T}}). \quad (59)$$

From this one may compute cumulants, similarly to the moments in Eq. (57):

$$\mathbf{K}_k \approx (\mathcal{F}_d(\mathbf{x}^{\otimes k} \odot \mathcal{F}_d^{-1}(\mathbf{r})))_{j^0}. \quad (60)$$

The moment generating function $M_\xi(\mathbf{t}) = \mathbb{E}(\exp\langle \mathbf{t} | \xi \rangle)$ Eq. (33) can in principle be generated in the same way as the characteristic function $\varphi_\xi(\mathbf{t}) = \mathbb{E}(\exp(i\langle \mathbf{t} | \xi \rangle))$ (Eq. (12) or Eq. (22)) with the help of the RV $\xi(\cdot)$ expressed as in Eq. (11) to give its tensor representation $\mathbf{M} = M_\xi(\hat{\mathbf{T}})$ on the grid $\hat{\mathbf{T}}$. Now its derivatives are directly the moments, so with the FT one has an alternative approximate computation of the moments Eq. (56) as follows:

$$\bar{\xi} \approx \mathbb{E}_{\mathcal{T}}(\mathbf{x}) = i (\mathcal{F}_d(\mathbf{x} \odot \mathcal{F}_d^{-1}(\mathbf{M})))_{j^0}, \quad \text{and} \quad (61)$$

$$\mathbf{X}_k \approx \mathbb{E}_{\mathcal{T}}(\mathbf{x}^{\otimes k}) = i^k (\mathcal{F}_d(\mathbf{x}^{\otimes k} \odot \mathcal{F}_d^{-1}(\mathbf{M})))_{j^0}. \quad (62)$$

Similarly to the discrete version of second characteristic function Eq. (59), the cumulant generating function $K_\xi(\mathbf{t}) = \log(M_\xi(\mathbf{t}))$ in Eq. (35) also has a discrete version, the point-wise logarithm of the discrete moment generating function \mathbf{M} :

$$\mathbf{Z} = \log(\mathbf{M}), \quad \text{such that } \mathbf{Z} = K_\xi(\hat{\mathbf{T}}). \quad (63)$$

Analogous as before in Eq. (62), the cumulants may be expressed via

$$\mathbf{K}_k \approx i^k (\mathcal{F}_d(\mathbf{x}^{\otimes k} \odot \mathcal{F}_d^{-1}(\mathbf{Z})))_{j^0}. \quad (64)$$

From Eq. (58) follows, that if discretised pcf Φ has a low tensor rank, then \mathbf{X}_k will also be of a low-rank. Note that we cannot say the same about \mathbf{K}_k from Eq. (60) (or Eq. (64)). The tensor rank of \mathbf{K}_k depends on the tensor rank of \mathbf{r} (or \mathbf{Z}), and the latest can have a high rank due to the involved $\log(\cdot)$ function. So, we assume here that the series expansion, described in Section 5.5 will allow us to approximate \mathbf{r} (or \mathbf{Z}) in a low-rank tensor format.

3.2 Computing divergences

Name of the divergence	$D_{\bullet}(p q)$
Kullback–Leibler-(KL) — D_{KL} :	$\int (\log(p(\mathbf{x})/q(\mathbf{x}))) p(\mathbf{x}) \, d\mathbf{x} = \mathbb{E}_p(\log(p/q))$
sqr. Hellinger distance — $(D_H)^2$:	$\frac{1}{2} \int \left(\sqrt{p(\mathbf{x})} - \sqrt{q(\mathbf{x})} \right)^2 d\mathbf{x}$
Bregman divergence — D_{ϕ} :	$\int [(\phi(p(\mathbf{x})) - \phi(q(\mathbf{x}))) - (p(\mathbf{x}) - q(\mathbf{x}))\phi'(q(\mathbf{x}))] d\mathbf{x}$
Bhattacharyya distance — D_{Bh} :	$-\log \left(\int \sqrt{p(\mathbf{x})q(\mathbf{x})} d\mathbf{x} \right)$

Table 1: List of some typical divergences and distances.

Let us now turn to quantities which characterise the whole distribution, or the difference or distance between them. Divergences are a kind of generalisation of distances, and unlike distances they do not have to be symmetric. The best known is probably the relative entropy, also known as the Kullback-Leibler (KL) divergence.

Let $p, q \in \mathfrak{D}$ be two probability densities, and $\mathbf{P}, \mathbf{Q} \in \mathcal{T}$ their low-rank tensor representations. A simple characterisation of a distribution is its entropy, for a continuous distribution p this is the *differential entropy*, requiring the point-wise logarithm of \mathbf{P} :

$$h(p) := \mathbb{E}_p(-\log(p)) \approx \mathbb{E}_{\mathbf{P}}(-\log(\mathbf{P})) = -\frac{V}{N} \langle \log(\mathbf{P}) \mid \mathbf{P} \rangle, \quad (65)$$

where the expectation $\mathbb{E}_{\mathbf{P}}(\cdot)$ is computed as in Eq. (49) resp. Eq. (55). To compare two probability densities p and q , one uses divergences or distances between them. Some well known divergences and distances are given in Table 1. For the Bregman divergence, ϕ has to be a real convex function, e.g. $\phi(t) = t^2$. These divergences and distances may be computed by the discrete approximations shown in Table 2.

Name of the divergence	Approximation of $D_{\bullet}(p q)$
Kullback–Leibler-(KL) — D_{KL} :	$\frac{V}{N} (\langle \log(\mathbf{P}) \mid \mathbf{P} \rangle - \langle \log(\mathbf{Q}) \mid \mathbf{P} \rangle)$
squared Hellinger distance — $(D_H)^2$:	$\frac{V}{2N} \langle \mathbf{P}^{\odot 1/2} - \mathbf{Q}^{\odot 1/2} \mid \mathbf{P}^{\odot 1/2} - \mathbf{Q}^{\odot 1/2} \rangle$
Bregman divergence — D_{ϕ} :	$\mathcal{S}((\phi(\mathbf{P}) - \phi(\mathbf{Q})) - (\mathbf{P} - \mathbf{Q}) \odot \phi'(\mathbf{Q}))$
Bhattacharyya distance — D_{Bh} :	$-\log \left(\frac{V}{N} \langle \mathbf{P}^{\odot 1/2} \mid \mathbf{Q}^{\odot 1/2} \rangle \right)$

Table 2: Discrete approximations for divergences listed in Table 1. Formulas for computations are given in Sections 2 and 5.4.2.

It is evident that one has to be able to compute the point-wise logarithm and the square root of a low-rank tensor. For the Bregmann divergence one has to be able to compute point-wise the convex function ϕ and its derivative ϕ' of a low-rank tensor representation, an easy task for $\phi(t) = t^2$.

The f -divergence is a way to define many divergences in a unifying way [83, 91], depending on a convex function f . One requires that f be a convex function, satisfying $f(1) = 0$. Then the f -divergence of p from q and its discrete approximation is defined as

$$D_f(p||q) := \mathbb{E}_q \left(f \left(\frac{p}{q} \right) \right) \approx \mathbb{E}_{\mathbf{Q}} \left(f(\mathbf{P} \odot \mathbf{Q}^{\odot -1}) \right) = \frac{V}{N} \langle f(\mathbf{P} \odot \mathbf{Q}^{\odot -1}) \mid \mathbf{Q} \rangle. \quad (66)$$

Many common divergences, such as the KL-divergence, the Hellinger distance, and the total variation distance, are special cases of the f -divergence, coinciding with a particular choice of f . In Table 3 the functions f for some common f -divergences [83, 91] are listed.

Name of the divergence	Corresponding $f(t)$
KL-divergence	$t \log(t)$
reverse KL-divergence	$-\log(t)$
squared Hellinger distance	$(\sqrt{t} - 1)^2$
total variation distance	$ t - 1 /2$
Pearson χ_P^2 -divergence	$(t - 1)^2$
Neyman χ_N^2 -divergence (reverse Pearson)	$t^{-1} - 1$
Pearson-Vajda χ_P^k -divergence	$(t - 1)^k$
Pearson-Vajda $ \chi _P^k$ -divergence	$ t - 1 ^k$
Jensen-Shannon-divergence	$t \log(t) - (t + 1) \log((t + 1)/2)$

Table 3: Some examples of the function f for the f -divergence.

Hence to compute the discrete approximation, one has to be able to compute not only the Hadamard inverse of a low rank tensor, but also the function f . These are essentially the ones which have been discussed already, the only new one is the absolute value.

4 Tensor formats

Our task is to approximate a high-dimensional function (e.g. a **pdf**) in a low-rank tensor format. After discretisation of the high-dimensional function on a grid, we obtain a tensor, which is also a high-dimensional object. Now we need an appropriate *tensor representation*, which will make efficient storage and efficient multi-linear algebra possible. In this section, we give a short overview of known tensor representations (tensor formats) and review definitions and properties of the canonical polyadic (CP) tensor format.

Many tensor formats are used in quantum physics under the name *tensor networks*, see [119, 106, 41, 94, 18, 14]. The CP [65] and *Tucker* [115] formats have been well known for a long time and are therefore very popular. For instance, CP and Tucker rank-structured tensor formats have been applied in chemometrics and in signal processing [112, 21]. The *Tensor Train* format was originally developed in quantum physics and chemistry as “matrix product states” (MPS), see [119] and references therein, and rediscovered and developed further in [100, 101, 7, 25] as tensor train. The hierarchical tensor (HT) format was introduced in [58], and further considered in [51].

The CP format is cheap, it is simpler than the Tucker or TT format, but, compared to others, there are no reliable algorithms to compute CP decompositions for $d > 2$ [59, 75]. The Tucker format has stable algorithms [73], but the storage and complexity costs are $\mathcal{O}(drn + r^d)$, i.e. they grow exponentially with d . The TT format is a bit more complicated, but does not have this disadvantage. Applications to UQ problems are described in [23, 24, 30].

A tensor is a multi-index array, where multi-indices are used instead of indices. As an example, consider a vector $\mathbf{w} \in \mathbb{R}^N$, $N = 10^{12}$ data points. We can *reshape* it into a matrix $\mathbf{W} \in \mathbb{R}^{10^6 \times 10^6} \cong \mathbb{R}^{10^6} \otimes \mathbb{R}^{10^6}$, which is a tensor of 2nd order. To get a tensor of 3rd order, we reshape it in the following way $\mathbb{R}^{10^4 \times 10^4 \times 10^4} \cong \bigotimes_{k=1}^3 \mathbb{R}^{10^4}$ and so on (see Section 1 in [39]). The higher the order of the tensor, the more possibilities there are to

find a low-rank approximation [59]. The tensors obtained in this way contain not only rows and columns, but also *slices* and *fibres* [77, 78, 22, 59]. These slices and fibres can be analysed for linear dependencies, super symmetry, or sparsity, and may result in a strong data compression [116].

4.1 The canonical polyadic (CP) tensor format

The CP representation of a multivariate function is one of the easiest tensor representations, it was developed in [65]. Schematically it is shown in Figure 1, where a full tensor $\mathbf{w} \in \mathbb{R}^{n_1 \times n_2 \times n_3}$ (on the left) is represented as a sum of tensor products (on the right). The lines on the right denote vectors $\mathbf{w}_{i,k} \in \mathbb{R}^{n_k}$, $i = 1, \dots, r$, $k = 1, 2, 3$.

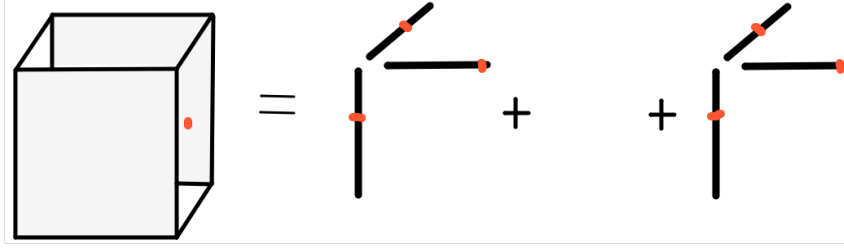


Figure 1: Representation of a 3D tensor in the CP tensor format.

Tensor representation is a multi-linear mapping. There are many different representations, e.g., CP tensor representation maps tensor \mathbf{w} into the sum with r terms $\sum_{i=1}^r \bigotimes_{\nu=1}^d \mathbf{w}_{i,\nu}$. The number r is called the tensor rank. The storage required to store a tensor in the CP tensor format is $\mathcal{O}(r d n)$ (assuming that $n = n_1 = \dots = n_d$). To compute an element (j_1, j_2, j_3) , denoted by the red point on the left, we should compute the following sum $\sum_{i=1}^r \mathbf{w}_{i,1}(j_1) \cdot \mathbf{w}_{i,2}(j_2) \cdot \mathbf{w}_{i,3}(j_3)$. The values $\mathbf{w}_{i,1}(j_1)$, $\mathbf{w}_{i,2}(j_2)$, and $\mathbf{w}_{i,3}(j_3)$ are denoted by the red points on the right hand side in Fig. 1.

Let us denote the set of all rank- r tensors by \mathcal{T}^r . We note that if $\mathbf{w}_1, \mathbf{w}_2 \in \mathcal{T}^r$, then $\mathbf{w}_1 + \mathbf{w}_2 \notin \mathcal{T}^r$, and, therefore, \mathcal{T}^r is not a vector space [40]. This sum belongs to \mathcal{T}^{2r} .

A complete description of fundamental operations in the canonical tensor format and a their numerical cost can be found in [59]. For recent algorithms in the canonical tensor format we refer to [55, 12, 35, 36, 37]. We remind few properties [39] of the CP format. To multiply a tensor \mathbf{w} by a scalar $\alpha \in \mathbb{R}$ costs $\mathcal{O}(r n d)$:

$$\alpha \cdot \mathbf{w} = \sum_{j=1}^r \alpha \bigotimes_{\nu=1}^d \mathbf{w}_{j,\nu} = \sum_{j=1}^r \bigotimes_{\nu=1}^d \alpha_{\nu} \mathbf{w}_{j,\nu}, \quad (67)$$

where $\alpha_{\nu} := \sqrt[d]{|\alpha|}$ for all $\nu > 1$, and $\alpha_1 := \text{sign}(\alpha) \sqrt[d]{|\alpha|}$.

The sum of two tensors costs only $\mathcal{O}(1)$:

$$\mathbf{w} = \mathbf{u} + \mathbf{v} = \left(\sum_{j=1}^{r_u} \bigotimes_{\nu=1}^d \mathbf{u}_{j,\nu} \right) + \left(\sum_{k=1}^{r_v} \bigotimes_{\mu=1}^d \mathbf{v}_{k,\mu} \right) = \sum_{j=1}^{r_u+r_v} \bigotimes_{\nu=1}^d \mathbf{w}_{j,\nu}, \quad (68)$$

where $\mathbf{w}_{j,\nu} := \mathbf{u}_{j,\nu}$ for $j \leq r_u$ and $\mathbf{w}_{j,\nu} := \mathbf{v}_{j-r_u,\nu}$ for $r_u < j \leq r_u + r_v$. The sum \mathbf{w} generally has rank $r_u + r_v$. The Hadamard product can be written as follows

$$\mathbf{w} = \mathbf{u} \odot \mathbf{v} = \left(\sum_{j=1}^{r_u} \bigotimes_{\nu=1}^d \mathbf{u}_{j,\nu} \right) \odot \left(\sum_{k=1}^{r_v} \bigotimes_{\nu=1}^d \mathbf{v}_{k,\nu} \right) = \sum_{j=1}^{r_u} \sum_{k=1}^{r_v} \bigotimes_{\nu=1}^d (\mathbf{u}_{j,\nu} \odot \mathbf{v}_{k,\nu}). \quad (69)$$

The new rank can increase till $r_u r_v$, and the computational cost is $\mathcal{O}(r_u r_v n d)$. The scalar product can be computed as follows:

$$\langle \mathbf{u} \mid \mathbf{v} \rangle_{\mathcal{T}} = \left\langle \sum_{j=1}^{r_u} \bigotimes_{\nu=1}^d \mathbf{u}_{j,\nu} \mid \sum_{k=1}^{r_v} \bigotimes_{\nu=1}^d \mathbf{v}_{k,\nu} \right\rangle_{\mathcal{T}} = \sum_{j=1}^{r_u} \sum_{k=1}^{r_v} \prod_{\nu=1}^d \langle \mathbf{u}_{j,\nu} \mid \mathbf{v}_{k,\nu} \rangle_{\mathcal{P}_{\nu}}. \quad (70)$$

The computational cost is $\mathcal{O}(r_u r_v n d)$. The tensor rank can be truncated via the ALS-method or Gauss-Newton-method [35, 40]. The scalar product above helps to compute the Frobenius norm $\|\mathbf{u}\|_2 := \sqrt{\langle \mathbf{u} \mid \mathbf{u} \rangle_{\mathcal{T}}}$.

4.2 The Tensor Train format

The tensor train (TT) format is described in [98, 101, 59, 75]. As already noted, it was originally developed in quantum chemistry as “matrix product states” (MPS), see [119] and references therein, and rediscovered later [100, 101].

Definition 4.1 (TT-Format, TT-Representation, TT-Ranks). *The TT-tensor format is for variable TT-representation ranks $\mathbf{r} = (r_0, \dots, r_d) \in \mathbb{N}^{d+1}$ — with $r_0 = r_d = 1$ and under the assumption that $d > 2$ — defined by the following multilinear mapping*

$$\begin{aligned} U_{\text{TT}} : \mathcal{P}_{\text{TT},\mathbf{r}} &:= \bigtimes_{\nu=1}^d \mathcal{P}_{\nu}^{r_{\nu-1} \times r_{\nu}} \rightarrow \mathcal{T}, \quad \mathcal{P}_{\nu} = \mathbb{R}^{M_{\nu}} \quad (\nu = 1, \dots, d), \\ \mathcal{P}_{\text{TT},\mathbf{r}} \ni \mathbf{P} = (\mathbf{W}^{(\nu)} = (\mathbf{w}_{j_{\nu-1}j_{\nu}}^{(\nu)}) \in \mathcal{P}_{\nu}^{r_{\nu-1} \times r_{\nu}} : 1 \leq j_{\nu} \leq r_{\nu}, 1 \leq \nu \leq d) \\ &\mapsto U_{\text{TT}}(\mathbf{P}) := \mathbf{w} = \sum_{j_0=1}^{r_0} \cdots \sum_{j_d=1}^{r_d} \bigotimes_{\nu=1}^d \mathbf{w}_{j_{\nu-1}j_{\nu}}^{(\nu)} \in \mathcal{T}. \end{aligned} \quad (71)$$

We call $\mathbf{w} := (w_{i_1 \dots i_d}) = U_{\text{TT},\mathbf{r}}(\mathbf{P})$ a tensor represented in the train tensor format. Note that the TT-cores $\mathbf{W}^{(\nu)}$ may be viewed as a vector valued $r_{\nu-1} \times r_{\nu}$ matrix with the vector $\mathbf{w}_{j_{\nu-1}j_{\nu}}^{(\nu)} \in \mathbb{R}^{M_{\nu}}$ with the components $w_{j_{\nu-1}j_{\nu}}^{(\nu)}[i_{\nu}] : 1 \leq i_{\nu} \leq M_{\nu}$ at index position $(j_{\nu-1}, j_{\nu})$. The representation in components is then

$$(w_{i_1 \dots i_d}) = \sum_{j_0=1}^{r_0} \cdots \sum_{j_d=1}^{r_d} w_{j_0 j_1}^{(1)}[i_1] \cdots w_{j_{\nu-1} j_{\nu}}^{(\nu)}[i_{\nu}] \cdots w_{j_{d-1} j_d}^{(d)}[i_d] \quad (72)$$

Alternatively, each TT-core $\mathbf{W}^{(\nu)}$ may be seen as a vector of $r_{\nu-1} \times r_{\nu}$ matrices $\mathbf{W}_{i_{\nu}}^{(\nu)}$ of length M_{ν} , i.e. $\mathbf{W}^{(\nu)} = (\mathbf{W}_{i_{\nu}}^{(\nu)}) : 1 \leq i_{\nu} \leq M_{\nu}$. Then the representation Eq. (72) reads

$$(w_{i_1 \dots i_d}) = \prod_{\nu=1}^d \mathbf{W}_{i_{\nu}}^{(\nu)}, \quad (73)$$

which explains the name matrix product state. Observe that the first matrix is always a row vector as $r_0 = 1$, and the last matrix is always a column vector as $r_d = 1$. The matrix components $\mathbf{W}_{i_{\nu}}^{(\nu)}$ of the TT-cores are also called “carriages” or “waggon” with “wheels” i_{ν} at the bottom, coupled to the next “carriage” or “waggon” via the matrix product. This explains the tensor train name. If one notes more carefully $\mathbf{W}^{(\nu)} \in \mathcal{P}_{\nu}^{r_{\nu-1} \times r_{\nu}} = \mathbb{R}^{r_{\nu-1}} \otimes \mathbb{R}^{M_{\nu}} \otimes \mathbb{R}^{r_{\nu}}$, then Eq. (73) can be written more concisely as

$$\mathbf{w} = U_{\text{TT}}(\mathbf{P}) = \mathbf{W}^{(1)} \times_3^1 \mathbf{W}^{(2)} \times_3^1 \cdots \times_3^1 \mathbf{W}^{(d)}, \quad (74)$$

where $\mathbf{U} \times_k^{\ell} \mathbf{V}$ is a contraction of the k -th index of \mathbf{U} with the ℓ -th index of \mathbf{V} , where one often writes just \times_k for \times_k^1 . Thus in Eq. (74) the contractions leave the indices from the $\mathbb{R}^{M_{\nu}}$ untouched, so that the tensor \mathbf{w} is formed.

Each TT-core (or *block*) $\mathbf{W}^{(\nu)}$ is defined by $r_{\nu-1} \times r_\nu \times M_\nu$ numbers. Assuming $n = M_\nu$ for all $\nu = 1, \dots, d$, the total number of entries scales as $\mathcal{O}(d n r^2)$, which is tractable as long as $r = \max\{r_k\}$ is moderate.

A pictorial representation of the schema for the TT tensor format is shown in Figure 2. It shows d connected waggons with one wheel. The waggons denote the TT-cores, and each wheel denotes the index i_ν . The waggons for $\nu = 2, \dots, (d-1)$ are connected with their neighbours by two indices $j_{\nu-1}$ and j_ν . The first and the last waggons are connected by only one index, namely j_1 and j_{d-1} respectively. Since by the convention in Definition 4.1 above, $r_0 = r_d = 1$, the indices j_0 and j_d run from 1 to 1, i.e. are purely formal.

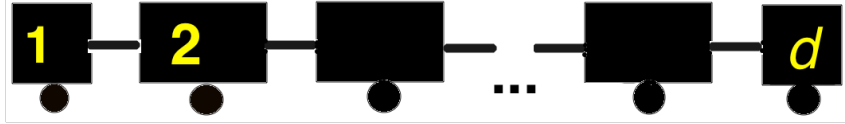


Figure 2: Schema of the TT tensor decomposition. The waggons denote the TT cores and each wheel denotes the index i_ν . Each waggon is connected with neighbours by indices $j_{\nu-1}$ and j_ν .

The waggon or carriage 2 — $\mathbf{W}^{(2)}$ — is a tensor of degree 3, described by three indices j_1 (the left hitch), i_2 (the wheel), and j_2 (the right hitch). Multiplication of the third TT-core with the second and forth cores means the tensor contraction by the indices j_2 and j_3 . If we perform tensor contraction of all TT-cores over the indices j_1, \dots, j_{d-1} , and disregard the purely formal constant indices j_0 and j_d , then the indices j_0, \dots, j_d — the hitches — will disappear, and only the indices i_1, \dots, i_d — the wheels — will be left.

Basic operations with the TT format We follow to the work of Oseledets [101] and list the major properties of the TT-tensor format.

The multiplication with scalar α could be simply done by multiplying one of the TT-cores $\mathbf{W}^{(\nu)}$ in the representation Eq. (74) for any ν in $\mathbf{w} = \mathbf{W}^{(1)} \times_3^1 \mathbf{W}^{(2)} \times_3^1 \dots \times_3^1 \mathbf{W}^{(d)}$. But to balance the effect better, define $\alpha_\nu := \sqrt[d]{|\alpha|}$ for all $\nu > 1$, and $\alpha_1 := \text{sign}(\alpha) \sqrt[d]{|\alpha|}$. Then $\tilde{\mathbf{w}} = \alpha \cdot \mathbf{w}$ is given by

$$\tilde{\mathbf{w}} = (\alpha_1 \cdot \mathbf{W}^{(1)}) \times_3^1 (\alpha_2 \cdot \mathbf{W}^{(2)}) \times_3^1 \dots \times_3^1 (\alpha_d \cdot \mathbf{W}^{(d)}) = \tilde{\mathbf{W}}^{(1)} \times_3^1 \dots \times_3^1 \tilde{\mathbf{W}}^{(d)}.$$

The new cores are given by $\tilde{\mathbf{W}}^{(\nu)} = (\tilde{\mathbf{W}}_{i_\nu}^{(\nu)}) = (\alpha_\nu \mathbf{W}_{i_\nu}^{(\nu)})$, a sequence of new “carriage” matrices. The computational complexity is $\mathcal{O}(d n r^2)$.

Addition of two TT-tensors Assume two tensors \mathbf{u} and \mathbf{v} are given in the TT-tensor format as in Eq. (73), i.e. $(u_{i_1 \dots i_d}) = \prod_{\nu=1}^d \mathbf{U}_{i_\nu}^{(\nu)}$ and $(v_{i_1 \dots i_d}) = \prod_{\nu=1}^d \mathbf{V}_{i_\nu}^{(\nu)}$. The sum $\mathbf{w} = \mathbf{u} + \mathbf{v}$ is given by the new cores $\mathbf{W}_{i_\nu}^{(\nu)}$ such that $(w_{i_1 \dots i_d}) = \prod_{\nu=1}^d \mathbf{W}_{i_\nu}^{(\nu)}$, where

$$\mathbf{W}_{i_\nu}^{(\nu)} = \begin{pmatrix} \mathbf{U}_{i_\nu}^{(\nu)} & \mathbf{0} \\ \mathbf{0} & \mathbf{V}_{i_\nu}^{(\nu)} \end{pmatrix}, \quad 1 \leq i_\nu \leq r_\nu, 2 \leq \nu \leq d-1.$$

and the first and the last cores will be

$$\mathbf{W}_{i_1}^{(1)} = \begin{pmatrix} \mathbf{U}_{i_1}^{(1)} & \mathbf{V}_{i_1}^{(1)} \end{pmatrix} \quad \text{and} \quad \mathbf{W}_{i_d}^{(d)} = \begin{pmatrix} \mathbf{U}_{i_d}^{(d)} \\ \mathbf{V}_{i_d}^{(d)} \end{pmatrix}.$$

As only storage may have to be concatenated, the computational cost is $\mathcal{O}(1)$, but as the carries resp. TT-cores grow, the final rank will generally be the sum of the ranks.

The Hadamard product $\mathbf{w} = \mathbf{u} \odot \mathbf{v}$ in the TT format is computed as follows. Assume two tensors \mathbf{u} and \mathbf{v} are given in the TT tensor format as in Eq. (73), i.e. $(u_{i_1 \dots i_d}) = \prod_{\nu=1}^d \mathbf{U}_{i_\nu}^{(\nu)}$ and $(v_{i_1 \dots i_d}) = \prod_{\nu=1}^d \mathbf{V}_{i_\nu}^{(\nu)}$. The Hadamard product is

$$(w_{i_1 \dots i_d}) = (u_{i_1 \dots i_d} \cdot v_{i_1 \dots i_d}).$$

The tensor \mathbf{w} has also the TT-tensor format, namely with the new cores

$$\mathbf{W}_{i_\nu}^{(\nu)} = \mathbf{U}_{i_\nu}^{(\nu)} \otimes_K \mathbf{V}_{i_\nu}^{(\nu)}, \quad 1 \leq i_\nu \leq r_\nu, 1 \leq \nu \leq d,$$

where \otimes_K is the Kronecker product of two matrices [59]. The rank of $\mathbf{W}^{(\nu)} = (\mathbf{W}_{i_\nu}^{(\nu)})$ is the product of the ranks of the TT-cores $\mathbf{U}^{(\nu)}$ and $\mathbf{V}^{(\nu)}$.

The Euclidean inner product of two tensors in the TT-format as in Eq. (71)

$$\mathbf{u} = \sum_{j_0=1}^{r_0^u} \cdots \sum_{j_d=1}^{r_d^u} \bigotimes_{\nu=1}^d \mathbf{u}_{j_{\nu-1}j_\nu}^{(\nu)}, \quad \mathbf{v} = \sum_{j_0=1}^{r_0^v} \cdots \sum_{j_d=1}^{r_d^v} \bigotimes_{\nu=1}^d \mathbf{v}_{j_{\nu-1}j_\nu}^{(\nu)},$$

with ranks \mathbf{r}^u and \mathbf{r}^v can be computed as follows:

$$\langle \mathbf{u} | \mathbf{v} \rangle_{\mathcal{T}} = \sum_{j_0=1}^{r_0^u} \cdots \sum_{j_d=1}^{r_d^u} \sum_{i_0=1}^{r_0^v} \cdots \sum_{i_d=1}^{r_d^v} \prod_{\nu=1}^d \langle \mathbf{u}_{j_{\nu-1}j_\nu}^{(\nu)} | \mathbf{v}_{i_{\nu-1}i_\nu}^{(\nu)} \rangle_{\mathcal{P}_\nu}.$$

The computational complexity is $\mathcal{O}(dnr^4)$, and can be reduced further [99].

Rank truncation in the TT format. The rank truncation operation is based on the SVD algorithm and requires $\mathcal{O}(dnr^3)$ operations [50]. The TT-rounding algorithm (p. 2305 in [101]) is based on QR decomposition and costs $\mathcal{O}(dnr^3)$.

Corollary 2.4 in [101] states that for a given tensor \mathbf{w} and rank bounds r_k , the best approximation to \mathbf{w} in the Frobenius norm with TT-ranks bounded by r_k always exist (denote it by \mathbf{w}^*), and the TT-approximation \mathbf{u} computed by the TT-SVD algorithm (p. 2301 in [101]) is quasi-optimal:

$$\|\mathbf{w} - \mathbf{u}\|_F \leq \sqrt{d-1} \|\mathbf{w} - \mathbf{w}^*\|_F. \quad (75)$$

In [80] the authors suggested a new re-compression randomised algorithm for Tucker and TT tensor formats. The rank-adaptive DMRG-cross algorithm see in [108], and its extension in [32].

5 Algorithms

This section gives the algorithms to actually compute functions from Table 3. As one may have gleaned from the preceding, very often not only the density $p_\xi(\mathbf{y})$ is of interest, but functions of density, e.g. in order to compute an f -divergence or the entropy. Below we will list algorithms, which approximate $f(p_\xi(\mathbf{y}))$ by $f(\mathbf{P})$, where

$$f(\cdot) = \{\text{sign}(\cdot), (\cdot)^{-1}, \sqrt{\cdot}, \sqrt[3]{\cdot}, (\cdot)^k, \log(\cdot), \exp(\cdot), (\cdot)^2, |\cdot|\}, \quad (76)$$

$k > 0$, and \mathbf{P} is a tensor which represents the values of $p_\xi(\mathbf{y})$ on a discretisation grid as explained in section 2.3.1, i.e. $\mathbf{P} = p_\xi(\hat{\mathbf{X}}) = \sum_{j=1}^{r_p} \bigotimes_{\nu=1}^d \mathbf{p}_{j,\nu}$. The p -th root is needed for scaling.

These algorithms are non-trivial and their detailed discussion is out of the scope of this work. Possible difficulties, which may appear are: the intermediate tensor ranks of iterates may become very large, a stable rank truncation procedure is either not available or very computationally intensive, and problems in choosing the starting value \mathbf{X}_0 .

5.1 Discrete low-rank representation and Fourier transforms

We start with the low-rank CP-format function tensor representation in Eq. (2). As each of the functions $p_{\ell,\nu}(x_\nu)$ is evaluated on the grid vector $\hat{\mathbf{x}}_\nu$ for its dimension ν (cf. Section 1 and section 2.3.1), giving $\mathbf{p}_{\ell,\nu} := p_{\ell,\nu}(\hat{\mathbf{x}}_\nu) = (p_{\ell,\nu}(\hat{x}_{1,\nu}), \dots, p_{\ell,\nu}(\hat{x}_{M_\nu,\nu})) \in \mathbb{R}^{M_\nu}$ (with grid spacing $\Delta_{x_\nu} = (\hat{x}_{M_\nu,\nu} - \hat{x}_{1,\nu})/(M_\nu - 1)$), the tensor \mathbf{P} can be approximated analogously to the low-rank function representation in the conceptually simplest CP-format, cf. Section 4:

$$\mathbf{P} \approx \tilde{\mathbf{P}} = \sum_{\ell=1}^R \bigotimes_{\nu=1}^d \mathbf{p}_{\ell,\nu}. \quad (77)$$

Applying \mathcal{F}_d to the discrete low-rank representation Eq. (77) results in

$$\boldsymbol{\Phi} := \varphi_\xi(\hat{\mathbf{T}}) \approx \tilde{\boldsymbol{\Phi}} = \mathcal{F}_d(\tilde{\mathbf{P}}) = \sum_{\ell=1}^R \bigotimes_{\nu=1}^d \mathcal{F}_1(\mathbf{p}_{\ell,\nu}) = \sum_{\ell=1}^R \bigotimes_{\nu=1}^d \boldsymbol{\varphi}_{\ell,\nu}, \quad (78)$$

with vectors $\boldsymbol{\varphi}_{\ell,\nu} = \mathcal{F}_1(\mathbf{p}_{\ell,\nu}) = \mathcal{F}_1(p_{\ell,\nu}(\hat{\mathbf{x}}_\nu)) = (\varphi_{\ell,\nu}(\hat{\mathbf{t}}_\nu)) = (\varphi_{\ell,\nu}(\hat{t}_{i_1,1}, \dots, \hat{t}_{i_d,d})) \in \mathbb{R}^{M_\nu}$, which are the samples of the low-rank component function $\varphi_{\ell,\nu}$ on the regular grid $\hat{\mathbf{t}}_\nu$ in its appropriate dimension; i.e. $\boldsymbol{\Phi}$ can be computed with $(d \times R)$ discrete 1D-Fourier transforms.

Observe that

$$\varphi_\xi(\hat{t}_{j_1^0,1}, \dots, \hat{t}_{j_d^0,d}) = \varphi_\xi(\mathbf{0}) = 1 = \int_{\mathbb{R}^d} p_\xi(\mathbf{x}) \, d\mathbf{x}. \quad (79)$$

If one were to start with the **pcf** instead and obtain a low-rank representation like Eq. (78) for the samples $\boldsymbol{\Phi}$ of φ_ξ on the grid $\hat{\mathbf{T}}$, the computations can be done in an analogous way in the other direction with the inverse discrete Fourier transform to obtain a low-rank representation like Eq. (77) for the samples \mathbf{P} of p_ξ on the grid $\hat{\mathbf{X}}$. We write this relation concisely as [55]

$$\boldsymbol{\Phi} = \mathcal{F}_d(\mathbf{P}), \text{ and } \mathbf{P} = \mathcal{F}_d^{-1}(\boldsymbol{\Phi}), \quad (80)$$

$$\boldsymbol{\varphi}_{\ell,\nu} = \mathcal{F}_1(\mathbf{p}_{\ell,\nu}), \text{ and } \mathbf{p}_{\ell,\nu} = \mathcal{F}_1^{-1}(\boldsymbol{\varphi}_{\ell,\nu}), \quad 1 \leq \ell \leq R, 1 \leq \nu \leq d. \quad (81)$$

Observe that the infinite integration domain—the whole space—for the Fourier transform in the continuous case in Subsection 2.2 in the discretisation process in a first step is shrunk to a finite hyper-rectangle in the space where the **pdf** is defined. This means that one computes a *windowed* transform with a rectangular window, functions are implicitly assumed to be periodic [16] on that finite hyper-rectangle, the **pcf** becomes an infinite sequence of discrete values, and the inverse Fourier transform from **pcf** to **pdf** now is a Fourier series. Upon truncating this infinite **pcf** sequence to a finite number of values, or alternately introducing a finite number of discrete integration points for the **pdf**, one finally arrives at the discrete Fourier transform, which is a finite series summed with the FFT algorithm in both directions. As was already remarked in Eq. (36) in section 2.3.1,

the total d -dimensional volume covered is $V = \prod_{\nu=1}^d M_{\nu} \Delta_{x_{\nu}}$, and the integration rule is implicitly the iterated trapezoidal rule on a periodic grid, hence, as was already mentioned in Eq. (48), each point carries the same integration weight V/N . In order to catch most of the “probability mass”, one may want to choose a large enough hyper-rectangle, and shift the mean $\bar{\xi}$ of the pdf into the middle of that hyper-rectangle. This means that the pdf now has a vanishing mean, i.e. one is looking at the RV $\tilde{\xi} = \xi - \bar{\xi}$ instead of ξ . In case the pcf is needed, this shift also avoids possible high-frequency modulation of the characteristic function, as from

$$\varphi_{\xi}(\mathbf{t}) = \mathbb{E}(\exp(i \langle \mathbf{t} | \xi \rangle)) = \mathbb{E}(\exp(i \langle \mathbf{t} | \tilde{\xi} + \bar{\xi} \rangle)) = \exp(i \langle \mathbf{t} | \bar{\xi} \rangle) \varphi_{\tilde{\xi}}(\mathbf{t}),$$

one may see that working with $\tilde{\xi}$ resp. $\varphi_{\tilde{\xi}}(\mathbf{t})$ avoids the modulating factor $\exp(i \langle \mathbf{t} | \bar{\xi} \rangle)$.

The effect of “rectangular windowing” by only integrating over a finite domain just alluded to, which implicitly makes functions in the pdf domain periodic [16] is an issue which has to be addressed in any serious computation. The outcome is that the two “ends” of the windowed function usually do not fit together very well, and this introduces an artificial discontinuity, with an subsequent artificially high amount of higher frequency components in the transform, so-called “spectral leakage”.

Even when the FFT is not used, this is an issue, and it can be dealt with by an additional smooth window, e.g. a cosine taper, applied to the pdf, so that the pdf vanishes smoothly at the boundary of the hyper-rectangle. Denoting the non-negative window values at the integration point by the rank-one tensor \mathbf{w} , the smoothed pdf \mathbf{P}_s is simply

$$\mathbf{P}_s = \mathbf{w} \odot \mathbf{P}. \quad (82)$$

Usually \mathbf{P}_s will not integrate to one (i.e. $\mathcal{S}(\mathbf{P}_s) < 1$), as some “probability mass” will have been cut off through the rectangular windowing from the primary \mathbf{P} , or “smoothed away” in Eq. (82), and the quantity $1 - \mathcal{S}(\mathbf{P}_s)$ can serve as an error measure for these discretisation steps. As typically there is still a residual error even after these adjustments, in the next Subsection 5.2 it is described in Eq. (84) how to correct this.

5.2 Consistency of data

Making sure the data one works with is consistent is of great importance, and should be checked before any other computations. This was already touched upon at the end of section 2.3.2 and in section 2.3.4. We recall that for the continuous case, the pdf has to be in the set \mathfrak{D} (Eq. (18)), and the pcf has to be in the set \mathfrak{C} (Eq. (23)).

The pdf is real valued, and the Fourier transform (FT) translates this into the pcf being Hermitean Eq. (26). The discrete FT preserves these properties. And as the FT is applied to the low-rank approximation without any approximation in Eq. (78), these properties are preserved also in the low-rank representation. Now checking that the pcf is Hermitean is directly not easy in the low-rank representation. On the other hand, for the pdf one only has to make sure that the imaginary part is zero — it does not even have to be represented. So this condition is most easily checked on the pdf.

The next condition is that the pdf is non-negative, and the Fourier transform (FT) translates this into the pcf being positive definite, see the relation in Eq. (27) which is preserved also by the discrete FT. It was already stated that for the pcf tensor Φ , resulting from the pdf tensor \mathbf{P} , being positive definite means that the convolution operator \mathbf{K}_{Φ} mentioned earlier in section 2.3.2 is positive definite. In section 2.3.4 it was concluded that its spectrum are the values of the pdf tensor \mathbf{P} . Hence, to check positive definiteness

is easiest by checking that $\mathbf{P} \geq 0$. It will be shown later that it is possible to compute the functions $\max(\mathbf{P})$ and $\min(\mathbf{P})$. The linear maps \mathbf{K}_Φ and $\mathbf{L}_\mathbf{P}$ are positive definite iff $\min(\mathbf{P}) \geq 0$. In case this condition is not satisfied, a possible remedy was already indicated in section 2.3.4: compute the level set function Λ_U from section 2.3.4 for the level set $U =]-\infty, 0]$, and for a corrected pdf tensor \mathbf{P}_c set

$$\mathbf{P}_c := \mathbf{P} - \Lambda_U(\mathbf{P}). \quad (83)$$

This new approximation has all the faulty negative values removed, so that $\mathbf{P}_c \geq 0$. This change will not affect the Hermitean or self-adjoint character discussed earlier. Having satisfied this condition we turn to the next, which can be affected by Eq. (83).

This condition is the requirement that the pdf integrate to unity, or equivalently (see Eq. (28)), that the pcf takes the value one at the origin. This condition should be preserved by the discrete approximation. It was already formulated at the very end of section 2.3.2, namely the requirement that $\Phi_{j^0} = \Phi_{j_1^0, \dots, j_d^0} = 1$. Completely equivalent is the condition that the discrete integral Eq. (48) of the pdf tensor is unity, i.e. $\mathcal{S}(\mathbf{P}) = 1$. In case this is not satisfied, say $\Phi_{j^0} = \mathcal{S}(\mathbf{P}) = \beta \neq 1$, for a re-scaled $\mathbf{P}^{(s)}$ one may set

$$\mathbf{P}^{(s)} := \mathbf{P}/\beta. \quad (84)$$

If one recomputes then the pcf tensor $\Phi^{(s)} = \mathcal{F}_d(\mathbf{P}^{(s)})$, it will also satisfy $\Phi_{j^0}^{(s)} = 1$.

5.3 Overview of methods to compute tensor functions

There are many methods to compute $f(\mathbf{w})$. Most of these only use the fact that the underlying structure (here of \mathcal{T}) is that of a unital C*-algebra [110]. It was already alluded to in section 2.3.4 that polynomials can trivially be computed in any unital algebra, whereas power series and Cauchy's integral can be computed in a unital C*-algebra, giving already a broad range of functions, namely the holomorphic ones. Using spectral calculus [110], the class of functions can be extended to all measurable functions, and we shall need this for some discontinuous functions like the sign.

Many algorithms developed [64] to compute functions of matrices—defined via the spectral calculus—use only operations from the underlying algebra. They can thus be used in any unital C*-algebra. Below we have adapted and listed some of the classical matrix algorithms, described in [64], for computing the tensor-functions listed above in Eq. (76).

Exponential sums to compute $\mathbf{w}^{\odot -1}$ in $[1, R]$, $1 \leq R \leq \infty$, are implemented in [17, 13]. Some other methods and estimates are developed in [49, 60, 74]. The function $\mathbf{w}^{\odot -1/2}$ was computed in [75, 74], and $\mathbf{w}^{\odot -\mu}$ in [61, 74]. A quadrature rule to compute the Dunford-Cauchy contour integral

$$f(\mathbf{w}) = \frac{1}{2\pi i} \int_{\Gamma} f(z)(z \cdot \mathbf{e} - \mathbf{w})^{\odot -1} dz$$

is presented in [42, 43, 56, 57, 84, 75]. Iterative methods of Newton and Newton-Schultz type are used in [35, 40, 34, 11, 33]. The inversion $\mathbf{w}^{\odot -1}$ in the Tucker format is done by the Newton-Schultz approximate iteration in [96].

The various TT-cross approximation algorithms are a well-known alternative to iterative methods and series expansions, and they are sketched later in Subsection 5.6. Whereas the previously mentioned algorithms work in any unital C*-algebra, the cross approximation algorithms make use of a specific representation. We focus here on the

tensor train (TT) representation. The TT-cross approximation computes a low-rank TT approximation of $f(\mathbf{w})$ for a given function $f(\cdot)$ and a tensor \mathbf{w} directly, “on the fly”. The TT-cross algorithms assume that the full tensor $\mathbf{v} := f(\mathbf{w})$ is not given explicitly, but rather as a function which can return any element $\mathbf{v}_i := f(\mathbf{w}_i)$ for a given index i . The Tucker cross algorithm to approximate $\mathbf{w}^{\odot -1}$ was used in [95]. In [117], the multigrid Cross 3D algorithm is used to calculate the Gauss polynomial. In [97], iterative methods in the Tucker format are used to compute $\mathbf{w}^{\odot 1/3}$. In [7, 36], the authors are using the cross method for the Hierarchical Tucker format to estimate various functionals of the solution in the UQ context. In [63, 84] the sinc quadrature is used to compute fractional derivatives of the d -dimensional Laplace operator. The TT-approximation of the sign function was computed in [23, 30], but the TT-ranks were large. The pointwise inverse, level sets, and sign functions are defined and computed in [33]. The pointwise inverse is required for computing the pointwise functions $\text{sign}(\mathbf{w})$ and $\sqrt{\mathbf{w}}$, [33]. The Newton algorithm for computing $\text{sign}(\mathbf{w})$ and $\exp(-\mathbf{w})$, its convergence and error analysis for hierarchical matrices were considered in [52].

5.4 Iterative methods

We want to compute $f(\mathbf{w})$ for some function $f : \mathcal{T} \rightarrow \mathcal{T}$ from the list at the beginning of this section. We describe how to do it through iteration (see also [39]). Thus we have an iteration function Ψ_f , which only uses operations from the Hadamard algebra on \mathcal{T} , and which is iterated, $\mathbf{v}_{i+1} = \Psi_f(\mathbf{v}_i)$, and converges to a fixed point $\Psi_f(\mathbf{v}_*) = \mathbf{v}_*$. When started with a \mathbf{v}_0 depending on \mathbf{w} , the fixed point is $\lim_{i \rightarrow \infty} \mathbf{v}_i = \mathbf{v}_* = \Psi_f(\mathbf{v}_*) = f(\mathbf{w})$. A Newton-type family of high-order iterative methods for some matrix functions was discussed in [3].

While performing algebraic operations on tensors in some compressed format, the tensor ranks are increasing. To keep computational cost low a tensor compression after each or after a number of algebraic operations may be necessary. We perform the *truncation* T_ϵ to low rank r with error ϵ [59, 11]. We thus allow that the algebraic operations are possibly only executed approximately.

5.4.1 Perturbed iteration

The standard iteration map Ψ_f is replaced by $T_\epsilon \circ \Psi_f$. Here one speaks about a *perturbed or truncated iteration* [62, 90, 39]. The general structure of the iterative algorithms for a post-processing task f or for an auxiliary function is shown in Algorithm 1. If the iteration

Algorithm 1 Iteration with truncation

- 1: Start with some initial *compressed* guess $\mathbf{v}_0 = \mathbf{w}$.
 - 2: $i \leftarrow 0$
 - 3: **while** *no convergence* **do**
 - 4: $\mathbf{v}_{i+1} \leftarrow T_\epsilon \circ \Psi_f(\mathbf{v}_i)$
 - 5: $i \leftarrow i + 1$
 - 6: **end while**
-

by Ψ_f is *super-linearly* convergent, the *truncated iteration* $T_\epsilon \circ \Psi_f$ will still *converge* super-linearly, but finally *stagnate* in an ϵ -neighbourhood of the fixed point \mathbf{v}_* [62]. if the iteration by Ψ_f is *linearly* convergent with *contraction* factor q , the *truncated iteration* $T_\epsilon \circ \Psi_f$ will still *converge* linearly, but finally *stagnate* in an $\epsilon/(1 - q)$ -neighbourhood of \mathbf{v}_* [90]. Ideas how to choose the starting value \mathbf{v}_0 are given in [39].

5.4.2 Iteration functions

The first function to consider is an auxiliary function which is needed for a different kind of “scaling”, namely iterated squaring or iterated inverse squaring. It will be used in subsequent algorithms. In some of the algorithms the scaling factor involves e.g. $\|\mathbf{w}\|_\infty$, we shall sketch at the end of this section how to compute that.

Computing $\mathbf{w}^{\odot m}$ for $m \in \mathbb{Z}$. This is a really simple and well known way to compute any *integer power*, and at the same time make sure that no unnecessary multiplications are performed. The Algorithm 2 computes $\mathbf{w}^{\odot m} = \Psi_{\text{pow}}(m, \mathbf{w})$ for positive and negative powers m and takes note of possibilities to use squaring. This is not really an iteration

Algorithm 2 Computing $\Psi_{\text{pow}}(m, \mathbf{w})$

Require: $(m \geq 0) \vee (\mathbf{w}^{\odot -1} \text{ exists})$.

Ensure: Output $\mathbf{v} = \mathbf{w}^{\odot m}$

```

1:  $\mathbf{v} \leftarrow \mathbf{1}$ 
2: if  $m < 0$  then
3:    $\mathbf{x} \leftarrow \mathbf{w}^{\odot -1}$ ;
4:    $n \leftarrow -m$ 
5: else
6:    $\mathbf{x} \leftarrow \mathbf{w}$ 
7:    $n \leftarrow m$ 
8: end if
9: while  $n > 0$  do
10:  if  $n$  is even then
11:     $\mathbf{x} \leftarrow \mathbf{x} \odot \mathbf{x}$ 
12:     $n \leftarrow n/2$ 
13:  else
14:     $\mathbf{v} \leftarrow \mathbf{x} \odot \mathbf{v}$ 
15:     $n \leftarrow n - 1$ 
16:  end if
17: end while

```

function to be used in Algorithm 1, but it is an auxiliary function which is used in a few other algorithms and iteration functions. For negative powers it needs $\mathbf{w}^{\odot -1}$, which is shown next.

Computing pointwise inverse $\mathbf{w}^{\odot -1}$. Let $F(\mathbf{x}) := \mathbf{w} - \mathbf{x}^{\odot -1}$. It is clear that for $\mathbf{w} = \mathbf{1}$ the solution is $F(\mathbf{1}) = \mathbf{0}$. This means that $\mathbf{v}_a = \mathbf{1}$ is one of the a priori known fixed points. Applying Newton’s method to $F(\mathbf{x})$ for approximating the inverse of a given tensor \mathbf{w} , one obtains [96] the following iteration function $\Psi_{\odot -1}$ — to be used with Algorithm 1 with the initial iterate $\mathbf{v}_0 = \alpha \cdot \mathbf{w}$ to bring \mathbf{v}_0 close to $\mathbf{v}_a = \mathbf{1}$:

$$\Psi_{\odot -1}(\mathbf{v}) = \mathbf{v} \odot (2 \cdot \mathbf{1} - \mathbf{w} \odot \mathbf{v}). \quad (85)$$

The iteration converges if the initial iterate \mathbf{v}_0 satisfies $\|\mathbf{1} - \mathbf{w} \odot \mathbf{v}_0\|_\infty < 1$. A possible candidate for the starting value is $\mathbf{v}_0 = \alpha \mathbf{w}$ with $\alpha < (1/\|\mathbf{w}\|_\infty)^2$. For such a \mathbf{v}_0 , the convergence initial condition $\|\mathbf{1} - \alpha \mathbf{w}^{\odot 2}\|_\infty < 1$ is always satisfied. As the initial iterate was scaled, the fixed point of the iteration is $\mathbf{v}_* = (1/\alpha) \cdot \mathbf{w}^{\odot -1}$, and thus the final result is $\mathbf{w}^{\odot -1} = \alpha \cdot \mathbf{v}_*$.

We did not assume that \mathbf{w} is invertible, as the iteration actually computes the pseudo-inverse (i.e. only the non-zero entries are inverted). It is easily seen from Eq. (85) that with $\mathbf{v}_0 = \alpha \mathbf{w}$ zero entries in \mathbf{w} stay zero during the iteration.

Computing pointwise $\sqrt{\mathbf{w}}$ (another notation $(\mathbf{w})^{\odot -1/2}$). Let $F(\mathbf{x}) := \mathbf{x}^{\odot 2} - \mathbf{w} = 0$. We assume that $\mathbf{w} \geq \mathbf{0}$, and again it is clear that for $\mathbf{w} = \mathbf{1}$ the solution is $F(\mathbf{1}) = \mathbf{0}$, so that $\mathbf{v}_a = \mathbf{1}$ is one of the a priori known fixed points. The Newton iteration for the above function uses the iteration function Eq. (86) together with Algorithm 1.

$$\psi_{\sqrt{}}(\mathbf{v}) = \frac{1}{2} \cdot (\mathbf{v} + \mathbf{v}^{\odot -1} \odot \mathbf{w}). \quad (86)$$

The starting value can be $\mathbf{v}_0 = (\mathbf{w} + \mathbf{1})/2$, other stating values obtained through scaling are described later.

Unfortunately, Eq. (86) contains an inverse power $\mathbf{v}^{\odot -1}$ and can thus not be computed directly only with operations from the algebra. Of course, one could use the just described algorithm for the inverse, but this would involve a nested iteration, which is mostly not so advantageous. An alternative is the well known stable inversion free Newton-Schulz iteration [64], which computes $\mathbf{v}_*^+ = \sqrt{\mathbf{w}} = \mathbf{w}^{\odot 1/2}$ and $\mathbf{v}_*^- = (\sqrt{\mathbf{w}})^{\odot -1} = \mathbf{w}^{\odot -1/2}$ at the same time. Hence we set $\mathbf{V}_0 = [\mathbf{y}_0, \mathbf{z}_0] = [\alpha \cdot \mathbf{w}, \mathbf{1}] \in \mathcal{T}^2$, and the iteration function is best written using the auxiliary function $A(\mathbf{y}, \mathbf{z}) = 3 \cdot \mathbf{1} - \mathbf{z} \odot \mathbf{y}$:

$$\psi_{\sqrt{}}\left(\begin{bmatrix} \mathbf{y} \\ \mathbf{z} \end{bmatrix}\right) = \frac{1}{2} \begin{bmatrix} \mathbf{y} \odot A(\mathbf{y}, \mathbf{z}) \\ A(\mathbf{y}, \mathbf{z}) \odot \mathbf{z} \end{bmatrix}. \quad (87)$$

The iteration converges to $\mathbf{V}_* = [\mathbf{v}_*^+, \mathbf{v}_*^-] = [\sqrt{\mathbf{y}_0}, (\sqrt{\mathbf{y}_0})^{\odot -1}]$ if $\|\mathbf{1} - \mathbf{y}_0\|_{\infty} < 1$, which can be achieved with a scaling factor $\alpha < 1/\|\mathbf{w}\|_{\infty}$. As the initial iterate was scaled, the fixed point of the iteration is $\mathbf{v}_*^+ = \sqrt{\alpha} \cdot \sqrt{\mathbf{w}}$ and $\mathbf{v}_*^- = (1/\sqrt{\alpha}) \cdot (\sqrt{\mathbf{w}})^{\odot -1}$. Thus the final result is $\sqrt{\mathbf{w}} = (1/\sqrt{\alpha}) \cdot \mathbf{v}_*^+$ and $(\sqrt{\mathbf{w}})^{\odot -1} = \sqrt{\alpha} \cdot \mathbf{v}_*^-$.

Computing $\mathbf{w}^{\odot 1/m}$ when $m \in \mathbb{N}$. This function may be needed for logarithmic scaling purposes, see Subsection 5.5. For the theory and required definitions see Section 7 in [64]. A new family of high-order iterative methods for the matrix m -th root was suggested in [4].

To compute the principal m -th root of \mathbf{w} , where it is assumed that $\mathbf{w} \geq \mathbf{0}$, one considers Newton's method for $F(\mathbf{x}) = \mathbf{x}^{\odot m} - \mathbf{w} = 0$. Again it is clear that for $\mathbf{w} = \mathbf{1}$ the solution is $F(\mathbf{1}) = \mathbf{0}$, so that $\mathbf{v}_a = \mathbf{1}$ is one of the a priori known fixed points. The iteration function with $\mathbf{v} = \mathbf{w}$ corresponding to Eq. (86) looks like

$$\psi_{m\text{-root}}(\mathbf{v}) = \frac{1}{m} ((m-1) \cdot \mathbf{v} + \psi_{\text{pow}}(1-m, \mathbf{v}) \odot \mathbf{v}_0). \quad (88)$$

If $m \geq 2$, this involves a negative power $\mathbf{v}^{\odot (1-m)} = \psi_{\text{pow}}(1-m, \mathbf{v})$. The convergence analysis is rather complicated, see more in Section 7.3, [64], but the algorithm converges for all $\mathbf{w} \geq \mathbf{0}$.

Just as there is a more stable version Eq. (87) for $m = 2$ avoiding inverses, so one has a “double iteration” [64] here as well. It is best written using the auxiliary function $A(\mathbf{y}, \mathbf{z}) = (1/m) \cdot ((m+1) \cdot \mathbf{1} - \mathbf{z})$:

$$\psi_{m\text{-root}}\left(\begin{bmatrix} \mathbf{y} \\ \mathbf{z} \end{bmatrix}\right) = \begin{bmatrix} \mathbf{y} \odot A(\mathbf{y}, \mathbf{z}) \\ \psi_{\text{pow}}(m, A(\mathbf{y}, \mathbf{z})) \odot \mathbf{z} \end{bmatrix}, \quad (89)$$

where $\mathbf{y}_i \rightarrow \mathbf{w}^{\odot -1/m}$. The starting values are $\mathbf{V}_0 = [\mathbf{y}_0, \mathbf{z}_0] = [\alpha \cdot \mathbf{1}, (\alpha)^m \mathbf{w}] \in \mathcal{T}^2$, with $\alpha < (\|\mathbf{w}\|_\infty / \sqrt{2})^{-1/m}$. For scaling purposes it is best used with $m = 2^k$.

Another way of computing the m -th root is Tsai's algorithm [114, 86], which uses the auxiliary function $B(\mathbf{y}) = (2 \cdot \mathbf{1} + (m-2) \cdot \mathbf{y}) \odot (\mathbf{1} + (m-1) \cdot \mathbf{y})^{\odot -1}$:

$$\psi_{Tsai} = \left(\begin{bmatrix} \mathbf{y} \\ \mathbf{z} \end{bmatrix} \right) = \begin{bmatrix} \mathbf{y} \odot \psi_{\text{pow}}(m, B(\mathbf{y})) \\ \mathbf{z} \odot (B(\mathbf{y})) \end{bmatrix}, \quad (90)$$

with starting value $\mathbf{V}_0 = [\mathbf{w}, \mathbf{1}]$. Then $\mathbf{z}_i \rightarrow \mathbf{w}^{\odot 1/m}$.

Computing $\text{sign}(\mathbf{w})$. The tensor $\text{sign}(\mathbf{w}) \in \mathcal{T}$ is defined pointwise for all $i \in \mathcal{I}$ by

$$(\text{sign}(\mathbf{w}))_i := \begin{cases} 1, & \mathbf{w}_i > 0; \\ -1, & \mathbf{w}_i < 0; \\ 0, & \mathbf{w}_i = 0. \end{cases} \quad (91)$$

The equation to be used for the Newton iteration is $F(\mathbf{x}) := \mathbf{x} \odot \mathbf{x} - \mathbf{1}$. With starting value $\mathbf{v}_0 = \mathbf{w}$ we obtain the following iteration function:

$$\psi_{\text{sign}}(\mathbf{v}) = \frac{1}{2}(\mu \cdot \mathbf{v} + \frac{1}{\mu} \cdot \mathbf{v}^{\odot -1}), \quad (92)$$

with $\mu = \|\mathbf{v}^{\odot -1}\|_\infty / \|\mathbf{v}\|_\infty$ (see Section 8.6 in [64]). This method converges to $\text{sign}(\mathbf{w})$.

Alternatively, one can rewrite this iteration function without computing $\mathbf{v}^{\odot -1}$, namely

$$\psi_{NS}(\mathbf{v}) = \frac{1}{2} \cdot \mathbf{v} \odot (3 \cdot \mathbf{1} - \mathbf{v} \odot \mathbf{v}), \quad (93)$$

with starting value $\mathbf{v}_0 = \alpha \cdot \mathbf{w}$, where $\alpha = \|\mathbf{w}^{\odot -1}\|_\infty / \|\mathbf{w}\|_\infty$. The last formula is called the Newton-Schulz iteration, it has quadratic (local) convergence to $\text{sign}(\mathbf{w})$ [35, 33, 38, 64].

Computing the absolute value $|\mathbf{w}|$ is simple if $\text{sign}(\mathbf{w})$ is available (see above): Having the $\text{sign}(\cdot)$ function, we can compute the absolute value, characteristic function of a set, and the level set function, see section 5.4.2:

$$|\mathbf{w}| = \mathbf{w} \odot \text{sign}(\mathbf{w}).$$

Computing the characteristic function of a set is done by using the shifted sign-function [37, 38, 39]. The *characteristic* function of $\mathbf{w} \in \mathcal{T}$ in an interval $I \subset \mathbb{R}$ is a tensor $\chi_I(\mathbf{w}) \in \mathcal{T}$. It is defined for every multi- index $i \in \mathcal{I}$ pointwise as

$$(\chi_I(\mathbf{w}))_i := \begin{cases} 1, & \mathbf{w}_i \in I; \\ 0, & \mathbf{w}_i \notin I. \end{cases} \quad (94)$$

Let $a, b \in \mathbb{R}$. If $I = (-\infty, b)$, then $\chi_I(\mathbf{w}) = \frac{1}{2}(\mathbf{1} + \text{sign}(b\mathbf{1} - \mathbf{w}))$. If $I = (a, +\infty)$, then $\chi_I(\mathbf{w}) = \frac{1}{2}(\mathbf{1} - \text{sign}(a\mathbf{1} - \mathbf{w}))$. And if $I = [a, b]$, then

$$\chi_I(\mathbf{w}) = \frac{1}{2}(\text{sign}(b\mathbf{1} - \mathbf{w}) - \text{sign}(a\mathbf{1} - \mathbf{w})).$$

Computing the level set function of a set is done by using the characteristic function [37, 38, 39]:

$$\Lambda_U(\mathbf{w}) = \chi_U(\mathbf{w}) \odot \mathbf{w}.$$

Computing $\|\mathbf{w}\|_\infty = \max \mathbf{w} = \varrho(\mathbf{w})$ and $\min \mathbf{w}$. We need these values in almost every algorithm above and for checking the consistency. For instance, if $\min \mathbf{w} \geq \mathbf{0}$ then $\mathbf{w} \geq \mathbf{0}$. It was already pointed out that $\|\mathbf{w}\|_\infty = \max \mathbf{w} = \varrho(\mathbf{w})$ is the largest—by magnitude—eigenvalue of the associated linear operator $\mathbf{L}_\mathbf{w} : \mathbf{v} \mapsto \mathbf{w} \odot \mathbf{v}$, and thus iterative eigenvalue algorithms can be used to compute it. One of the simplest is the power iteration. It can be modified in this special case here to greatly increase its convergence speed, essentially by repeated squaring. The modified power iteration algorithm is described in [53, 39]. The convergence is *exponential* with the rate $|\lambda_2/\lambda_1|^{2^i}$, where λ_1 and λ_2 are the largest and the second largest eigenvalues of $\mathbf{L}_\mathbf{w}$.

To compute $\min \mathbf{w}$ (the smallest eigenvalue) or some intermediate eigenvalues of $\mathbf{L}_\mathbf{w}$ resp. \mathbf{w} we suggest to use the well-known shifting or inverse shifting functions [33, 39]. These and similar techniques are well known from eigenvalue calculations of large / sparse symmetric matrices [45, 103, 105, 120].

5.5 Series expansions

Computing $\log(\mathbf{w})$. We assume that $\mathbf{w} > 0$. Various algorithms, improvement ideas, stability issues and tricks to compute $\log(\mathbf{w})$ are discussed in [20]. Improved inverse scaling and squaring algorithms for the matrix logarithm were suggested later in [2]. We suggest to follow these works for the case when \mathbf{w} is a tensor. The stability of the matrix arithmetic-geometric mean iterations for computing the matrix logarithm is investigated in [19]. For the algorithms to work well, \mathbf{w} has to be close to the identity $\mathbf{1}$, which can be achieved by taking roots: for $\lambda \in [-1, 1]$ one has $\log(\mathbf{w}^\lambda) = \lambda \log \mathbf{w}$.

From matrix calculus it is known [20, 2] that one of the ways (for \mathbf{w} close to the identity) to compute $\log(\mathbf{w})$ is to truncate the Taylor series (radius of convergence $\|\mathbf{x}\|_\infty < 1$):

$$\log(\mathbf{1} - \mathbf{x}) = - \sum_{n=1}^{\infty} \frac{1}{n} \cdot \mathbf{x}^{\odot n}$$

where $\mathbf{x} := \mathbf{1} - \mathbf{w}$. If \mathbf{w} is not near to the identity, then one may use the relation $\log(\mathbf{w}) = 2^k \log(\mathbf{w}^{\odot 1/2^k})$, where $\mathbf{w}^{\odot 1/2^k} \rightarrow \mathbf{1}$ as k increases [69].

Another way to compute the logarithm of a positive \mathbf{w} is Gregory's series [64], which converges for all $\mathbf{w} > 0$. Setting $\mathbf{z} = (\mathbf{1} - \mathbf{w}) \odot (\mathbf{1} + \mathbf{w})^{\odot -1}$, one has

$$\log \mathbf{w} = -2 \sum_{k=0}^{\infty} \frac{1}{2k+1} \cdot \mathbf{z}^{\odot (2k+1)}. \quad (95)$$

Obviously, \mathbf{z} involves an inverse, but it has to be computed only once. We note that the tensor ranks (according to Section 4.2) in Eq. (95) may increase very fast. For instance, a naive calculation of \mathbf{w} in Eq. (95) (without the rank truncation procedure) results in the tensor rank $3^6 = 729$ even for a few terms.

Computing $\exp \mathbf{w}$. One of the standard algorithms using power series together with scaling and squaring is explained in [64] (Chapter 10):

$$\mathbf{u}_{r,s} = \left(\sum_{k=0}^r \frac{1}{k! s^k} \mathbf{w}^{\odot k} \right)^{\odot s}. \quad (96)$$

Here $\lim_{r \rightarrow \infty} \mathbf{u}_{r,s} = \lim_{s \rightarrow \infty} \mathbf{u}_{r,s} = \exp \mathbf{w}$. It is of advantage to use s from the series of powers of 2, $s = 1, 2, 4, \dots, 2^k$, then the s -th power can be computed by squaring. For the scaling the best choice is $\alpha > \|\mathbf{w}\|_\infty$.

5.6 Direct approximation of $\mathbf{v} := f(\mathbf{w})$

In this section, we discuss the so-called cross algorithms [100, 7, 25, 24]. Some extensions of the TT-Cross and ALS-Cross algorithms (e.g. the AMEn algorithm) were suggested by S. Dolgov and co-authors, and can be found here [28].

A general cross algorithm computes the following TT-representation, see Subsection 4.2, the definition Eq. (71), and in particular Eq. (72):

$$f(\mathbf{w}) = \mathbf{v}(\alpha_1, \dots, \alpha_M) = \sum_{s_1=1}^{r_1} \sum_{s_2=1}^{r_2} \dots \sum_{s_{M-1}=1}^{r_{M-1}} \mathbf{v}_{s_0, s_1}^{(1)}(\alpha_1) \mathbf{v}_{s_1, s_2}^{(2)}(\alpha_2) \dots \mathbf{v}_{s_{M-1}, s_M}^{(M)}(\alpha_M). \quad (97)$$

For analytic $f(\cdot)$ the TT-ranks often depend only logarithmically on the accuracy [71, 109].

These algorithms are an alternative to iterations and series expansions, they are tailored specifically to low-rank approximations in a particular tensor format. They allow one to compute a low-rank approximation of $\mathbf{v} = f(\mathbf{w})$ for a given function $f(\cdot)$ and a tensor \mathbf{w} directly, “on the fly”. We assume here that the full tensor $\mathbf{v} := f(\mathbf{w})$ is not given explicitly, but rather as a function which can return any element $\mathbf{v}_i := f(\mathbf{w}_i)$ of \mathbf{v} .

For example, the AMEn algorithm can compute the representation Eq. (97) using only $\mathcal{O}(dnr^2)$ entries of \mathbf{v} and $\mathcal{O}(dnr^3)$ additional arithmetic operations. The pseudocode is listed in [24]. It is based on the skeleton decomposition (another name is adaptive cross approximation) of a matrix [47, 9, 8], and the *maxvol* algorithms [46]. The idea of the *maxvol* algorithms is to find a rank- r matrix approximation A_r of a $n \times m$ matrix A , the rank of which is r . The *maxvol* algorithm suggests to select among all $r \times r$ submatrices the one that has the largest volume (determinant). The computational complexity is $\mathcal{O}(r(n+m))$, and the approximation error $\|A - A_r\|_\infty \leq (r+1)\sigma_{r+1}$, where σ_{r+1} is the $(r+1)$ -th singular value of A .

6 Numerical examples

A few numerical examples are provided to validate and show the power of the proposed approach. This includes a validation example, where Kullback-Leibler divergences (KLD) are computed with well known analytical formulas and the `amen_cross` algorithm [32, 108] from the TT-toolbox for d -dimensional Gaussian `pdfs` are compared, as well as the Hellinger distances again computed with well-known analytical formulas and the `amen_cross` algorithm. To show the approach on a distribution where the `pdf` is not known analytically, the d -variate elliptically contoured α -stable distributions are chosen and accessed via their `pcfs`, and again KLD and Hellinger distances for different value of d , n and the parameter α are computed.

For the numerical tests below we used the Matlab package *TT-Toolbox* [101], which is well known in the tensor community. To compute $f(\mathbf{w})$, we use the *alternating optimization with enrichment (AMEn)* method [32], provided in the TT-toolbox library. This is a block cross algorithm with an error-based enrichment. It tries to interpolate the function $f(\mathbf{w})$ via the error-enriched *maxvol-cross* method. All computations are done on a MacBook Pro computer produced in 2018, equipped with 6-Core Intel Core i7, 2.2 GHz, and 16 GB RAM. We started by computing the point-wise inverse, squared root, and exponent of a given discretised `pdf` represented as a TT tensor. For this, iterative methods, series expansions, and the AMEn algorithm [32, 108] were used in order to make sure that the AMEn method gives the same results as other methods.

The first Example 6.1 is a validation example, where the analytical formula for the KLD is known analytically. This exact value is compared with the approximate KLD

(denoted by $\widetilde{D}_{\text{KL}}$) for high values of d and n . One may observe that they are almost the same. Additionally, the absolute error ($\text{err}_a := |D_{\text{KL}} - \widetilde{D}_{\text{KL}}|$) as well as the relative error ($\text{err}_r := |D_{\text{KL}} - \widetilde{D}_{\text{KL}}|/|D_{\text{KL}}|$) and the computing times (last row) are shown.

Example 6.1 (Validation example 1 — KLD). *Consider two Gaussian distributions $\mathcal{N}_1 := \mathcal{N}(\boldsymbol{\mu}_1, \mathbf{C}_1)$ and $\mathcal{N}_2 := \mathcal{N}(\boldsymbol{\mu}_2, \mathbf{C}_2)$, where $\mathbf{C}_1 := \sigma_1^2 \mathbf{I}$, $\mathbf{C}_2 := \sigma_2^2 \mathbf{I}$, $\boldsymbol{\mu}_1 = (1.1 \dots, 1.1)$ and $\boldsymbol{\mu}_2 = (1.4, \dots, 1.4) \in \mathbb{R}^d$, $d = \{16, 32, 64\}$, \mathbf{I} is the identity matrix, and $\sigma_1 = 1.5$, $\sigma_2 = 22.1$. The well known analytical formula is [102]*

$$D_{\text{KL}}(\mathcal{N}_1 \parallel \mathcal{N}_2) = \frac{1}{2} \left(\text{tr}(\mathbf{C}_2^{-1} \mathbf{C}_1) + (\boldsymbol{\mu}_2 - \boldsymbol{\mu}_1)^T \mathbf{C}_2^{-1} (\boldsymbol{\mu}_2 - \boldsymbol{\mu}_1) - d + \log \left(\frac{|\mathbf{C}_2|}{|\mathbf{C}_1|} \right) \right). \quad (98)$$

After discretisation of the two *pdfs*, one obtains the tensors \mathbf{P} and \mathbf{Q} (see Eq. (77)). Then the KLD $\widetilde{D}_{\text{KL}}$ is computed as in Table 2. The results are summarised in Table 4.

d	16	32	64
n	2048	2048	2048
D_{KL} (exact)	35.08	70.16	140.32
$\widetilde{D}_{\text{KL}}$	35.08	70.16	140.32
err_a	4.0e-7	2.43e-5	1.4e-5
err_r	1.1e-8	3.46e-8	8.1e-8
comp. time, sec.	1.0	5.0	18.7

Table 4: D_{KL} computed via TT tensors (AMEn algorithm) and the analytical formula Eq. (98) for various values of d . TT tolerance = 10^{-6} , the stopping difference between consecutive iterations.

An important ingredient of the KLD computation is the $f(\cdot) = \log(\cdot)$ function, which can be computed via the AMEn method (see Subsection 5.6), or the Gregory series Eq. (95). We observed that the TT ranks are increasing very fast in the Gregory series Eq. (95), and it is not so transparent how and when to truncate them. Therefore, we recommend using the AMEn algorithm in the TT Toolbox, and the small absolute err_a and relative err_r errors show that the AMEn method can be used for computing the KLD.

The next validation test is with the Hellinger distance:

Example 6.2 (Validation example 2 — Hellinger distance). *For the Gaussian distributions from Example 6.1, the Hellinger distances computed via the AMEn algorithm—denoted by \widetilde{D}_H —and the analytical formula Eq. (99) denoted by D_H are compared in Table 5. The squared Hellinger distances for two multi-variate Gaussian distributions can be computed analytically as follows (see p.51 and p.45 in [102]):*

$$D_H(\mathcal{N}_1, \mathcal{N}_2)^2 = 1 - K_{1/2}(\mathcal{N}_1, \mathcal{N}_2), \quad \text{where} \quad (99)$$

$$K_{1/2}(\mathcal{N}_1, \mathcal{N}_2) = \frac{\det(\mathbf{C}_1)^{1/4} \det(\mathbf{C}_2)^{1/4}}{\det\left(\frac{\mathbf{C}_1 + \mathbf{C}_2}{2}\right)^{1/2}} \cdot \exp\left(-\frac{1}{8}(\boldsymbol{\mu}_1 - \boldsymbol{\mu}_2)^\top \left(\frac{\mathbf{C}_1 + \mathbf{C}_2}{2}\right)^{-1} (\boldsymbol{\mu}_1 - \boldsymbol{\mu}_2)\right) \quad (100)$$

d	16	32	64
n	2048	2048	2048
D_H (exact)	0.99999	0.99999	0.99999
\tilde{D}_H	0.99992	0.99999	0.99999
err_a	3.5e-5	7.1e-5	1.4e-4
err_r	2.5e-5	5.0e-5	1.0e-4
comp. time, sec.	1.7	7.5	30.5

Table 5: The Hellinger distance D_H computed via TT tensors (AMEn algorithm) and the analytical formula Eq. (99) for various values of d . TT tolerance = 10^{-6} . The Gaussian mean values and covariance matrices are defined in Example 6.1.

The results in Table 5 show that the AMEn algorithm is able to compute the D_H Hellinger distance between two multivariate Gaussian distributions for large dimensions $d = \{16, 32, 64\}$, and for large $n = 2048$. The exact and approximate values are identical, and the error is small. The absolute and relative errors (err_a , err_r) can be further decreased by taking a smaller TT tolerance.

After these validation tests, we choose the d -variate elliptically contoured α -stable distribution, where no analytical formula for the pdf is known, and which generalises the normal law. These distributions have heavy tails and are often used for modelling financial data [92]. We access the distribution in the next example 6.3 through its pcf, which is known analytically Eq. (101).

Example 6.3 (α -stable distribution). *The pcf of a d -variate elliptically contoured α -stable distribution is given by*

$$\varphi_{\xi}(\mathbf{t}) = \exp \left(i \langle \mathbf{t} | \boldsymbol{\mu} \rangle - \langle \mathbf{t} | \mathbf{C} \mathbf{t} \rangle^{\alpha/2} \right). \quad (101)$$

We approximate $\varphi_{\xi}(\mathbf{t})$ as in Eq. (6), but in the TT format Eq. (71) and Eq. (97). The tolerance used in the AMEn algorithm is 10^{-9} . Further, from the inversion theorem, the pdf of ξ on \mathbb{R}^d can be computed as in Eq. (7) via the FFT.

We start by computing the KLD between two α -stable distributions for fixed $\alpha_1 = 2.0$, $\alpha_2 = 1.9$ (with $\boldsymbol{\mu}_1 = \boldsymbol{\mu}_2 = 0$, $\mathbf{C}_1 = \mathbf{C}_2 = \mathbf{I}$); the results are summarised in Table 6. From

d	16	16	16	16	16	16	16	32	32	32
n	8	16	32	64	128	256	512	64	128	256
$D_{\text{KL}}(2.0, 1.9)$	0.016	0.059	0.06	0.062	0.06	0.06	0.06	0.09	0.14	0.12
comp. time, sec.	0.8	3	8.9	14	22	61	207	46	100	258
max. TT rank	40	57	79	79	59	79	77	80	78	79
memory, MB	1.8	7	34	54	73	158	538	160	313	626

Table 6: Computation of $D_{\text{KL}}(\alpha_1, \alpha_2)$ for between two α -stable distributions for $\alpha_1 = 2.0$, $\alpha_2 = 1.9$, and different d and n . The AMEn tolerance is 10^{-9} .

Table 6 one may see that $n = 32$ (for $d = 16$) is sufficient, and there is no need to take a higher resolution n , the KLD value is (almost) not changing. One may also see that for $d = 32$ one needs to take $n = 256$ or higher, but a higher n requires more memory.

These values in the last column in Table 6, namely $d = 32$ and $n = 256$, can be used to illustrate the amount of data and computation which would be involved in a—here

impossible—full representation. The values $d = 32$ and $n = 256$ mean that the amount of data in full storage mode would be $N = n^d = 265^{32} \approx 1.16\text{E}77$, and assuming 8 bytes per entry, this would be ca. 1E78 bytes. Compare this to the estimated number of hadrons in the universe (1E80), to see that alone the storage of such an object is not possible in full mode, whereas in a TT-low-rank approximation it did not require more than ca. 626MB, and fits on a laptop. And as for the computation of the Kullback-Leibler divergence (KLD) shown in that table, assume that the computation of the logarithms per data point could be achieved at a rate of 1GHz. Then the KLD computation in full mode would require ca. 1.2E68sec, or more than 3E60 years, and even with a perfect speed-up on a parallel super-computer with say 1,000,000 processors, this would require still more than 3E54 years; compare this with the estimated age of the universe of ca. 1.4E10 years.

Continuing our tests, in Table 7 the KLD $D_{\text{KL}}(\alpha_1, \alpha_2)$ between two α -stable distributions for different pairs of (α_1, α_2) and fixed $d = 8$ and $n = 64$ is computed. The mean and covariance matrices were taken $\boldsymbol{\mu}_1 = \boldsymbol{\mu}_2 = 0$, $\mathbf{C}_1 = \mathbf{C}_2 = \mathbf{I}$. The tolerance for the AMEn algorithm was 10^{-12} . These results demonstrate that a TT approximation is possible (although the TT ranks are not so small) for various values of the parameters α in Eq. (101).

(α_1, α_2)	(2.0, 0.5)	(2.0, 1.0)	(2.0, 1.5)	(2.0, 1.9)	(1.5, 1.4)	(1.0, 0.4)
$D_{\text{KL}}(\alpha_1, \alpha_2)$	2.27	0.66	0.3	0.03	0.031	0.6
comp. time, sec.	8.4	7.8	7.5	8.5	11	8.7
max. TT rank	78	74	76	76	80	79
memory, MB	28.5	28.5	27.1	28.5	35	29.5

Table 7: Computation of $D_{\text{KL}}(\alpha_1, \alpha_2)$ between two α -stable distributions for various α with fixed $d = 8$ and $n = 64$. AMEn tolerance is 10^{-12} . $\boldsymbol{\mu}_1 = \boldsymbol{\mu}_2 = 0$, $\mathbf{C}_1 = \mathbf{C}_2 = \mathbf{I}$.

From the Kullback-Leibler divergence we turn again to the computation of the Hellinger distance, this time for the d -variate elliptically contoured α -stable distribution. Table 8 shows the Hellinger distance $D_H(\alpha_1, \alpha_2)$ computed for two different α -stable distributions with values of $\alpha = 1.5$ and $\alpha = 0.9$ for different d and n . The mean values and the covariances are the same $\boldsymbol{\mu}_1 = \boldsymbol{\mu}_2 = 0$, $\mathbf{C}_1 = \mathbf{C}_2 = \mathbf{I}$. The maximal TT ranks and the computation times are comparable to the KLD case in Table 6.

d	16	16	16	16	16	16	32	32	32	32
n	8	16	32	64	128	256	16	32	64	128
$D_H(1.5, 0.9)$	0.218	0.223	0.223	0.223	0.219	0.223	0.180	0.176	0.175	0.176
comp. time, sec.	2.8	3.7	7.5	19	53	156	11	21	62	117
max. TT rank	79	76	76	76	79	76	75	71	75	74
memory, MB	7.7	17	34	71	145	283	34	66	144	285

Table 8: Computation of $D_H(\alpha_1, \alpha_2)$ between two α -stable distributions for different d and n . AMEn tolerance is 10^{-9} . $\boldsymbol{\mu}_1 = \boldsymbol{\mu}_2 = 0$, $\mathbf{C}_1 = \mathbf{C}_2 = \mathbf{I}$.

To show the influence of the TT (AMEn) tolerance, in Table 9 shows the D_H distance computed with different TT (AMEn) tolerances. Additionally, the maximal tensor rank (there are d ranks in total), the computing times, and the required storage cost are provided.

TT(AMEn) tolerance	10^{-7}	10^{-8}	10^{-9}	10^{-10}	10^{-14}
$D_H(1.5, 0.9)$	0.1645	0.1817	0.176	0.1761	0.1802
comp. time, sec.	43	86	103	118	241
max. TT rank	64	75	75	78	77
memory, MB	126	255	270	307	322

Table 9: Computation of $D_H(\alpha_1, \alpha_2)$ between two α -stable distributions ($\alpha = 1.5$ and $\alpha = 0.9$) for different AMEn tolerances. $n = 128$, $d = 32$, $\boldsymbol{\mu}_1 = \boldsymbol{\mu}_2 = 0$, $\mathbf{C}_1 = \mathbf{C}_2 = \mathbf{I}$.

A note about software. Several tensor toolboxes developed for low-rank tensor calculus are available. The CP and Tucker decompositions are implemented in the Tensor Toolbox [5, 6, 1], and in the Tensorlab [118, 22]. The TT and QTT tensor formats are implemented in TT-toolbox [101]. The hierarchical Tucker tensor format is realised in the Hierarchical Tucker Toolbox `htucker toolbox` [82]. For a more detailed overview, see [54, 76]. Almost all available implementations (e.g. TT-toolbox and htucker) are have been used to solve (stochastic) PDEs [27], integral equations, linear systems in tensor format, or to perform arithmetic operations such as the scalar product, addition, etc. But, to the best of our knowledge, we do not know any attempts for computing the KLD and other divergences or distances, or the entropy of high-dimensional probability distributions.

7 Conclusion

The task considered here was the numerical computation of characterising statistics of high-dimensional probability density functions (**pdfs**), as well as their divergences and distances, where the **pdf** in the numerical implementation was assumed discretised on some regular grid. Even for moderate dimension d , the full storage and computation with such objects become very quickly infeasible.

We have demonstrated that high-dimensional probability density functions (**pdfs**), probability characteristic functions (**pcfs**), and some functions of them can be approximated and represented in a low-rank tensor data format. Utilisation of low-rank tensor techniques helps to reduce the computational complexity and the storage cost from exponential $\mathcal{O}(n^d)$ to linear in the dimension d , e.g. $\mathcal{O}(dnr^2)$ for the TT format. Here n is the number of discretisation points in one direction, $r \ll n$ is the maximal tensor rank, and d the problem dimension. The particular data format is rather unimportant, any of the well-known tensor formats (CP, Tucker, hierarchical Tucker, tensor-train (TT)) can be used, and we used the TT data format. Much of the presentation and in fact the central train of discussion and thought is actually independent of the actual representation.

In the beginning in Section 1 it was motivated through three possible ways how one may arrive at such a representation of the **pdf**. One was if the **pdf** was given in some approximate analytical form, e.g. like a function tensor product of lower-dimensional **pdfs** with a product measure, or from an analogous representation of the **pcf** and subsequent use of the Fourier transform, or from a low-rank functional representation of a high-dimensional random variable (RV), again via its **pcf**. The theoretical underpinnings of the relation between **pdfs** and **pcfs** as well as their properties were recalled in Section 2, as they are important to be preserved in the discrete approximation. This also introduced the concepts of the convolution and of the point-wise multiplication Hadamard algebra, concepts which become especially important if one wants to characterise sums

of independent random variables (RVs) or mixture models, a topic we did not touch on for the sake of brevity but which follows very naturally from the developments here. Especially the Hadamard algebra is also important for the algorithms to compute various point-wise functions in the sparse formats. The Section 2, as well as the following Section 3 and Section 5 are actually completely independent of any particular discretisation and representation of the data

Some statistics, divergences, and distance measures were collected in Section 3 together with the abstract discrete expressions on how to compute them numerically, independent of any particular numerical representation. To demonstrate our idea, one of the easiest tensor formats—the CP tensor format—was described first in Section 4. In the numerical part, we used the tensor-train (TT) format, which is also sketched in Section 4, together with how to implement the operations of the Hadamard algebra. As Section 3 shows, point-wise functions are required in order to compute the desired statistics, and some algorithms to actually perform this in an algebra were collected in Section 5. These were originally developed for matrix algebra algorithms [64], but they work just as well in any other associative C^* -algebra. In using such algorithms, one assumes that the ranks of the involved tensors are not increasing strongly during iterations and linear algebra operations.

In the numerical computations in Section 6, the first example is one where the analytic answer was known, and this validates the approach and shows the accuracy of the low-rank computation in the computation of Kullback-Leibler divergences (KLD) and Hellinger distances, which were taken as examples of characterising functionals resp. statistics. As a more taxing problem, we then took elliptically contoured α -stable distributions to evaluate the KLD and Hellinger distances between them. For these distributions, the pdf is not known analytically, but the pcf is, which we took as our starting point. The AMEn TT-Cross algorithm [23, 24] was used to compute the low-rank approximations, and the pdfs were then computed via FFT. This also nicely demonstrates the smooth integration of the FFT into low-rank tensor formats, and made it subsequently possible to compute the required quantities.

In total, these examples showed the viability of this concept, namely that it is possible to numerically operate on discretised versions of high-dimensional distributions with a reasonable computational expense, whereas in a full format the computations would not have been feasible at all. All that we required was that the data in its discretised form can be considered as an element of a commutative C^* -algebra with an inner product, where the algebra operations only have to be numerically computed in an approximative fashion. Such an algebra is isomorphic to a commutative sub-algebra of the usual matrix algebra, allowing the use of matrix algorithms.

Acknowledgments

The research reported in this publication was partly supported by funding from the Alexander von Humboldt Foundation (AvH), the Deutsche Forschungsgemeinschaft (DFG), and a Gay-Lussac Humboldt Research Award. We also would like to thank Sergey Dolgov (University of Bath, UK) for his assistance with the TT-toolbox.

References

- [1] E. Acar, D. M. Dunlavy, and T. G. Kolda, *A scalable optimization approach for fitting canonical tensor decompositions*, Journal of Chemometrics **25** (2011), no. 2, 67–86, doi:10.1002/cem.1335.
- [2] A. H. Al-Mohy and N. J. Higham, *Improved inverse scaling and squaring algorithms for the matrix logarithm*, SIAM Journal on Scientific Computing **34** (2012), no. 4, C153–C169, doi:10.1137/110852553.
- [3] S. Amat, S. Busquier, and A. A. Magrenan, *On a Newton-type family of high-order iterative methods for some matrix functions*, AIP Conference Proceedings **1978** (2018), no. 1, 330005, doi:10.1063/1.5043941.
- [4] S. Amat, J. A. Ezquerro, and M. A. Hernandez-Veron, *On a new family of high-order iterative methods for the matrix p -th root*, Numerical Linear Algebra with Applications **22** (2015), no. 4, 585–595, doi:10.1002/nla.1974.
- [5] B. W. Bader and T. G. Kolda, *Algorithm 862: MATLAB tensor classes for fast algorithm prototyping*, ACM Transactions on Mathematical Software **32** (2006), no. 4, 635–653, doi:10.1145/1186785.1186794.
- [6] B. W. Bader, T. G. Kolda, et al., *Matlab tensor toolbox version 2.6*, Available online, February 2015, Available from: <http://www.sandia.gov/~tgkolda/TensorToolbox/>.
- [7] J. Ballani and L. Grasedyck, *Hierarchical tensor approximation of output quantities of parameter-dependent PDEs*, SIAM/ASA Journal on Uncertainty Quantification **3** (2015), 852–872, doi:10.1137/140960980.
- [8] M. Bebendorf, *Adaptive cross approximation of multivariate functions*, Constructive approximation **34** (2011), no. 2, 149–179, doi:10.1007/s00365-010-9103-x.
- [9] M. Bebendorf and S. Rjasanow, *Adaptive low-rank approximation of collocation matrices*, Computing **70** (2003), no. 1, 1–24. MR MR1972724 (2004a:65177)
- [10] D. Belomestny and L. Iosipoi, *Fourier transform MCMC, heavy-tailed distributions, and geometric ergodicity*, Mathematics and Computers in Simulation **181** (2021), 351–363, doi:10.1016/j.matcom.2020.10.005.
- [11] U. Benedikt, H. Auer, M. Espig, W. Hackbusch, and A. A. Auer, *Tensor representation techniques in post-Hartree–Fock methods: matrix product state tensor format*, Molecular Physics **111** (2013), no. 16–17, 2398–2413, doi:10.1080/00268976.2013.798433.
- [12] P. Benner, M. Ohlberger, A. Cohen, and K. Willcox, *Model reduction and approximation*, Society for Industrial and Applied Mathematics, Philadelphia, PA, 2017, doi:10.1137/1.9781611974829.
- [13] G. Beylkin and L. Monzon, *On approximation of functions by exponential sums*, Applied and Computational Harmonic Analysis **19** (2005), 17–48, doi:10.1016/j.acha.2005.01.003.

- [14] J. Biamonte and V. Bergholm, *Quantum tensor networks in a nutshell* [online], arXiv: 1708.00006 [quant-ph], July 2017, Available from: <https://arxiv.org/abs/1708.00006>, arXiv:1708.00006.
- [15] D. Bigoni, A. P. Engsig-Karup, and Y. M. Marzouk, *Spectral tensor-train decomposition*, SIAM Journal on Scientific Computing **38** (2016), no. 4, A2405–A2439, doi:10.1137/15M1036919.
- [16] R. N. Bracewell, *The Fourier transform and its applications*, McGraw-Hill, New York, NY, 1978.
- [17] D. Braess and W. Hackbusch, *Approximation of $1/x$ by exponential sums in $[1, \infty[$* , IMA Journal of Numerical Analysis **25** (2005), 685–697, doi:10.1093/imanum/dri015.
- [18] J. C. Bridgeman and C. T. Chubb, *Hand-waving and interpretive dance: An introductory course on tensor networks*, J. Phys. A: Math. Theor. **50** (2017), 223001, doi:10.1088/1751-8121/aa6dc3.
- [19] J. R. Cardoso and R. Ralha, *Matrix arithmetic-geometric mean and the computation of the logarithm*, SIAM Journal on Matrix Analysis and Applications **37** (2016), no. 2, 719–743, doi:10.1137/140998226.
- [20] S. H. Cheng, N. J. Higham, C. S. Kenney, and A. J. Laub, *Approximating the logarithm of a matrix to specified accuracy*, SIAM Journal on Matrix Analysis and Applications **22** (2001), no. 4, 1112–1125, doi:10.1137/S0895479899364015.
- [21] A. Cichocki, , and S. Sh. Amari, *Adaptive blind signal and image processing: Learning algorithms and applications*, Wiley, 2002.
- [22] L. De Lathauwer, B. De Moor, and J. Vandewalle, *A multilinear singular value decomposition*, SIAM J. Matrix Anal. Appl. **21** (2000), 1253–1278.
- [23] S. Dolgov, B. N. Khoromskij, A. Litvinenko, and H. G. Matthies, *Polynomial chaos expansion of random coefficients and the solution of stochastic partial differential equations in the tensor train format*, IAM/ASA J. Uncertainty Quantification **3** (2015), no. 1, 1109–1135.
- [24] S. Dolgov, A. Litvinenko, and D. Liu, *Kriging in tensor train data format*, Proceedings, 3rd International Conference on Uncertainty Quantification in Computational Sciences and Engineering, 2019, pp. 309–329, Available from: https://files.eccomasproceedia.org/papers/e-books/uncecomp_2019.pdf, doi:10.7712/120219.6343.18651.
- [25] S. Dolgov and R. Scheichl, *A hybrid Alternating Least Squares - TT Cross algorithm for parametric PDEs* [online], arXiv: 1707.04562 [math.NA], 2017, Available from: <http://arxiv.org/abs/1707.04562>, arXiv:1707.04562.
- [26] S. V. Dolgov, B. N. Khoromskij, and D. V. Savostyanov, *Superfast Fourier transform using QTT approximation*, J. Chem. Phys. **18** (2012), no. 5, 915–953.
- [27] S. Dolgov, *Additional UQ and statistical procedures for TT-toolbox*, 2021, Available from: <https://people.bath.ac.uk/sd901/research/software/>.

- [28] ———, *Tensor Train ALS-cross algorithm and experiments*, 2021, Available from: <https://people.bath.ac.uk/sd901/als-cross-algorithm/>.
- [29] S. Dolgov, K. Anaya-Izquierdo, C. Fox, and R. Scheichl, *Approximation and sampling of multivariate probability distributions in the tensor train decomposition*, *Statistics and Computing* **30** (2020), no. 3, 603–625, [doi:10.1007/s11222-019-09910-z](https://doi.org/10.1007/s11222-019-09910-z).
- [30] S. Dolgov, B. N. Khoromskij, A. Litvinenko, and H. G. Matthies, *Computation of the response surface in the tensor train data format* [online], arXiv: 1406.2816 [math.NA], Available from: <https://arxiv.org/abs/1406.2816>, [arXiv:1406.2816](https://arxiv.org/abs/1406.2816).
- [31] S. Dolgov, D. Kressner, and C. Strössner, *Functional Tucker approximation using Chebyshev interpolation* [online], arXiv: 2007.16126 [math.NA], 2020, Available from: <https://arxiv.org/abs/2007.16126>, [arXiv:2007.16126](https://arxiv.org/abs/2007.16126).
- [32] S. Dolgov and D. Savostyanov, *Alternating minimal energy methods for linear systems in higher dimensions*, *SIAM Journal on Scientific Computing* **36** (2014), no. 5, A2248–A2271 (English), [doi:10.1137/140953289](https://doi.org/10.1137/140953289).
- [33] M. Espig, W. Hackbusch, A. Litvinenko, H. G. Matthies, and E. Zander, *Efficient analysis of high dimensional data in tensor formats*, *Sparse Grids and Applications* (J. Garcke and M. Griebel, eds.), *Lecture Notes in Computational Science and Engineering*, vol. 88, Springer, Berlin, 2013, pp. 31–56 (English), [doi:10.1007/978-3-642-31703-3_2](https://doi.org/10.1007/978-3-642-31703-3_2).
- [34] M. Espig, M. Schuster, A. Killaitis, N. Waldren, P. Waehnert, S. Handschuh, and H. Auer, *TensorCalculus, C++ library*, 2012, Available from: <http://gitorious.org/tensorcalculus>.
- [35] M. Espig, *Effiziente Bestapproximation mittels Summen von Elementartensoren in hohen Dimensionen*, Ph.D. thesis, Universität Leipzig, Germany, 2008.
- [36] M. Espig, L. Grasedyck, and W. Hackbusch, *Black box low tensor-rank approximation using fiber-crosses*, *Constructive Approximation* **30** (2009), 557–597, [doi:10.1007/s00365-009-9076-9](https://doi.org/10.1007/s00365-009-9076-9).
- [37] M. Espig and W. Hackbusch, *A regularized Newton method for the efficient approximation of tensors represented in the canonical tensor format*, *Numerische Mathematik* **122** (2012), no. 3, 489–525, [doi:10.1007/s00211-012-0465-9](https://doi.org/10.1007/s00211-012-0465-9).
- [38] M. Espig, W. Hackbusch, S. Handschuh, and R. Schneider, *Optimization problems in contracted tensor networks*, *Computing and Visualization in Science* **14** (2011), no. 6, 271–285, [doi:10.1007/s00791-012-0183-y](https://doi.org/10.1007/s00791-012-0183-y).
- [39] M. Espig, W. Hackbusch, A. Litvinenko, H. G. Matthies, and E. Zander, *Iterative algorithms for the post-processing of high-dimensional data*, *Journal of Computational Physics* **410** (2020), 109396, [doi:10.1016/j.jcp.2020.109396](https://doi.org/10.1016/j.jcp.2020.109396).
- [40] M. Espig, W. Hackbusch, T. Rohwedder, and R. Schneider, *Variational calculus with sums of elementary tensors of fixed rank*, *Numerische Mathematik* **122** (2012), no. 3, 469–488, [doi:10.1007/s00211-012-0464-x](https://doi.org/10.1007/s00211-012-0464-x).

- [41] G. Evenbly and G. Vidal, *Tensor network states and geometry*, J Stat Phys **145** (2011), 891–918, [doi:10.1007/s10955-011-0237-4](https://doi.org/10.1007/s10955-011-0237-4).
- [42] I. Gavriluk, W. Hackbusch, and B. N. Khoromskij, *Data-sparse approximation of a class of operator-valued functions*, Mathematics of Computation **74** (2005), 681–708.
- [43] I. P. Gavriluk, W. Hackbusch, and B. N. Khoromskij, *Hierarchical tensor-product approximation to the inverse and related operators for high-dimensional elliptic problems*, Computing **74** (2005), no. 2, 131–157.
- [44] R. Ghanem, D. Higdon, and H. Owhadi, *Handbook of uncertainty quantification*, Springer, 2017, Available from: <http://lib.ugent.be/catalog/ebk01:434000000062028>.
- [45] G. Golub and C. F. van Loan, *Matrix computations*, Johns Hopkins University Press, Baltimore, MD, 1996.
- [46] S. A. Goreinov, I. V. Oseledets, D. V. Savostyanov, E. E. Tyrtyshnikov, and N. L. Zamarashkin, *How to find a good submatrix*, Matrix Methods: Theory, Algorithms, Applications (V. Olshevsky and E. Tyrtyshnikov, eds.), World Scientific, Hackensack, NY, 2010, pp. 247–256.
- [47] S. A. Goreinov, E. E. Tyrtyshnikov, and N. L. Zamarashkin, *A theory of pseudo-skeleton approximations*, Linear Algebra Appl. **261** (1997), 1–21. MR MR1448862 (99d:15015)
- [48] A. Gorodetsky, S. Karaman, and Y. Marzouk, *A continuous analogue of the tensor-train decomposition*, Computer Methods in Applied Mechanics and Engineering **347** (2019), 59–84, [doi:10.1016/j.cma.2018.12.015](https://doi.org/10.1016/j.cma.2018.12.015).
- [49] L. Grasedyck, *Existence and computation of low Kronecker-rank approximations for large linear systems of tensor product structure*, Computing **72** (2004), no. 3, 247–265, [doi:10.1007/s00607-003-0037-z](https://doi.org/10.1007/s00607-003-0037-z).
- [50] L. Grasedyck and W. Hackbusch, *An introduction to hierarchical (H-) rank and TT-rank of tensors with examples*, Comput. Methods Appl. Math. **11** (2011), no. 3, 291–304, [doi:10.2478/cmam-2011-0016](https://doi.org/10.2478/cmam-2011-0016).
- [51] L. Grasedyck, *Hierarchical singular value decomposition of tensors*, SIAM Journal on Matrix Analysis and Applications **31** (2010), 2029–2054, [doi:10.1137/090764189](https://doi.org/10.1137/090764189).
- [52] L. Grasedyck, W. Hackbusch, and B. N. Khoromskij, *Solution of large scale algebraic matrix Riccati equations by use of hierarchical matrices*, Computing **70** (2003), no. 2, 121–165, [doi:10.1007/s00607-002-1470-0](https://doi.org/10.1007/s00607-002-1470-0).
- [53] L. Grasedyck, L. Juschka, and C. Löbber, *Finding entries of maximum absolute value in low-rank tensors* [online], arXiv: 1912.02072 [math.NA], December 2019, Available from: <https://arxiv.org/abs/1912.02072>, [arXiv:1912.02072](https://arxiv.org/abs/1912.02072).
- [54] L. Grasedyck, D. Kressner, and C. Tobler, *A literature survey of low-rank tensor approximation techniques*, GAMM-Mitteilungen **36** (2013), 53–78, [doi:10.1002/gamm.201310004](https://doi.org/10.1002/gamm.201310004).

- [55] W. Hackbusch, *Tensor Spaces and Numerical Tensor Calculus*, Springer Series in Computational Mathematics, Springer Verlag, 2012, [doi:10.1007/978-3-642-28027-6](https://doi.org/10.1007/978-3-642-28027-6).
- [56] W. Hackbusch, B. N. Khoromskij, and E. E. Tyrtysnikov, *Hierarchical Kronecker tensor-product approximations*, J. Numer. Math. **13** (2005), no. 2, 119–156, [doi:10.1515/1569395054012767](https://doi.org/10.1515/1569395054012767). MR MR2149863 (2006d:65152)
- [57] W. Hackbusch and B. Khoromskij, *Low-rank Kronecker-product approximation to multi-dimensional nonlocal operators. I. Separable approximation of multi-variate functions*, Computing **76** (2006), no. 3-4, 177–202. MR MR2210094 (2006k:65117)
- [58] W. Hackbusch and S. Kühn, *A new scheme for the tensor representation*, Journal of Fourier Analysis and Applications **15** (2009), no. 5, 706–722, [doi:10.1007/s00041-009-9094-9](https://doi.org/10.1007/s00041-009-9094-9).
- [59] W. Hackbusch, *Tensor Spaces and Numerical Tensor Calculus*, Springer, Berlin, 2012, [doi:10.1007/978-3-642-28027-6](https://doi.org/10.1007/978-3-642-28027-6).
- [60] W. Hackbusch and B. N. Khoromskij, *Low-rank Kronecker-product approximation to multi-dimensional nonlocal operators. Pt. 1: Separable approximation of multi-variate functions*, Computing **76** (2006), no. 3/4, 177–202, [doi:10.1007/s00607-005-0144-0](https://doi.org/10.1007/s00607-005-0144-0).
- [61] W. Hackbusch and B. N. Khoromskij, *Tensor-product approximation to operators and functions in high dimensions*, J. Complexity **23** (2007), no. 4-6, 697–714, Available from: <http://dx.doi.org/10.1016/j.jco.2007.03.007>, [doi:10.1016/j.jco.2007.03.007](https://doi.org/10.1016/j.jco.2007.03.007). MR 2372023 (2008k:65042)
- [62] W. Hackbusch, B. N. Khoromskij, and E. E. Tyrtysnikov, *Approximate iterations for structured matrices*, Numerische Mathematik **109** (2008), no. 3, 365–383, [doi:10.1007/s00211-008-0143-0](https://doi.org/10.1007/s00211-008-0143-0).
- [63] G. Heide, V. Khoromskaia, B. N. Khoromskij, and V. Schulz, *Tensor approach to optimal control problems with fractional d-dimensional elliptic operator in constraints* [online], arXiv: 1809.01971 [math.NA], 2018, Available from: <https://arxiv.org/abs/1809.01971>, [arXiv:1809.01971](https://arxiv.org/abs/1809.01971).
- [64] N. Higham, *Functions of matrices — theory and computation*, SIAM, Philadelphia, PA, 2008.
- [65] F. L. Hitchcock, *The expression of a tensor or a polyadic as a sum of products*, J. Math. Physics **6** (1927), 164–189.
- [66] S. Janson, *Gaussian Hilbert spaces*, Cambridge Tracts in Mathematics, vol. 129, Cambridge University Press, Cambridge, 1997. MR MR1474726 (99f:60082)
- [67] K. Karhunen, *Zur Spektraltheorie stochastischer Prozesse*, Annales Academiae Scientiarum Fennicae, Ser. A. I, Math.-Phys. **34** (1946), 1–7.
- [68] ———, *Über lineare Methoden in der Wahrscheinlichkeitsrechnung*, Annales Academiae Scientiarum Fennicae, Ser. A. I, Math.-Phys. **37** (1947), 3–79, Engl. translation: RAND Corporation, 1960, Available from: <https://www.rand.org/pubs/translations/T131.html>.

- [69] C. Kenney and A. J. Laub, *Condition estimates for matrix functions*, SIAM Journal on Matrix Analysis and Applications **10** (1989), no. 2, 191–209.
- [70] V. Khoromskaia and B. N. Khoromskij, *Tensor numerical methods in quantum chemistry*, Walter de Gruyter GmbH & Co KG, 2018.
- [71] B. N. Khoromskij, *Structured rank- (r_1, \dots, r_d) decomposition of function-related operators in \mathbb{R}^d* , Comp. Meth. Appl. Math **6** (2006), no. 2, 194–220.
- [72] ———, *Introduction to tensor numerical methods in scientific computing*, Preprint, Lecture Notes 06-2011, University of Zürich, 2010, Available from: http://www.math.uzh.ch/fileadmin/math/preprints/06_11.pdf.
- [73] B. Khoromskij and V. Khoromskaia, *Low rank Tucker-type tensor approximation to classical potentials*, Cent. Eur. J. Math. **5** (2007), no. 3, 523–550 (electronic). MR MR2322828 (2008c:65118)
- [74] B. N. Khoromskij, *Structured rank- (r_1, \dots, r_d) decomposition of function-related tensors in \mathbb{R}^d* , Computational methods in applied mathematics **6** (2006), no. 2, 194–220, doi:[10.2478/cmam-2006-0010](https://doi.org/10.2478/cmam-2006-0010).
- [75] B. N. Khoromskij, *Tensor numerical methods in scientific computing*, Walter de Gruyter GmbH & Co KG, 2018.
- [76] B. N. Khoromskij, *Tensor Numerical Methods for Multidimensional PDEs: Basic Theory and Initial Applications*, ESAIM: Proceedings and Surveys, N. Champagnat, T. Lelièvre, A. Nouy, eds **48** (January 2015), 1–28, doi:[10.1051/proc/201448001](https://doi.org/10.1051/proc/201448001).
- [77] T. G. Kolda, *Orthogonal tensor decompositions*, SIAM Journal on Matrix Analysis and Applications **23** (2001), no. 1, 243–255, doi:[10.1137/S0895479800368354](https://doi.org/10.1137/S0895479800368354).
- [78] T. G. Kolda and B. W. Bader, *Tensor decompositions and applications*, SIAM Review **51** (2009), no. 3, 455–500, doi:[10.1137/07070111X](https://doi.org/10.1137/07070111X).
- [79] S. Kotz, N. Balakrishnan, and N. L. Johnson, *Continuous multivariate distributions, volume 1, models and applications*, Wiley Series in Probability and Statistics, Philadelphia, PA, 2005.
- [80] D. Kressner and L. Perisa, *Recompression of Hadamard products of tensors in Tucker format*, SIAM Journal on Scientific Computing **39** (2017), no. 5, A1879–A1902, doi:[10.1137/16M1093896](https://doi.org/10.1137/16M1093896).
- [81] D. Kressner and C. Tobler, *Low-rank tensor Krylov subspace methods for parametrized linear systems*, SIAM J. Matrix Anal. Appl. **32** (2011), no. 4, 1288–1316, doi:[10.1137/100799010](https://doi.org/10.1137/100799010). MR 2854614
- [82] D. Kressner and C. Tobler, *Algorithm 941: Htucker—a Matlab toolbox for tensors in hierarchical Tucker format*, ACM Trans. Math. Softw. **40** (2014), no. 3, doi:[10.1145/2538688](https://doi.org/10.1145/2538688).
- [83] F. Liese and I. Vajda, *On divergences and informations in statistics and information theory*, IEEE Transactions on Information Theory **52** (2006), no. 10, 4394–4412, doi:[10.1109/TIT.2006.881731](https://doi.org/10.1109/TIT.2006.881731).

- [84] A. Litvinenko, D. E. Keyes, V. Khoromskaia, B. N. Khoromskij, and H. G. Matthies, *Tucker tensor analysis of matérn functions in spatial statistics*, Computational Methods in Applied Mathematics **19** (2019), 101–122, [doi:10.1515/cmam-2018-0022](https://doi.org/10.1515/cmam-2018-0022).
- [85] M. Loève, *Probability theory I. graduate texts in mathematics, vol. 45, 46.*, fourth ed., Springer, Berlin, 1977. MR MR0651017 (58 #31324a)
- [86] E. Lorin and S. Tian, *A numerical study of fractional linear algebraic systems*, Mathematics and Computers in Simulation **182** (2021), 495–513, [doi:10.1016/j.matcom.2020.11.010](https://doi.org/10.1016/j.matcom.2020.11.010).
- [87] E. Lukacs, *Characteristic Functions*, Griffin, London, 1970.
- [88] H. G. Matthies and A. Keese, *Galerkin methods for linear and nonlinear elliptic stochastic partial differential equations*, Comput. Methods Appl. Mech. Engrg. **194** (2005), no. 12–16, 1295–1331, [doi:10.1016/j.cma.2004.05.027](https://doi.org/10.1016/j.cma.2004.05.027). MR MR2121216 (2005j:65146)
- [89] H. G. Matthies, *Uncertainty quantification with stochastic finite elements*, Encyclopedia of Computational Mechanics (E. Stein, R. de Borst, and T. J. R. Hughes, eds.), vol. 1, Wiley, 2007, [doi:10.1002/0470091355.ecm071](https://doi.org/10.1002/0470091355.ecm071).
- [90] H. G. Matthies and E. Zander, *Solving stochastic systems with low-rank tensor compression*, Linear Algebra and its Applications **436** (2012), 3819–3838, [doi:10.1016/j.laa.2011.04.017](https://doi.org/10.1016/j.laa.2011.04.017).
- [91] F. Nielsen and R. Nock, *On the Chi square and higher-order Chi distances for approximating f-divergences* [online], arXiv: 1309.3029 [cs.IT], 2013, Available from: <https://arxiv.org/abs/1309.3029>, [arXiv:1309.3029](https://arxiv.org/abs/1309.3029).
- [92] J. P. Nolan, *Multivariate elliptically contoured stable distributions: theory and estimation*, Computational Statistics **28** (2013), no. 5, 2067–2089, [doi:10.1007/s00180-013-0396-7](https://doi.org/10.1007/s00180-013-0396-7).
- [93] W. Nowak and A. Litvinenko, *Kriging and spatial design accelerated by orders of magnitude: Combining low-rank covariance approximations with FFT-techniques*, Mathematical Geosciences **45** (2013), no. 4, 411–435, [doi:10.1007/s11004-013-9453-6](https://doi.org/10.1007/s11004-013-9453-6).
- [94] R. Orús, *A practical introduction to tensor networks: Matrix product states and projected entangled pair states*, Annals of Physics **349** (2014), 117–158, [doi:10.1016/j.aop.2014.06.013](https://doi.org/10.1016/j.aop.2014.06.013).
- [95] I. Oseledets, D. Savostianov, and E. Tyrtysnikov, *Tucker dimensionality reduction of three-dimensional arrays in linear time*, SIAM Journal on Matrix Analysis and Applications **30** (2008), no. 3, 939–956, [doi:10.1137/060655894](https://doi.org/10.1137/060655894).
- [96] I. V. Oseledets, D. V. Savostyanov, and E. E. Tyrtysnikov, *Linear algebra for tensor problems*, Computing **85** (2009), no. 3, 169–188, [doi:10.1007/s00607-009-0047-6](https://doi.org/10.1007/s00607-009-0047-6).
- [97] ———, *Cross approximation in tensor electron density computations*, Numerical Linear Algebra with Applications **17** (2010), no. 6, 935–952, [doi:10.1002/nla.682](https://doi.org/10.1002/nla.682).

- [98] I. V. Oseledets and E. Tyrtyshnikov, *Breaking the curse of dimensionality, or how to use SVD in many dimensions*, SIAM J. Scientific Computing **31** (2009), no. 5, 3744–3759.
- [99] I. Oseledets, *Matlab TT-toolbox, version 2.2*, 2011, Available from: http://spring.inm.ras.ru/osel/?page_id=24.
- [100] I. Oseledets and E. Tyrtyshnikov, *TT-cross approximation for multidimensional arrays*, Linear Algebra and its Applications **432** (2010), 70–88, [doi:10.1016/j.laa.2009.07.024](https://doi.org/10.1016/j.laa.2009.07.024).
- [101] I. V. Oseledets, *Tensor-train decomposition*, SIAM J. Sci. Comput. **33** (2011), no. 5, 2295–2317, Software <https://github.com/oseledets/TT-Toolbox.git>, [doi:10.1137/090752286](https://doi.org/10.1137/090752286).
- [102] L. Pardo, *Statistical inference based on divergence measures*, CRC press, 2018.
- [103] B. N. Parlett, *The symmetric eigenvalue problem*, SIAM, Philadelphia, PA, 1998.
- [104] P. B. Rohrbach, S. Dolgov, L. Grasedyck, and R. Scheichl, *Rank Bounds for Approximating Gaussian Densities in the Tensor-Train Format* [online], arXiv:2001.08187 [math.NA], 2020, Available from: <https://arxiv.org/abs/2001.08187>, [arXiv:2001.08187](https://arxiv.org/abs/2001.08187).
- [105] Y. Saad, *Numerical methods for large eigenvalue problems: Theory and algorithms*, Manchester University Press, Manchester, 1992.
- [106] S. Sachdev, *Tensor networks—a new tool for old problems*, Physics **2** (2009), 90, [doi:10.1103/Physics.2.90](https://doi.org/10.1103/Physics.2.90).
- [107] Z. Sasvari, *Multivariate characteristic and correlation functions*, vol. 50, De Gruyter, 2013.
- [108] D. V. Savostyanov and I. V. Oseledets, *Fast adaptive interpolation of multidimensional arrays in tensor train format*, Proceedings of 7th International Workshop on Multidimensional Systems (nDS), IEEE, 2011, [doi:10.1109/nDS.2011.6076873](https://doi.org/10.1109/nDS.2011.6076873).
- [109] R. Schneider and A. Uschmajew, *Approximation rates for the hierarchical tensor format in periodic sobolev spaces*, Journal of Complexity **30** (2014), no. 2, 56–71, [doi:10.1016/j.jco.2013.10.001](https://doi.org/10.1016/j.jco.2013.10.001).
- [110] I. E. Segal and R. A. Kunze, *Integrals and Operators*, Springer, Berlin, 1978.
- [111] N. Shephard, *From characteristic function to distribution function: a simple framework for the theory*, Econometric Theory **7** (1991), 519–529.
- [112] A. Smilde, R. Bro, and P. Geladi, *Multi-way analysis with applications in the chemical sciences*, Wiley, 2004.
- [113] T. L. Toulas and C. P. Kitsos, *Information divergence and the generalized normal distribution: A study on symmetry*, Communications in Mathematics and Statistics (2020), [doi:10.1007/s40304-019-00200-8](https://doi.org/10.1007/s40304-019-00200-8).

- [114] J. S. H. Tsai, L. S. Shieh, and R. E. Yates, *Fast and stable methods for computing the principal n th root of a complex matrix and the matrix sector function*, Comput. Math. Appl. **15** (1988), no. 11, 903–913, doi:[10.1016/0898-1221\(88\)90034-x](https://doi.org/10.1016/0898-1221(88)90034-x).
- [115] L. R. Tucker, *Some mathematical notes on three-mode factor analysis*, Psychometrika **31** (1966), 279–311.
- [116] M. Udell and A. Townsend, *Why are big data matrices approximately low rank?*, SIAM Journal on Mathematics of Data Science **1** (2019), no. 1, 144–160, doi:[10.1137/18M1183480](https://doi.org/10.1137/18M1183480).
- [117] D. V. Savostyanov, E. Tyrtysnikov, B. Khoromskij, and H.-J. Flad, *Verification of the cross 3d algorithm on quantum chemistry data*, Russian Journal of Numerical Analysis and Mathematical Modelling **23** (2008), 329–344, doi:[10.1515/RJNAMM.2008.020](https://doi.org/10.1515/RJNAMM.2008.020).
- [118] N. Vervliet, O. Debals, L. Sorber, M. Van Barel, and L. De Lathauwer, *Tensorlab 3.0*, online, 2016, Available from: <http://www.tensorlab.net>.
- [119] G. Vidal, *Efficient classical simulation of slightly entangled quantum computations*, Phys. Rev. Lett. **91** (2003), 147902, doi:[10.1103/PhysRevLett.91.147902](https://doi.org/10.1103/PhysRevLett.91.147902).
- [120] D. Watkins, *The matrix eigenvalue problem: GR and Krylov subspace methods*, SIAM, Philadelphia, PA, 2007.
- [121] V. Witkovsky, *Numerical inversion of a characteristic function: An alternative tool to form the probability distribution of output quantity in linear measurement models*, ACTA IMEKO **5** (2016), no. 3, 32–44.
- [122] V. Witkovsky, G. Wimmer, and T. Duby, *Computing the aggregate loss distribution based on numerical inversion of the compound empirical characteristic function of frequency and severity*, arXiv preprint:1701.08299, 2017, Available from: <http://arxiv.org/abs/1701.08299>.